A PROPOSAL FOR CORING INTO DEEP PERMAFROST IN NORTHERN CANADA

(RESPONSE TO NAI REVIEWER'S COMMENTS IN ITALICS)

INTRODUCTION

Deep permafrost/subpermafrost brine environments are important terrestrial analogues for the Martian subsurface. A highly collaborative drilling and sampling project in northern Canada is proposed for characterizing the microbial ecosystem present within the deep permafrost and determine how it differs from that of the underlying brine and brine pockets. The results from this coring expedition and the subsequent sample analyses will provide crucial science and engineering requirements for a Mars deep-drilling exploration program. Near term astrobiological goals for the proposed NAI-collaborative permafrost coring project include (long term goals in italics that are not part of this specific proposal):

1. Comparison of the rock/ice/gas geochemistry and the microbial density, diversity and activity of deep permafrost relative to that within the underlying brine saturated zone and potential brine pockets or cryopegs. The results can also be compared to microbial studies of shallow Siberian permafrost (Rivkina et al., 2004) and cryopegs (Gilichinsky et al., 2003) environments, nearby sub-glacial environments (Skidmore et al., 2000) and Arctic cold springs (Andersen et al., 2002). *Although microbial results have yet to be published from cold-spring discharge, both the proposed subsurface samples and surface springs are potential windows into permafrost and subpermafrost environments that can be evaluated and compared. Core samples can be surveyed for biogenic signatures using life-detection probes that are being planned for deployment on future Mars exploration missions. These include probes that analyze crushed rock as well as fluid from boreholes and in situ borehole devices.*
2. Comparison of core and fluid recovery, preservation and contamination using 0.2 μm filtered, fresh water versus using 0.2 μm filtered N_2 gas as a drilling fluid. Evaluation of microbial and organic contamination of the permafrost rock cores and fluids is an essential part of this task. How best to minimize the contamination and operate within the constraints of Planetary Protection guidelines for future Mars missions is an anticipated outcome. Gas derived either from compression of the Martian atmosphere or from sublimation of ground ice will play an essential role when drilling or coring deep into the Martian surface (Zacny and Cooper, 2003; Zacny et al., 2004). The proposed goal will also gather important data on the gas flow required

for varying rock/ice/brine ratios, temperatures and penetration rates. *Defining and refining technologies that best suit acquisition of rock and fluid samples from deep permafrost and sub-permafrost regions on Mars will include testing of drilling apparatuses that are currently being developed for flight and acquisition of data (e.g. bit penetration, temperature effects, jamming frequency, etc.) essential for evaluation of the apparatus and its autonomous drilling protocol. Evaluation should include various strategies for removing rock material from the borehole, stabilizing the borehole and management of any fluid pressure changes during future drilling/coring campaigns. Geoff Briggs of NASA Ames is developing an ASTEP proposal to utilize our northern Canadian sties for development of a fully autonomous drilling platform capable of penetrating the deep permafrost at the range of depths and pressures accessible from the underground workings.*

3. Measurement of the dielectric permittivity of the rock/ice is essential characterizing the radar attenuation and velocity at frequencies comparable to the MARSIS instrument currently orbiting Mars. Determining the heterogeneity and spatial distribution of these properties over the transition from permafrost to brine saturated rock will be essential for interpreting the data from MARSIS (Picardi et al., 2004). *Determining which geophysical prospecting tool or combination of tools are best for locating subsurface brines or brines situated within sub-vertical fractures within the permafrost is a longer term research goal at northern Candian sites. Steve Clifford has submitted a proposal to NASA's ISE program to utilize these underground mines with ramps that penetrate the deep permafrost to test EM, seismic and radar instruments at varying depths and distances.*
4. Detection and isolation of a brine-filled fracture is a high priority of this coring proposal. Because the rate of fluid flow from such a fracture may be very slow we will utilize a down hole televiewer to survey the borehole as has been done previously at Lupin Mine (Ruskeeniemi et al., 2004). The Geological Survey of Finland will be contributing televiewer to the project. A packer will then be used to isolate this fracture and over time water and gas samples will be removed for analyses. *The development of down-hole geophysical tools that can distinguish a brine-filled fracture from rock/ice prior to intersection is an extremely important long term objective and is an integral part of a proposed by Geoff Briggs intended for submission to ASTEP.*
5. The acquisition of rock/permafrost cores stored in evacuated stainless steel canisters will be a high priority for the coring campaign. Isotopic analyses of the noble gases released by the cores will determine the age of the pore ice (Lippmann et al., 2003) and isotopic analyses of the $C_{1\text{-}4}$ hydrocarbons and H_2 constrain the *in situ* microbial

activity (Price and Sowers, 2004). *The recent discovery and confirmation of CH_4 in the Martian atmosphere (Krasnopolsky et al., 2004) increases the urgency for determining the distribution and origin of methane and other natural gases in deep permafrost and subpermafrost brine systems at the proposed northern Canadian sites. Development of instruments capable of C and H isotopic analyses of trace CH_4 in the field or down-hole is the subject of an ASTID proposal by Lehmann and Onstott. Using a series of box experiments deployed on the surface above cryopegs and other fractures to identify CH_4 and other gases emanating from the subsurface and to asses which gases are readily detectable and most reliably reflect subsurface microbial activity is another long term research goal at this site.*

6. Core and fluid samples destined for molecular and geochemical analyses are frozen on site with dry ice and stored in sterile packaging immediately after recovery to inhibit oxidation of the rock matrix and alteration of the microbial community by the growth of any indigenous or contaminating microorganisms. *The effects of temperature cycling on the biomarker signatures, organic and inorganic chemistry and mineralogy are not well known. The temperature cycling to be experienced by permafrost rock samples acquired during the Mars Sample Return mission have been modeled (Amundsen et al., 2000) . Cores obtained in the proposed drilling campaign could be exposed to a range of temperatures/time trajectories prior to molecular and geochemical analyses. The results of such analyses could be compared to those of untreated samples to delineate any detrimental effects from thermal cycling.*

The proposed coring project will generate a wealth of information about deep permafrost and subpermafrost microbial biogeochemistry. In addition, constraining the history of arctic permafrost formation is of interest to many nations from the perspective of understanding long-term sequestration of radioactive waste and the impact of global warming. The cores will provide also provide data relevant to the MARSIS experiment and to NASA's MSR mission. The cores and fluid samples will be archived in a -80^{o}C freezer and made available to other researchers upon request, particularly to those group developing instruments for organic analyses or life detection that will be flow on upcoming Mars rover missions.

Supplemental funds are requested from NAI because drilling and coring of deep permafrost was not proposed in our CAN 3 proposal. In addition, numerous scientists associated with other NAI lead teams and other NASA research groups have requested collaborative participation in research at our Canadian Arctic sites since development of our CAN3 proposal. *The proposed supplement covers actual costs of shipping, equipment, supplies, and personnel directly associated with drilling and core acquisition. Due to difficulties encountered in culturing cold-tolerant anaerobic organisms from our*

initial Artic water samples, funds are requested to include Tom Kieft in the scientific personnel present during the drilling campaign and to allow for preliminary culturing tests in his laboratory at the University of New Mexico. Costs for sample analyses are derived from our existing CAN 3 budget. Funds are also requested to support travel to the Canadian Arctic for a videographer and a writer working with IPTAI's education and public outreach effort. We think it is particularly important to include these support personnel in order to allow documentation of research activities at remote sites, which is a critical component of astrobiological exploration. We expect travel costs, equipment, and supplies for outside collaborators to be covered by other funding sources.

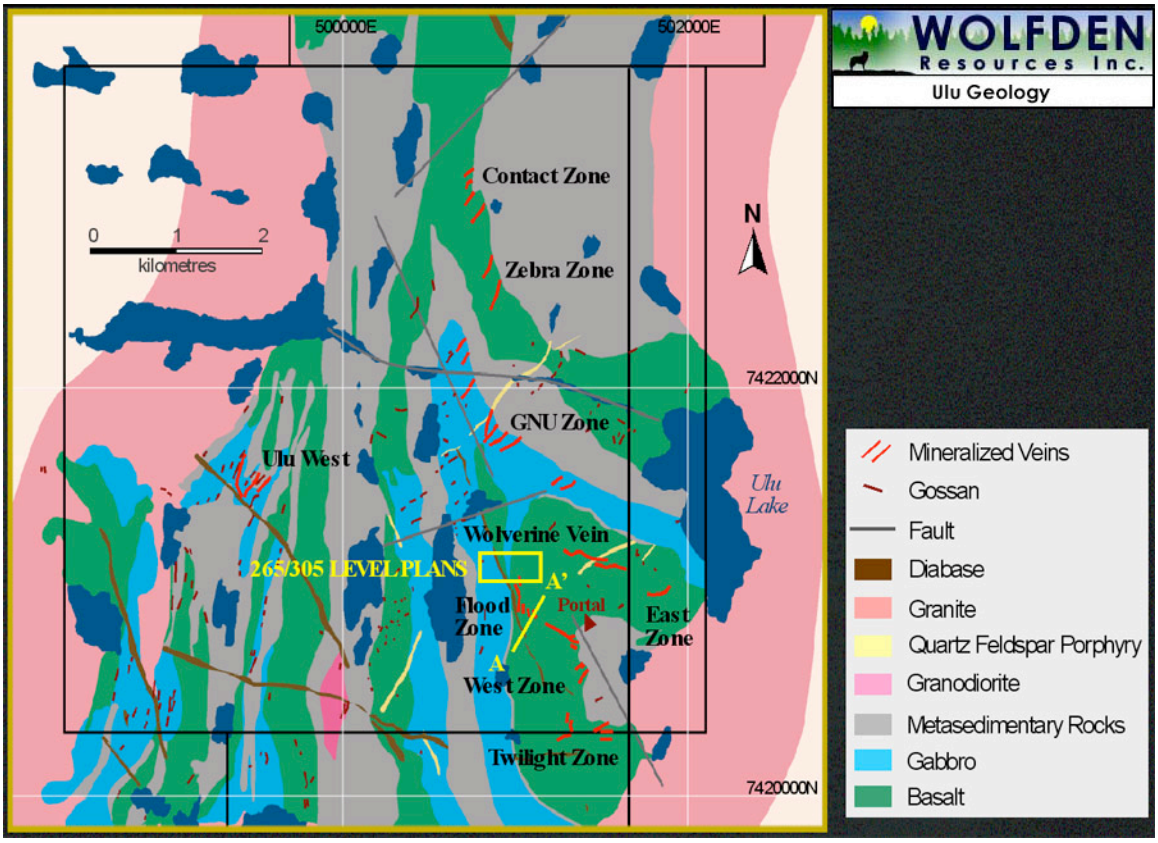

Fig. 1. Geological map of the Archean greenstone belt that comprises the Ulu exploration property. Portal marks the entrance to the inclined tunnel.

CANDIDATE SITES

Attention is focused on active commercial mines in the Canadian Arctic that provide direct access to permafrost/rock and subpermafrost brines and gases. Logistics of running a scientific drilling campaign where mineral exploration drilling is already

occurring greatly reduces the costs for transport and on-site support. We examined three potential sites for this project: Lupin (gold), Ulu (gold), and Ekati (diamond).

Lupin is a gold mine (owned by Kinross) hosted by 2.8 billion year old metasedimentary rock including banded iron formation. It possesses methane-bearing brine beneath a 500 meter thick permafrost layer of unknown age. The subsurface is accessible by a 1.5 km deep helical tunnel and by cage. It is currently accessible by weekly flights from Edmonton and, 3 months out of the year, by road from Yellowknife. In the near future, however, underground operations will cease, thereby limiting access. Surface operations will probably persist for at least another 2 to 3 years since Lupin acts as a supply hub for other mines in the region.

Ulu is an Au exploration property (owned by Wolfden Resources) comprised a 155 meter deep, inclined tunnel with horizontal access drifts located every 25 meters. The deposit is located in 2.8 billion year old mafic metavolcanic and metasedimentary strata of the Archean Slave Province (see Fig. 1). Ulu is located about 130 km north of Lupin and is accessed by the same winter road from Yellowknife and flights from Edmonton. Exploration drilling of 15,000' of core is being scheduled for '06 by Wolfden Resources.

Ekati is a diamond mine (owned by DeBeers) located about 100 km south of Lupin in Cretaceous kimberlite intruding 2.8 billion year old granite. The upper breccia facies of the pipe is mined from an open pit. A 400-meter-thick permafrost layer and the deeper root of the kimberlite are accessed by a drive-down tunnel located in the adjacent granite.

RECONNAISSANCE TRIP TO LUPIN Au MINE

NASA Astrobiology Institute scientists from IPTAI (Indiana University-Princeton University-University of Tennessee Astrobiology Initiative) Biosustaining Energy and Nutrient Cycles in the Deep Subsurface of Earth and Mars, and MSU (Michigan State University) Center for Genomic and Evolutionary Studies of Life at Low Temperatures and URI (Univ. of Rhode Island) have participated in sampling aerobic and anaerobic microbial communities from fractures intersected by existing sealed boreholes at Lupin Au mine. Previous hydrogeochemical research at Lupin by the Geological Survey of Finland and the University of Waterloo, Canada resulted in the establishment of a borehole array that is ideally suited for multi-year monitoring of biogeochemical reactions. Distinct microbial communities are anticipated in deep permafrost, cryopegs, and subpermafrost brines. Microbial diversity at Lupin is being assessed and rates of

microbial reactions are being determined in subsurface settings extending from about 200 to 1500 m below the surface. Ongoing field investigations of psychrophilic microbial communities at Lupin are directly related to the stated goals of the IPTAI team and are built on expertise developed during 5 years of work on thermophilic microbial communities in the deep and ultra-deep Au mines of South Africa. It is particularly exciting to link IPTAI's deep-subsurface experience with MSU's resources as a center for research on psychrophilic microorganisms from Siberian permafrost and Antarctic lake ice. Results of this preliminary field investigation are reported in Appendix A.

UNANSWERED QUESTIONS REGARDING SUBSURFACE LIFE IN PERMAFROST

Extensive hydrogeochemical, geophysical, and isotopic characterizations of the Lupin mine site completed during Phases 1-2 of the Canadian-Finnish-Swedish Permafrost Project provide a basis for formulating specific questions regarding the spatial and temporal distribution of microbial activity(Ruskeeniemi *et al.*, 2004; Ruskeeniemi et al., 2002).

- **Are microbial communities associated with Na-Ca brines at Lupin distinct from microbial communities associated with meteoric water of Holocene age?** A related question is whether the brine represents a Precambrian metamorphic fluid, in which case it should have been sterile, or ancient seawater, in which case ancient marine microorganisms may have been entrapped in the rock fractures. Initial He concentrations suggest an age of at least tens of millions of years.
- **Is the microbial community structure and activity within the rock pores significantly different in the permafrost zone compared to the rock fractures/pores immediately beneath the permafrost zone?** Microbial communities associated with sea ice are distinct from those found in the underlying sea water (Bowman et al., 1997). This difference is believed to be due to a combination of selection and adaptation of microorganisms to the thin, intercrystalline brine films within the sea ice in which they are trapped. In the case of deep permafrost, however, the low porosity and small pore throat diameter present within the rock already imposes a significant environmental selection that may be quite similar to frozen rock with residual thin films of brine. Very little is known about how diverse microbial communities are in permafrost.
- **What is the age of the permafrost?** Did the lowermost permafrost form more recently than the upper permafrost as would be predicted during the last deglaciation in which case the permafrost may only be ~10 kyr (Ruskeeniemi *et al.*, 2002)? If so,

is there any variation in the microbial communities or preserved molecular biomarkers with depth in the permafrost? If the permafrost is this young then why does the underlying brine appear so old?

- **Are microorganisms active in deep permafrost?** Amino acid analyses of shallow Siberian permafrost (Brinton et al., 2002) and laboratory studies of psychrophiles (Christner, 2002; Jakosky et al., 2003) appear to indicate that microorganisms are actively metabolizing substrates albeit at a 100x slower rate than in the liquid saline environments (Rivkina *et al.*, 2004). If *in situ* metabolic rates are governed by temperature as proposed by Price and Sowers (Price and Sowers, 2004), then *in situ* microbial respiration rates may actually increase with depth (and temperature) rather than decrease as observed at subsurface sites in the ocean and in terrestrial environments (Onstott et al., 1998). The slowest *in situ* metabolic rates reported by Price and Sowers (Price and Sowers, 2004) were based upon observations of deep ice cores (Price, 1999). Are the metabolic rates of deep permafrost in rock greater than, equal to or slower than those of deep ice?
- **Is the distribution of CH_4 gas in the subpermafrost fracture water correlated with the presence of methanogens, particularly CO_2 reducing methanogens?** Methanogenic activity has been documented in Siberian permafrost (Rivkina *et al.*, 2004), but methanogens have yet to be identified in the same deposits (Gilichinsky *et al.*, 2003). What effect does the formation of CH_4 clathrate have on the microbial community and activity? Specifically, how does the change in the pH_2/pCH_4 affect microbially mediated redox reactions? The methanogens will likely be less prevalent in the Ca-rich brines where DIC is less abundant.
- **Are deep permafrost microbial communities obtaining organic carbon from ancient, thermally altered organic carbon (originally photosynthetic in origin) or from acetogenesis?** The Gibbs free energy for autotrophic acetogenesis increases with decreasing temperature, whereas that for fermentation reactions decreases with increasing temperature. This suggests autotrophy could be favored in permafrost environments.
- **What are the dominant N species, and what is their origin?** Other than studies of ice covered Antarctica lakes, we do not know of any studies regarding the biogeochemical cycling of N in permafrost. With respect to identifying habitable environments on Mars where the only identified N species is N_2 in the atmosphere, this is an important question.

With respect to subpermafrost environments, these questions are being addressed by utilizing a multidisciplinary approach that combines molecular, microbial, geochemical and stable isotope data for water samples of Lupin Au mine. To address the questions

relevant to deep permafrost microbial and geochemical processes the acquisition of cores using aseptic protocols is required. Of the three potential sites, both Lupin and Ekati present problems in terms of contamination of the permafrost zone during their long history of mining and Lupin, in particular, presents logistical difficulties as it is near the end of its lifetime. Ulu, therefore, offers the best opportunity to core into the permafrost as it has the smallest contamination foot print of the three sites. Finally an extensive suite of exploration cores will be collected at Ulu by Wolfden this coming year.

CORING PLAN AT ULU

We propose collecting cores for this study during sub-vertical drilling within the Ulu tunnel from either the bottom of the ramp or from the 100 level (see Fig. 2). These locations are also closest to a western fault, which is believed to be a highly conductive, water-bearing fracture. Our initial plan will be to drill two sub-vertical holes starting at one of the underground levels and extending to below the permafrost to obtain pristine subpermafrost water. We are requesting funds for only one core as the second core will be funded by the Finnish team. Since the tunnel has yet to extend beneath the permafrost zone, this water will hopefully not be contaminated. We plan to employ the same drilling company hired by Wolfden to eliminate the cost of moving a drill rig to Ulu. For this reason the first drilling campaign is planned for winter/spring '06.

Major tasks include the following:

1. The drilling will be preceded by an EM survey of the site to identify the depth to the subpermafrost brine, examination of the existing cores with particular attention to the fracture filling minerals and selection of the location of the borehole in agreement with Wolfden Resources mining management. The final boreholes need to be located away from future mining operations at Ulu. An EM survey just completed this summer by the Finnish team indicates that the base of the permafrost at Ulu is at ~500 meters (Ruskeeniemi pers. comm., 2005).
2. One borehole will be cored using filtered fresh water as the drilling fluid as was done at Lupin during the Finnish Phase II study (Ruskeeniemi *et al.*, 2004). Uranine (Na fluorescein) at a concentration of 500 $\mu g\ L^{-1}$ will be used as a chemical tracer and fluorescent microspheres will be used as a physical tracer (Onstott et al., 2003). Following the approach of Colwell et al. (Colwell et al., 1992) the second core will employ filtered, high pressure N_2 gas for the drilling fluid in the permafrost zones where the cores for microbial studies are taken and for the portion of the borehole drilled beneath the permafrost. In this case perfluorocarbon will be utilized as the chemical tracer and fluorescent microspheres will be used as the physical tracer

(Colwell *et al.*, 1992). The latter will reduce microbial contamination and oxidation of core and any subpermafrost brines. The core barrel will be sterilized prior to each microbial coring run.

3. The conductivity of the drilling water from the first coring will be monitored to identify any brine intersections. Drilling will be followed by a borehole televiewer log to identify any weeping fracture zones and the top of the subpermafrost brine zone. The televiewer was successfully used during borehole surveys at Lupin mine and provide images of mineral grains and gas and water emitting fractures at high resolution. It will be provided by the Finnish team for no charge to this project. This information will be used to plan the second coring.
4. Cores designated for microbial studies and for which chemical and physical tracers were in the drilling fluid will be removed from the core barrel, photographed, and chopped on site. The chopped cores that are designated for activity experiments and microbial enrichments will be placed immediately into sterile whirl paks and deposited into sterile anaerobic jars flushed with high grade N_2 gas and carrying Paladium catalysts. The chopped cores designated for molecular and geochemical analyses will be placed into sterile whirl paks and deposited immediately in a cooler with dry ice. The dry ice is manufactured on site with a portable dry ice maker. The chopped cores designated for pore gas analyses and dating are placed in stainless steel canisters and sealed under vacuum using a mechanical vacuum pump on site after multiple exchanges with high grade N_2 gas. The cores will be transported to investigators home sites in this condition. Any investigators who want to initiate enzymatic analyses as soon as possible can do so at the lab that will be located in Lupin. This lab will contain an autoclave, wet bench and anaerobic glove bag. Drilling fluid samples will be collected before, during and after each microbial coring event. Fluid samples will also be collected during any conductivity spikes. The number and proportion of cores that will be collected using these procedures will depend upon the number of investigators who are interested in obtaining cores for analyses and upon the exact site selected for the coring and the distance to the subpermafrost brine or brine filled fracture. All microbial cores that have not been processed will be archived in -80^{o}C freezers at Princeton University.
5. Following the termination of coring activities the borehole will be sealed with a compression packer fitted with a valve and pressure gauge to monitor any fluid accumulation in the borehole. Based upon a review of the drilling fluid data, cores and televiewer log, the fractures that appear to be weeping brine will be identified. Nonmetallic compression packers constructed from PVDF and PEEK tubing will be

constructed at Princeton and sterilized prior to insertion into the borehole on a subsequent trip. These packers are designed to minimize the void volume. The peek tubing will be fitted with a valve and pressure gauge to determine if the brine attains hydrostatic equilibrium at depth. Fluid samples can then be collected for as long as Ulu underground operations remain open.

6. Depending upon the pressure and the storage capacity of the packered zones, fluid and gas samples can be withdrawn following the procedures that have been developed at Lupin. After a short burst of water to clear the valve outlet, sterile tubing with Swagelock fittings is screwed directly onto the valve. Sterile needles at the other end of the tubing are inserted into sterile serum vials for fluid collection. For microbial enrichments, the sterile needles are inserted directly into the media-containing Balsch tubes. For filter samples used in molecular
7. analyses the sterile hollow fiber filters are connected to the tubing and the valve left open

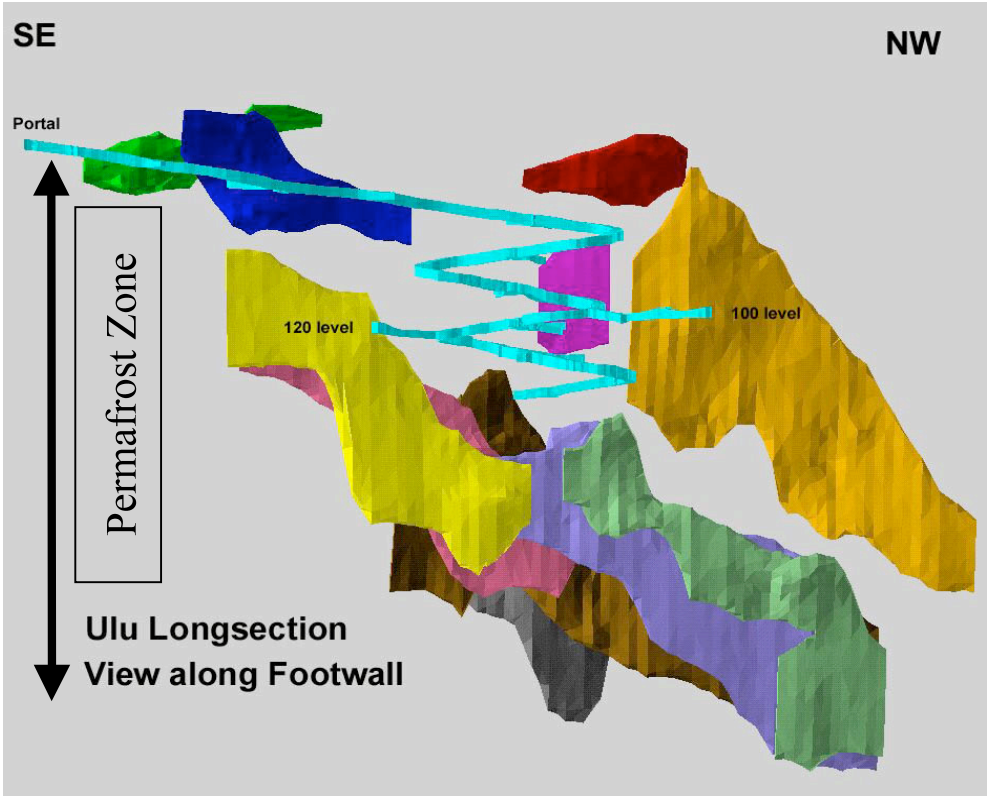

Fig. 2. Cross section of Ulu inclined tunnel showing potential locations of subsurface coring activities.

8. with water flowing for however long is required to obtain sufficient biomass for analyses. The flow rate will depend upon the recharge rate of the fracture zone, but the filters can be left on for days if need be. The hollow fiber filters are then back flushed into a sterile, anaerobic serum vial by reversing the direction of fluid flow from the tubing. For gas isotopic analyses a high pressure membrane system is used to concentrate the gas (Ruskeeniemi *et al.*, 2004) or sterile, evacuated serum vials are filled from an inverted bucket. (Ward et al., 2004). In most cases fluid samples are preserved by freezing, although in some cases depending upon the sample type various fixatives are utilized.

Fig. 3. Surface facilities at Ulu exploration site

FACILITIES AT ULU

Ulu has a 50-person Weatherhaven facility with attached mechanical/electrical shop (see Fig. 3). Modifications of the available surface facilities at Ulu to enable implementation of microbial processing procedures with more stringent quality control protocols will likely prove necessary to reduce the potential of microbial mine contaminants in future core samples. The Ulu mine site offers a surfeit of targets when it comes to borehole sampling, *in situ* borehole analyses, coring into permafrost and subpermafrost rock strata thanks to the willingness of the mine to accommodate such activities. Access to the underground will be provided by the mine using Toyota Land Cruisers fitted for underground transport. In the past exploration drilling at Ulu has not encountered any pressurized waters or gases or loss of return water while drilling through the permafrost, which bodes well for application of gas drilling. A drilling contractor is being selected who will be in charge of exploratory drilling for the next 2 to 3 years.

RESEARCH TEAM AND ACTIVITIES

The two NASA Astrobiology Institute teams, IPTAI and MSU, are comprised of scientists with varied and complementary expertise. Protocols for sampling anaerobic and aerobic eukaryotes will be developed for the Lupin project by a third Astrobiology team which is directed by Mitch Sogin at the Marine Biological Laboratory, Woods Hole Oceanographic Institutes. To address unanswered questions about subsurface life in the arctic we propose the following collaborative research activities:

1. Implementation of aseptic coring procedures, gas coring and tracer protocols to permafrost environments (Phelps-Oak Ridge National Lab; Kieft-New Mexico Tech).
2. Growth, isolation and characterization of psychrophilic aerobic and anaerobic microorganisms from environmental (i.e. filter or permafrost cores) samples (Bakermans-Michigan State and Amaral-Marine Biological Laboratory). Characterization of isolates would include phylogenetic identity, membrane lipid composition (Pfiffner-Tennessee), temperature tolerance (including freezing tolerance), salt tolerance, pH range, utilization of substrates (i.e. short chain fatty acids and H_2) for carbon and energy sources and stable isotope fractionation (Pratt-Indiana and Sherwood-Lollar-Toronto).
3. DNA (both 16SrDNA and functional genes) analyses of environmental (i.e. filter or permafrost cores) samples and flow cytometry of water samples (Onstott-Princeton) to determine biodiversity and biomass of all microorganisms including those noncultivatable.
4. Phospholipid fatty acid (PLFA) analyses of environmental (i.e. filter or cores) samples (Pfiffner-Tennessee) to determine biodiversity, stress level, and biomass of cultivable and noncultivable samples.

5. Sulfur isotope analyses of both sulfide and sulfate species (Pratt-Indiana) will be combined with ^{35}S activity measurements and DSR and APS reductase gene analyses to delineate the microbial S cycle in environmental (i.e. both water and rock core) samples. ^{35}S microautoradiography could be performed on freshly obtained rock/permafrost core to determine the spatial distribution of this activity with respect to mineralogy and physical properties (Onstott-Princeton). The results of these analyses would also complement the S and O isotopic analyses of sulfate being performed by Frape (Waterloo) to identify the sources of sulfate.
6. Microbial activity measurements of rock cores using ^{3}H, ^{14}C and ^{35}S (Soffientino-Univ. of Rhode Island) to delineate any trends with microbial activity associated with proximity of subpermafrost brine and temperature.
7. Organic chemistry of environmental (water and rock core) samples and C isotopes of organic and inorganic carbon (Pratt-Indiana University) to establish important electron donors and carbon substrates for microbial respiration and growth. The results of these analyses would also complement the inorganic aqueous chemistry being performed by Frape (Waterloo) and Ruskeeniemi (Geological Survey Finland).
8. H and C isotopic analyses of C_{1-4} and H_2 in water and core samples (Sherwood-Lollar - Univ. of Toronto) to determine whether microbial and/or abiogenic hydrocarbons are present. Dissolved H_2, CH_4 and CO by residual gas analysis of water and core samples (Onstott-Princeton) to establish abundance of these important electron donors for microbial respiration and growth (CO). These results would also complement the gaseous chemistry analyses being performed by Frape (Waterloo).
9. N-cycle. Concentration and N isotopic composition of dissolved NH_4^+ (if any) of environmental samples (water and permafrost core) to constrain the origin of N for microbial growth. DNA analyses of functional genes (e.g., NAR, NIR, NOR, NIF, and AMO) utilized by nitrate reducers, N_2 fixers and nitrifiers (Onstott-Princeton). These results would also complement the nitrate and N_2 isotopic chemistry being performed by Frape (Waterloo).
10. Depending upon the success of 1 and 2, perform microbial activity measurements under *in situ* conditions and determine the S and C isotopic fractionation associated with microbial sulfate reduction and methanogenesis at low temperatures (Pratt-Indiana,, Sherwood-Lollar-Toronto, Bakermans-Michigan State, Pfiffner-Tennessee). These data can be combined with qPCR of the methanogenic gene (MCR) to assess *in situ* rates of methanogenesis. The results of these studies would complement ongoing characterization of stable isotopic composition of aqueous, gas and rock pore species by Frape (Waterloo).

11. Examine the adaptations of microorganisms to low temperature with depth (which corresponds to time of exposure to low temperatures) to understand the evolution of these low temperature adaptive traits (Bakermans-Michigan State). Examine changes in the composition of the microbial community with depth to determine how low temperatures are selecting for and against individuals within the community.
12. Determine the physical (porosity and pore throat diameters) and geophysical (dielectric permittivity) properties of the rock cores (Clifford – Lunar Planetary Institute) and perform and ground penetrating radar (GPR) survey at low frequencies using the European Space Agency (ESA) Netlander GPR, a version of which is currently deployed around Mars on ESA Mars Odyssey Orbiter. This GPR device is designed to penetrate ~1 km into Martian subsurface, but has not been tested at all on Earth, let alone in a terrain analogous to Mars like that present at Lupin. The subsurface characterization permits unprecedented ground truthing and will constrain interpretations of the current MARSIS instrument on the ESA Mars Express orbiter.

A very important component of this research project is the development of devices and instruments for borehole analyses, fluid management, life detection, and autonomous drilling in permafrost terrain with low water/rock ratios. The proposed supplement includes travel support for IPTAI scientists working on the design of a life-detection probe that is specific for the energy-transfer molecule ATP. Additional funding for instrument development and testing is currently being sought from NASA (ASTID and ASTEP programs) by US collaborators and could be sought from the Canadian Space Agency and the Canadian Institute for Advanced Research by Frape and Sherwood-Lollar. Another important aspect of coring in permafrost will be testing of alternative drilling fluids, such as CO_2 and N_2, thereby minimizing contamination and facilitating preservation of ice and methane clathrates. Dry-gas drilling is a critical consideration in development of drilling and sampling systems appropriate for Martian surface conditions. Initial time frame for the proposed NAI-collaborative permafrost drilling is 3 years.

ADDITIONAL COLLABORATORS:

A number of investigators from within NAI and outside of NAI have expressed interest in collaborating on this field project. Two of the collaborators, Timo Ruskeeniemi and Shaun Frape, are responsible for having developed the infrastructure at Lupin Mine, established contacts with the mining industry, have developed a multiyear project there supported by Canadian, Finnish, Swedish and British nuclear waste management companies and have invited us to participate in their project. The current list of collaborators includes the following:

IPTAI
Lisa Pratt prattl@indiana.edu
Terry Hazen TCHazen@lbl.gov
Stephen Clifford Clifford@lpi.usra.edu
Barbara Sherwood-Lollar bslollar@chem.utoronto.ca
Daniel McGown ratspaw@ratspaw.com
Tullis Onstott tullis@princeton.edu
T. J. Phelps phelpstj@ornl.gov
Susan Pfiffner pfiffner@utkux.utcc.utk.edu
Tom Kieft tkieft@nmt.edu

Berkeley AI
Jill Banfield jill@eps.berkeley.edu

Carnegie Institute
Andrew Steele a.steele@gl.ciw.edu

Michigan State University AI
Corien Bakermans bakerm16@msu.edu
Mike Thomashow thomash6@msu.edu

NASA Ames AI
Geoffrey Briggs gbriggs@mail.arc.nasa.gov
"McKay, Chris" cmckay@mail.arc.nasa.gov
Carol Stoker cstoker@mail.arc.nasa.gov
Joern A. Jernsletten Joern@Jernsletten.name

University of Rhode Island AI
Steve D'Hondt dhondt@gso.uri.edu
Art Spivak spivack@gso.uri.edu
Bruno Soffientino bruno@gso.uri.edu

Woods Hole AI
Mitch Sogin sogin@evol5.mbl.edu

Johnson Space Center

Kennda Lynch kennda.l.lynch@jsc.nasa.gov
Norman Wainwright nwainwri@mbl.edu

Honeybee Robotics
Stephen Gorevan gorevan@honeybeerobotics.com

LBNL
Susan Hubbard shubbard@ccs.lbl.gov

Finland
Timo Ruskeeniemi Timo.Ruskeeniemi@gsf.fi

Canada
Ian Clark idclark@uottawa.ca
Shaun Frape shaun@sciborg.uwaterloo.ca

Kinross Mines-Lupin
Wayne Grudzinski andMike Tansey

Classified according to their primary interests and expertise, their role in the project would be as follows:

Geology and hydrology

Timo Ruskeeniemi and his team who work with the mine geologists and perform hydraulic testing and modeling.

Geophysics, including surface and borehole geophysics.

Timo Ruskeeniemi and his team have performed surface GPR and multi frequency EM soundings at Lupin. Similar EM soundings will be carried out in Ulu as well.

Stephen Clifford-geophysical rock properties and GPR surveys.

Susan Hubbard-primarily borehole seismic and pulsed neutron logging

Geochemistry and Isotope analyses

Shaun Frape and his research group and Timo Ruskeniemi focus on stable (O, D, C and S) and cosmogenic isotope analyses and geochemical analyses of fracture water, ice, rock pore water, dissolved methane and fluid inclusions.

Ian Clark and his research group perform noble gas isotopic analyses of the fracture water in order to determine its age.

Barbara Sherwood-Lollar performs C and H isotopic analyses of dissolved hydrocarbon gases and H_2.

Lisa Pratt's group is focusing on S isotopic analyses and its relationship to the microbiology, but will also perform aqueous and rock geochemical analyses as needed.

T.C. Onstott's group can perform low level H_2 and CO analyses and provide aqueous and rock geochemical analyses if needed.

Microbial Diversity

Michael Thomashow and Corein Bakermans group is focusing on psychrophilic organisms using both culture dependent and independent approaches on the fracture fluids and core material.

Jill Banfield's group has expressed interest in examining psychrophilic S oxidizing communities that may be present in the biofilms developed in open boreholes.

Mitch Sogin as expressed interest in genomic analyses particularly of eukaryotic communities, but bacterial/archaeal as well.

Onstott, McGown and Hazen are focusing on the development of genomic analyses of subsurface samples as an approach to characterizing the communities in the fracture fluids and the permafrost/rock cores.

Tom Kieft, T.J. Phelps and S. Pfiffner are primarily interested in psychrophilic anaerobes from the fracture fluids and cores and development of coring procedures in permafrost and on Mars.

Chris McKay is primarily interested in microorganism preservation in ancient permafrost and has been acting primarily as an unpaid consultant with respect to this project to date.

Biomarker Detection and Microbial Activity

Andrew Steele's group has been developing field based methods, MASSE, for biomarker detection and would primarily be interested in applying this approach to fluid, rock and permafrost samples.

Norm Wainwright and Kennda Lynch would be interested in applying their Horseshoe Crab immunological detection scheme to samples of fluid and permafrost.
Susan Pfiffner will focus on PLFA analyses.
Steve D'Hondt and Art Spivak are interested in applying their ^{3}H hydrogenase activity measurement on fluids and permafrost cores.
T.C. Onstott's group is interested in applying ^{35}S autoradiography on the permafrost samples.

Drilling Technology, Microbial Contamination and Tracer Analyses

Geoff Briggs is interested in testing their Baker Hughes assembly for coring at various levels within Ulu.
Carol Stoker and Steve Gorevan are interested in testing their deeper drilling device currently employed at Rio Tinto, but also testing of the Honeybee "inch worm" for much greater depths (up to ~1 km).
T.J. Phelps is interested in contributing his expertise on the use of various drilling fluids and tracers.

Education and Outreach

Ruth Droppo and Susan Pfiffner are in charge of the outreach for the drilling project.

DRAFT BUDGET FOR DRILLIING AT ULU:

Salary	year 1
L.M. Pratt, PI	0
T.C. Onstott, Princeton Co-PI	0
Supplies	
Cryogenic shipping containers suitable for commercial airlines	
2 Thermolyne Arctic Express-10 canisters @$1400/ea	2,800
High-pressure tanks of N2 and tank rental, 20 tanks purchased in Edmonton, Alberta @$99/ea	1,980
2-person minivinyl glove bag	5,000
Portable electric autoclave	700
-20 degree freezer	500
In-line PVDF 0.2 micron air filters	500
Portable dry ice maker, 1 pound blocks	500
Tank CO2 and tank rental, 4 cylinders @ $99/ea	396
Regulation mine gear (boots, helmets, gloves for 9 people @$450/each)	4,050
Total Supplies	16,426
Travel	
Foreign travel to, and expenses at, Ulu Mine for team members not covered by NAI CAN-3 award:	
5 investigators, airfare, lodging and per diem, 1 week at Ulu	11,250
Travel costs for drilling crew (airfare)	4,000
Total Travel	15,250
Other Direct Expenses	
Contractural Services to Boart/Longyear	
Drilling crew salary for 3 weeks	10,000
*Diamond-bit drilling/coring of one borehole in hard rock	25,000
Rig moving costs $200/hour for 50 hours	10,000
Acid test and consumables	6,000
Contractural Services to Wolfden Mining	
Rehab costs at drillsite, base of ramp or 100 level (50% cost share Finnish Geological Survey)	20,000
Delivery charge for N2 gas tanks to Yellowknife (via truck)	2,000
Delivery of N2 gas tanks to Ulu (air shipment from Edmonton to Ulu)	6,000
Roundtrip shipping of microbiological sampling equipment	4,000
Return shipping of core samples	3,000
Total Other Direct Expenses	86,000
Subcontracts	
Tom Kieft, New Mexico Technical Institute: Gene sequencing and microbial enrichments	15,000
Total Subcontracts	15,000

Total Direct Costs	132,676
Indirect costs	
Base = Modified total direct costs (MTDC) excludes subcontracts > $25K	132,676
indirect cost rate for off campus 26%	
Indirect Costs = rate x base (26% x 132,676)	34,496
Total Direct and Indirect Costs	**167,172**

*Second core to be provided by the Finnish Geological Society at no cost to the project

APPENDIX A: RESULT OF RECONNAISSANCE TRIP TO LUPIN

With the assistance of Timo Ruskeeniemi (Geological Survey of Finland) and Monique Hobbs (Ontario Power Generation), brines of widely varying salinity were collected from 11 subsurface sites in May 2004 and March 2005. Brines below the permafrost were collected from six drill holes outfitted with valves and pressure gages and located at the 1130 and 880 m levels. Dripping water from open fractures in the roof was collected at the 1130 and 250 m levels. Dripping water at the 250 m level is within the current permafrost. Water recirculated within the mine for drilling activities (service water) was sampled from an open drain at the 1130 m level. Water and biofilms from a cold spring at 1130 meters were collected. The following aliquot types were collected:

1. Filters for DNA analyses.
2. Filters for enrichment of cultivable, anaerobic and aerobic psychrophiles.
3. Anaerobic media (sulfate reducers, fermenters, Fe (III) reducers and methanogens) inoculated with borehole water.
4. Gas samples for isotopic analyses and measurement of dissolved H_2 and CO.
5. Water sample for isotopic analyses, including N isotopes of NH_4^+ (Waterloo)
6. Noble gas samples (Ottawa).
7. Dissolved sulfate/sulfide samples for isotopic analyses.
8. Samples for FISH (Fluorescent In Situ Hybridization) and flow cytometer (cell density).
9. Multiple samples for analyses of cations, anions, and short-chain fatty acids.
10. Water samples for ^3H enzymatic analyses.

Field parameters, pH, Eh, dissolved O_2, temperature and conductivity were measured on site. Conductivity ranged from 4.9 to 60.4 mS/cm. Temperatures varied from 13.4 to 1.5^{o}C. The pH ranged from 7 to 9. Visible ZnS precipitates were observed in the sulfur isotope syringes after one day of storage at room temperature indicating the presence of significant sulfide concentrations. Although Eh values as low as -143 mV were measured, Eh values were higher than expected for a sulfate/sulfide redox couple at the observed pH and temperature. One possible explanation is that mixing of water with different reduction potentials from separate fractures is occurring within boreholes. Televiewer logs indicate the presence of multiple fractures, and fracture water chemistry seems highly variable based upon observations of seeps. A very thick (~2 cm), white and fluffy biofilm beneath a flowing, spitting fracture in the machine shop at 1130 level was sampled. Finally, a large mineralized fracture (20 cm in thickness and laterally traceable

for more than 2 m) bearing calcite, quartz and sulfide was collected from the 540 m level along the ramp.

The integrity of borehole installations at Lupin is a tribute to the technical ability of the Finish/Canadian collaborators on the Permafrost at Lupin Project. We know of no equivalent borehole array available for scientific study at a deep mine. Of particular interest for sampling deep subsurface microbes, there are high *in situ* water pressures (300 to 700 psi), sulfide is present, dissolved O_2 is absent, and boreholes have been isolation for time periods up to 14 months. These are all positive indicators that the borehole communities will likely represent indigenous microbial constituents in the rock formation. Over the next several months, the sulfur isotopic and DNA analyses combined with the results of microbial enrichments should allow us to determine the extent of potential mining contamination of the environment and to target specific boreholes for more detailed sampling via a borehole packer system being developed in Frape's lab at Waterloo.

Laboratory analyses reveal that the brines are rich in sulfate and acetate (μM levels). Positive enrichments on sulfate reducing media have been successful as have aerobic plate enrichments and phylogenetic identification is underway. The ^4He concentrations indicate that brines are very old, yet H_2 concentrations are low, suggesting active H_2 consumption.

REFERENCES

Andersen, D. T., Pollard, W. H., McKay, C. P. and Heldmann, J. (2002) Cold springs in permafrost on Earth and Mars. *Journal of Geophysical Research* 107, 10,1029.

Bowman, J. P., Mccammon, S. A., Brown, M. V., Nichols, D. S. and Mcmeekin, T. A. (1997) Diversity and Association of Psychrophilic Bacteria
in Antarctic Sea Ice. *Applied and Environmental Microbiology* 63, 3068-3078.

Brinton, K. L. F., Tsapin, A. I., Gilichinsky, D. and McDonald, G. D. (2002) Aspartic Acid Racemization and Age–Depth Relationships for Organic Carbon in Siberian Permafrost. *Astrobiology Journal* 2, 77-82.

Christner, B. C. (2002) Incorporation of DNA and Protein Precursors into Macromolecules by Bacteria at -15^{o}C. *Applied and Environmental Microbiology* 68, 6435-6438.

Colwell, F. S., Stormberg, G. J., Phelps, T. J., Birnbaum, S. A., McKinley, J., Rawson, S. A., Veverka, C., Goodwin, S., Long, P. E., Russell, B. F., Garland, T., Thompson, D.,

Skinner, P. and Grover, S. (1992) Innovative techniques for collection of saturated and unsaturated subsurface basalts and sediments for microbiological characterization. *Journal of Microbiological Methods* 15, 279-292.

Gilichinsky, D., Rivkina, E., Shcherbakova, V., Laurinavichuis, K. and Tiedje, J. (2003) Supercooled Water Brines Within Permafrost—An Unknown Ecological Niche for Microorganisms: A Model for Astrobiology. *Astrobiology Journal* 3, 331-341.

Jakosky, B. M., Nealson, K. H., Bakermans, C., Ley, R. E. and Mellon, M. T. (2003) Subfreezing Activity of Microorganisms and the Potential Habitability of Mars' Polar Regions. 3, 343-350.

Krasnopolsky, V. A., Maillard, J. P. and Owen, T. C. (2004) Detection of methane in the martian atmosphere: evidence for life? *Icarus*

Lippmann, J., Stute, M., Torgersen, T., Moser, D. P., Hall, J., Lin, L., Borcsik, M., Bellamy, R. E. S. and Onstott, T. C. (2003) Dating ultra-deep mine waters with noble gases and ^{36}Cl, Witwatersrand Basin, South Africa. *Geochim. Cosmochim. Acta.* 67, 4597-4619.

Onstott, T. C., Moser, D. P., Fredrickson, J. K., Brockman, F. J., Pfiffner, S. M., Phelps, T. J., White, D. C., Peacock, A., Balkwill, D., Hoover, R., Krumholz, L. R., Borscik, M., Kieft, T. L. and Wilson, R. B. (2003) Indigenous versus contaminant microbes in ultradeep mines. *Environmental Microbiology* 5, 1168-1191.

Picardi, G., Biccari, D., Seu, R., Marinangeli, L., Johnson, W. T. K., Jordan, R. L., Plaut, J., Safaenili, A., Gurnett, D. A., Ori, G. G., Orosei, R., Calabrese, D. and Zampolini, E. (2004) Performance and surface scattering models for the Mars Advanced Radar for Subsurface and Ionosphere Sounding (MARSIS). *Planetary and Space Science* 52, 149-156.

Price, P. B. (1999) A habitat for psychrophiles in deep Antarctic ice. *Proceedings of the National Academy of Sciences* 97, 1247-1251.

Price, P. B. and Sowers, T. (2004) Temperature dependence of metabolic rates for microbial growth, maintenance, and survival. *Proceedings of the National Academy of Science* 101, 4631-4646.

Rivkina, E., Laurinavichius, K., McGrath, J., Tiedje, J., Shcherbakova, V. and Gilichinsky, D. (2004) Microbial life in permafrost. *Advances in Space Research* 33, 1215-1221.

Ruskeeniemi, T., Ahonen, L., Paananen, M., Frape, S., Stotler, R., Hobbs, M., Kaija, J., Degnan, P., Blomqvist, R., Jensen, M., Lehto, K., Moren, L., Puigdomenech, I. and Snellman, M. (2004) Permafrost at Lupin: Report of Phase II. 89.

Ruskeeniemi, T., Paananen, M., Ahonen, L., Kaija, J., Kuivamäki, A., Frape, S., Moren, L. and Degnan, P. (2002) Permafrost at Lupin: Report of Phase 1. 67.

Skidmore, M. L., Foght, J. M. and Sharp, M. J. (2000) Microbial Life beneath a High Arctic Glacier. *Applied and Environmental Microbiology* 66, 3214-3230.

Ward, J. A., Slater, G. F., Moser, D. P., Lin, L.-H., Lacrampe-Couloume, G., Bonin, A. P., Davidson, M., Hall, J. A., Mislowack, B., Bellamy, R. E. S., Onstott, T. C. and Sherwood Lollar, B. (2004) Microbial Hydrocarbon Gases in the Witwatersrand Basin, South Africa: Implications for the Deep Biosphere. *Geochim. Cosmochim. Acta.* 68, 3239-3250.

Zacny, K. A. and Cooper, G. A. (2003) Investigation of diamond-impregnated drill bit wear while drilling under Earth and Mars conditions. *Journal of Geophysical Research* 109, E07S10.

Zacny, K. A., Quayle, M. C. and Cooper, G. A. (2004) Laboratory drilling under Martian conditions yields unexpected results. *Journal of Geophysical Research* 109, E07S16.

Amendment A to Proposal for Coring into Deep Permafrost in Northern Canada: Sample Transportation, Storage, Access and Moratorium

In response to comments from the initial technical review, the following amendment is submitted to clarify transportation of time-critical microbiological, gas, and water samples and to outline a protocol for long-term storage of and access to samples from rock cores.

Time-critical samples include inoculated growth media, enzyme-based metabolic assays, and various types of filters and membranes used to concentrate biomass by filtration of tens to hundreds of liters of ground water. Time-critical samples will be collected by the field team following detailed instructions and using sampling kits provided by researchers not present at the time of sampling. Instructions and kits for time-critical sampling will be tested for feasibility and safety by the field team prior to accepting responsibility for acquisition of samples. Transportation of samples back to laboratories will be done as excess baggage on commercial airlines using either cooler boxes packed with blue ice (about 0^oC) or shippable cryogenic dewars with liquid N_2 absorbent cores (about -196^oC). After arrival in the U.S., time-critical samples will be re-packed on blue ice, on dry ice (about -78^oC), or in shippable dewars and transported to individual researchers by overnight carriers.

Gas samples in syringes, glass bottles or serum vials will be stored and transported on blue ice or poisoned with $HgCl_2$ to inhibit microbial activity. Water samples in plastic or glass bottles will be stored and transported on blue ice. Depending upon the type of analyses some of these water samples will be fixed in the field. Samples that cannot be fixed will be shipped frozen (e.g. anion samples). Filters from water samples will also be stored in sterile whirlpak bags frozen for molecular or on blue ice for inoculation experiments or activity measurements. Small sections of rock cores containing fractures or other evidence of enhanced permeability will be sub-sampled from the long cores with a clean chisel, wrapped in annealed (500^oC for 12 hours) Al foil, packaged in low-volatility plastic bags, and stored on blue ice or dry ice. Rock cores will be stored in corrugated, low-volatility plastic boxes and shipped as commercial air fright. Sub-samples of rock cores intended for analyses of redox sensitive chemistry or molecular composition will be placed in sterile whirlpaks and shipped using liquid N_2 dewars or dry ice. Rock cores collected for long term incubation experiments at in situ temperatures will be sealed in sterile whirlpaks in gas tight ammo cans under high grade N_2 gas and shipped with blue ice. Rock cores to be analyzed for gas pore compositions and pore fluid dating with noble gases will be placed immediately into stainless steel vacuum canisters, evacuated and sealed. No special conditions are required for shipment of noble gas samples.

Rock cores will be stored at room temperature (range $18\text{-}28^oC$) at Indiana University and will be accessible to researchers for a minimum of five years. Sections of rock cores sub-

sampled for molecular work and redox chemistry will be stored at Princeton University in a –80^{o}C freezer and also will be accessible for 5 years. Photographs and logs of cores will be available on the IPTAI website (http://www.indiana.edu/~deeplife/). Requests for samples will be limited to the original Ulu drilling participants for the first 6 months after drilling and then open to other researchers. Letters of request for samples from the Ulu rock cores must explicitly state the goal and time frame of the research, analytical or descriptive methods to be used, optimal size/weight of samples, and specific depth intervals or rock types needed for the research. If multiple requests are received for a particular depth interval or rock-type, then priority will be given to requests from NASA-funded researchers and to requests based on methods or approaches not utilized by the original participants.

Amendment B to Ulu drilling proposal: Explanation of Drilling Estimates

The following is the proposed drilling contract between Boart Longyear and Wolfden Resources, Inc., the owner of the Ulu mining property, for 15 kms. of exploration coring. This is being provided to the reviewer of our proposal who claimed that our estimated costs for coring were quite low. Our costs estimates were based upon this proposed contract. This contract was sent to us by Boart-Longyear in March 2004 as a means of providing a basis for estimating the cost of collecting one ~200-400 m long core at Ulu while Boart Longyear was on site. Any final negotiation with Boart-Longyear on the terms of a drilling contract with our project clearly is pending approval of funds for said drilling project. Note that these rates are no longer guaranteed after Dec. 31st, 2005.

Having said this, the rates for drilling, #3 and #8, therefore apply to our proposal to NAI for the estimated duration of 2 weeks, which in turn was based upon drilling performed at Lupin mine. Providing an adequate drilling station, #4, is relevant to the rehabilitation cost of our NAI budget. The delay rate, #9, of $50/hour applies to our proposal, which shouldn't be a serious problem given that in order to process the core there will be at least 6 people on site, 3 per 12 hour shift. The stand by, #10, doesn't apply to our drilling operation in the sense that only Wolfen can place drilling rigs on stand-by because of mining operations. Ground conditions, #11, applies to our proposal. Drilling fluids utilized by our project, #12, are different from those provided by Ulu and are provided in our budget. Inclinometer tests, #13, applies to our coring operation. Redrilling old holes, #14, and moving between holes, #16, applies to the cost estimate of set up and reorientation of the drill rig between our hole and that drilled by the Geological Survey of Finland will be shared between our two groups. Mobilization and demobilization, #15, obviously does not apply to our drilling operation as Boart Longyear will already be on site. Items #1 and #6 will be provided by Wolfden and #2 and #5 will be provided by Boart-Longyear. Items #17 to #29, but not #25, apply to our drilling operation, but are irrelevant to budget. Wolfden provides the right of way, #25.

AGREEMENT, entered into this 29th day of December 2004.

between*:*

Wolfden Resources Inc.
309 Court Street South
Thunder Bay, Ontario
P7J 2Y1

the party of the first part, hereinafter referred to as the Client.

and:

Boart Longyear Inc.
P.O. Box 789, 310 Niven Street
Haileybury, ON
P0J 1K0

the party of the second part, hereinafter referred to as the Contractor.

WHEREAS the Client wishes to have performed certain underground diamond drilling at the ULU Mine Site located near the Lupin Mine in the province of Nunavut and whereas the Contractor, in consideration of payments hereinafter contained, undertakes to do the said diamond drilling.

1. ***Guaranteed***

The Client guarantees a minimum of 15,000 meters of diamond drilling, in a series of NQ holes, collared at –90° to +80° degrees, to a maximum depth of 600 meters. All measurements are to be taken from top of casing.

2. ***Core Size***

The Contractor agrees to supply two (2) LM75 electric-hydraulic diamond drill rig (125 hp) and associated equipment and to drill the specified minimum footage recovering NQ-U Wireline Core, approximately 47.6 mm in diameter, at the following schedule of rates.

3. ***Schedule of Rates for Diamond Drilling***

Depth of Hole Range	NQ Wireline
0 – 150	$60.00 per meter
150 – 300	$67.50 per meter
300 – 450	$77.00 per meter
450 – 600	$84.50 per meter

If holes of a greater depth than 600 meters are desired, such drilling shall be performed only upon such conditions and at such rates as may be agreed upon before commencement of such drilling.

The drilling shall be conducted so as to produce maximum core recovery with every reasonable precaution taken to prevent crushing, wearing or grinding of core.

The Contractor agrees that all its labour, industrial diamond cost, and all other operating expenses, except as hereinafter provided, shall be for its own account.

4. ***Drill Stations***

The Client agrees to provide drill stations of sufficient size to accommodate the following rod pulls:

Drill	Hole Depth	Pull Length	Pull Space Required
LM75	0 – 600 m	3.0 m	5.5 m

It is understood that the Company will scale and rock bolt the drill stations, where necessary, to ensure a safe working area for the Contractor's employees.

5. ***Boart Longyear Responsibilities***

To Provide:

- Two electric hydraulic LM75 diamond drill's
- Experienced labour
- Drilling tools (i.e. bits, rods, etc.)
- Drill spares and maintenance
- Miscellaneous tools to perform the work required
- Hoses and fittings
- Management, Safety Supervisor to make regular visitations
- WHMIS certification, NWT supervisor certification, St. John's Ambulance certificate
- PPE for drill crew
- Survey equipment, Reflex Easy Shot
- Crew transportation to Yellowknife airport
- Full-time Supervision for two drills; operating foreman for one drill

6. ***Client Responsibilities***

To Provide (at no cost to Boart Longyear)

- Site specific orientation
- Mine plans at appropriate scale to adequately depict drill stations and hole set-ups
- All markings of proposed drill hole set-ups
- Core boxes
- Ventilation as per industry standards
- Rock bolted and screened drill stations as per industry standard
- Miners' lamps
- Power (600 volts to 60 hz) to diamond drill
- Brine water (12 gallons/minute) and compressed air (750 cfm @ 100 psi) within 100 feet of set-up
- Phone/fax line
- Loader for off-loading of drills and related equipment
- Office and dry facilities
- Room and board
- Transportation to and from site from Yellowknife Airport
- Lumber as required for proper staging and drill leveling

- Tractor for underground transportation

7. Work Schedule

The Contractor agrees to commence the work on or about mid – May 2005, but is contingent upon permitting and agreed that the Contractor will require 6 – 8 weeks prior notice of the intended start date. It is further understood that the Contractor will operate on a two 12-hour shift, twenty-four hours per day basis, seven (7) days per week on a four week in and two week out work schedule.

8. Hourly Rate

The Hourly Rate shall be interpreted here and hereinafter to be $135.00 per hour, per drill outfit.

It is agreed that the Contractor shall include in the Hourly Rate, the cost of supplying a regular two-man crew, supervision and maintenance as required, drill rig and associated equipment.

It is also agreed and understood that when the Contractor is working at the Hourly Rate, the cost of pipe, casing, down-hole equipment and diamond articles lost or left in the hole, and materials and supplies consumed in the work shall be for the Client's account, at cost, plus 15%.

9. Delay Rate

It is agreed that the Delay Rate shall be interpreted here and hereinafter to be $50.00 per man per hour.

Delays in excess of a one half (1/2) hour shall be reported to the Client at the earliest possible time. In such cases, the Client reserves the right to utilize Boart Longyear personnel for other work on site for which they are suitably qualified. Delay claims resultant from causes as outlined in this agreement will be reimbursed to the Contractor up to a maximum number of hours equivalent to the regular number of hours per shift. Examples of possible delays are:

- Waiting for instructions from the Client
- Blasting delays (smoked out, gas check)
- Delays caused by other mine equipment or personnel
- Lack of available work site

- Excess water in the airlines
- Delay by surveyors
- Site specific orientation or site induction
- Waiting for services to be provided by the Client (air, power, water, ventilation and prints).
- Scaling, screening of work site.
- Weather delays

10. ***<u>Standby Equipment</u>***

It is understood that a diamond drill and related equipment maybe placed on standby from time to time, in the event that this standby time exceeds a period of two (2) months the Client shall be charged $4,000.00 per month per drill outfit retro-active from the first day the drill went on standby.

11. ***<u>Ground Conditions</u>***

In the event that cavities, loose or caving materials, swelling ground, or hydrostatic pressures are encountered of a nature as to prevent the successful completion of any hole, the Contractor does not, under such conditions, guarantee to drill to a predetermined depth, and in the event that it becomes necessary to abandon the hole, the Client agrees to pay for such uncompleted holes at the rates herein specified for all footage completed.

In the event it becomes necessary to resort to cementing, reaming, hole reduction, or pumping lost circulation materials, the Client agrees to reimburse the Contractor at the Hourly Rate for cementing, reaming, hole reduction, or pumping lost circulation materials.

Wherever pipe, casing, down-hole equipment, and diamond articles are lost, or left in a hole on the instructions of the Client's Representative, the Client agrees to pay the Contractor for such at replacement cost, F.O.B. drill site.

12. ***<u>Circulating Fluids, Additives and Rod Grease</u>***

In the event drilling mud, polymers, additives and rod grease are required as a normal circulating medium in the hole, all costs associated with their supply shall be for the Client’s account at cost, plus 15%.

These products will be charged to the Client as consumed.

13. Tests

The Contractor agrees to supply one Reflex-Easy Shot instrument at a rental rate of $ 2,500.00 per month per unit.

The Contractor agrees to conduct Reflex-Easy Shot surveys or Clinometer dip test at the Hourly Rate per survey at depths specified by the Client.

14. Re-Drilling Old Holes

If at any time the Client desires the Contractor to move back onto a setup to deepen a previously drilled hole, all hours and supplies consumed to ream, clean, and condition the hole to the depth where coring may commence, are for the Client's account at the Hourly Rate.

15. Mobilization and Demobilization

The Client agrees to pay the mobilization of drilling equipment and interim shipments of equipment and supplies at invoice price plus 15% from the Contractor's shop and warehouse facilities in Haileybury, Ontario to the Client's warehousing yard in Yellowknife.

The Client further agrees to pay the demobilization of drilling equipment and interim shipments of equipment and supplies at invoice price plus 15% from the Client's warehousing yard in Yellowknife to the Contractor's shop and warehouse facilities in Haileybury, Ontario.

It is also agreed that the Client shall be responsible for the arrangement for the movement to and from of all drilling equipment and supplies including interim shipments from the Wolfden's Yellowknife warehouse to the Ulu Mine Site. All costs associated with this movement shall be the responsibilities of the Client.

It is agreed that the cost of mobilizing and demobilizing the crew to and from Yellowknife on completion of their maximum four week tour shall be charged to the Client at a lump sum of $2,250.00 per person. Included in the lump sum rate are all travel time cost and travel expenses.

16. Moving

The labour cost to move in from surface and set-up on the initial hole(s) plus tear down and move out to surface from the final hole(s) shall be for the Client's account at the hourly rate plus 15%.

All labour costs on moves between holes underground shall be for the Client's account at the hourly rate plus 15%.

The Client agrees to pay the hourly rate plus 15% for moving on, cleaning and moving off previously drilled holes.

Transportation of the Contractor's equipment for all moving shall be the responsibility of the Client.

17. Daily Reports

The Contractor shall make and deliver to the Client, daily drilling reports as to the progress of the drilling, including the depth of each hole, together with an explanation of any shutdown time, the reasons therefore, and what is being done to remedy them.

The Client agrees that it will verify that the daily drilling reports accurately describe the work performed, including, without limitation, the depth of each hole and ancillary charges.

The Client agrees that it is responsible for the verification of the daily drilling reports and that it will report any inaccuracies to the Contractor within twenty-one days of receiving an invoice containing the alleged inaccuracies. The Client agrees that if it fails to give notice to the Contractor of any alleged inaccuracies in the daily drilling reports within such twenty-one day period, the Client shall be deemed to have fully accepted the accuracy of the daily drilling reports and shall have waived any claims arising out of any such inaccuracies.

18. Core

Core shall be delivered to the Client at the end of every shift with the use of the Company tractor, to the core shack. Core boxes are to be furnished by the Client.

19. Security

The Contractor will not give out any information regarding drill results or permit access to any drill core, to any person other that the Client's accredited representatives, except upon specific permission of responsible officials of the Client.

It is agreed that the contents of this agreement shall remain confidential between the Management of the Client and the Contractor.

20. ***Safety and Health***

The Contractor will conduct the work with the highest regard to the safety and health of its employees and others. The Contractor has a “zero tolerance” for accidents or incidents and will actively work to achieve this standard by ensuring the following:

- Hiring only qualified and trained personnel
- Conducting pre-shift inspections on every shift
- Conducting weekly safety meetings
- Audit safety systems, training records and equipment logs
- Immediately suspending operations in order to remedy deficiencies with respect to safety
- Cooperate fully with other mine personnel and supervisors and follow all directions to ensure the safety of the crew
- Conduct preventative maintenance and ensure that all tools are in “first class” operating condition.
- Provide on-site orientation for all employees

21. ***Hydraulic Oil and Lubes***

The Contractor agrees to provide all lubes for the underground diamond drill on site.

22. ***Discipline***

The Contractor shall, at all times, enforce strict discipline and maintain good order among its employees, and shall not retain on the work any unfit person or anyone not skilled in the work assigned to him.

Any employees of the Contractor who are objectionable or unsatisfactory to the Client, shall be removed from the work and replaced by an employee satisfactory to the Client.

23. ***Insurance***

The Contractor shall maintain such insurance as will protect it from all claims and damage for personal injury, including death resulting therefrom, and from claims for property damage resulting from activities of Boart Longyear Inc. under this contract, in an amount not to exceed $2,000,000.00 inclusive for all liabilities for any one accident or occurrence.

The Contractor shall be responsible for and will pay promptly all dues and assessments payable under any Worker's Compensation Act, or other similar Act, whether Provincial or Federal, in respect of its employees.

24. Environment

The Contractor during 2004 became ISO 14001 certified, currently we are the only diamond drill contractor to do so and will follow all, the policies and procedures as set out in our guidelines. The Contractor shall keep the Client's premises free from accumulation of waste material or rubbish and upon completion of the work, shall remove all tools, scaffoldings, surplus materials and rubbish, and leave the premises in a clean condition.

25. Rights of Way

The Client shall provide, at no cost to the Contractor, all necessary permits and rights of way to all lands that may be required to enable the Contractor to carry out the work specified.

The Contractor shall execute the work in a good and workmanlike manner and the Client shall hold the Contractor harmless from any assessment for stumpage, land use or reclamation, or other charges of similar kind and nature.

26. Payment for Work

The Client agrees to pay the Contractor, in Canadian funds, the above prices. Payment must be made within thirty days of the date the account is rendered. Invoices shall be submitted twice monthly. Interest at the rate of 1_% per month shall be charged on overdue accounts.

27. Alterations to Agreement

This Agreement may be altered only by written consent of both parties hereto.

28. ***<u>Term of Agreement</u>***

This Agreement shall be valid until December 31st, 2005.

29. ***<u>Wording of Agreement</u>***

The parties expressly request that this Agreement, as well as all documents relating thereto be drawn up in English.

Les parties ont expressément exigé que cette convention ainsi que tous les documents s'y rattachant soient rédigés en anglais.

30. ***<u>Time</u>***

Time is of the essence in this Agreement.

BOART LONGYEAR INC.

_____ _____

Witness

_____

WOLFDEN RESOURCES INC.

_____ _____

Witness

_____

Amendment C to Ulu Proposal: Papers on technical methods (Ar drilling and other technologies)

See following reports (Colwell et al., 1992; Ruskeeniemi et al., no date).

Journal of Microbiological Methods 15 (1992) 279 – 292

MIMET 00500

Innovative techniques for collection of saturated and unsaturated subsurface basalts and sediments for microbiological characterization

F.S. Colwell[1], G.J. Stormberg[1], T.J. Phelps[2], S.A. Birnbaum[3], J. McKinley[4], S.A. Rawson[1], C. Veverka[4], S. Goodwin[4], P.E. Long[4], B.F. Russell[5], T. Garland[4], D. Thompson[1], P. Skinner[6] and S. Grover[7]

[1]*Idaho National Engineering Laboratory, Idaho Falls, ID 83415, U.S.A.,* [2]*The University of Tennessee, Institute for Applied Microbiology, Knoxville, TN 37932, U.S.A.,* [3]*Division of Earth and Physical Sciences, University of Texas – San Antonio, San Antonio, TX 78285, U.S.A.,* [4]*Pacific Northwest Laboratory, Richland, WA 99352, U.S.A.,* [5]*Golder Associates, Inc., Richland, WA 99352, U.S.A.,* [6]*Whitman College, Walla Walla, WA 99362, U.S.A. and* [7]*Idaho State University, Pocatello, ID 83209, U.S.A.*

(Received 3 October 1991; revision received and accepted 27 January 1992)

Summary

Basalt and sediment samples were cored from depths of up to 183 m at the Idaho National Engineering Laboratory (INEL) for evaluation of microbial abundance and diversity in the subsurface. The overall goal of the research is to understand subsurface microbial ecology to effectively conduct in situ bioremediation. To minimize the impact of sampling on the biological and chemical integrity of subsurface strata, argon (Ar) was used as an inert drilling fluid. Upon retrieval, cores were placed into Ar-filled chambers for processing. Subsamples for microbiological analyses were pared by hydraulic splitting and milled to diameters of 0.1 – 0.5 cm and then aseptically packaged for distribution to investigators. Multiple tracers measured potential contamination which may have occurred during drilling or coring. Fluorescent microspheres and lithium bromide (Br^-) served as downhole tracers while gaseous perfluorocarbon tracers (PFTs) were used to monitor intrusion of drilling fluids into the cored zone. Tracer concentrations in samples indicated that microsphere and Br^- occurrence and quantity was not necessarily correlated to the type of material cored but possibly related to characteristics of individual cores such as presence of fractures or core length. Microsphere and Br^- concentrations indicated that, in samples provided to the investigators, any contaminating microbes or chemicals introduced during the coring process would have been diluted to the extent that they would have been insignificant. PFTs indicated gaseous intrusion into sediments and basalts deeper than the drill bit-stratum interface and provided evidence of Ar intrusion into the sample and ahead of the drill bit. Tracer data provided evidence that the quality control techniques employed protected the integrity of the subsurface samples.

Key words: Subsurface; Argon; Sediment; Basalt; Quality assurance

Correspondence to: F.S. Colwell, Idaho National Engineering Laboratory, P.O. Box 1625, Idaho Falls, ID 83415, U.S.A.

Introduction

Abundance, diversity and activities of microbial communities residing in deep Eastern Coastal Plain sediments has recently been established. These studies provided evidence of aerobic [1, 2, 6], anaerobic [9], microaerophilic [3], and eukaryotic [12] microbes as well as spatial differences in microbial populations [2]. Sparse microbial populations have also been reported from arid unsaturated sediments [5]. Such findings are important as they relate to potential subsurface bioremediation schemes.

Accurate subsurface characterization requires techniques that allow deep sample acquisition while minimizing possible microbial or chemical contamination of the sampled strata. Previous studies primarily focused on sedimentary formations and were either shallow [15] or used liquid viscosifying agents in the drilling medium [4, 10]. Many problems may arise if liquid drilling fluids are used to acquire samples for chemical and biological analysis. Liquid drilling fluids can be a major source of bacterial contamination [13]. Sodium bentonite viscosifying agents provide attachment surfaces for microorganisms and, as drilling fluids are recirculated, nutrients may be acquired that facilitate microbial growth. Chemical contamination may occur through the introduction of sulfate which is common in many viscosifiers [10] or by altering the in situ redox conditions [7]. Liquid drilling fluids surround the drill stem from the drill bit – stratum interface to the land surface. Fluid circulation provides a mechanism for cross-contamination with deeper, unsampled strata. The drilling fluid is typically 10 – 25% denser than water and the fluid column may be higher than the groundwater head. In such cases, a large hydraulic head is exerted on the strata at the bottom of the hole contributing to potential contamination of unsampled strata.

For this study, drilling and coring techniques were sought which would facilitate chemical and biological characterization of subsurface formations without the deleterious effects of aqueous drilling fluids. Such techniques should be amenable to a variety of formations and have the capability to expand the knowledge of subsurface microbial ecology and chemistry. Chemical, particulate and gaseous tracers should also be used to assess the extent that drilling operations affect the samples. This report describes coring techniques and quality assurance protocols for sampling subsurface consolidated basalts and sediments for use in microbial ecology, geochemical and physical studies.

Techniques and Procedures

Site description

The borehole was located on the INEL reservation, 68 km from Idaho Falls and 13 km NE of Idaho highways 20 and 26 (NW 1/4 Sec31 T3N R30E). The site was located atop the basalt flows of the Eastern Snake River Plain, the age of the basalts ranging from approximately 233,000 to over 600,000 years before present. The site geology is characterized by a thin layer of unconsolidated surficial sediment (1 – 4 m thick) overlying numerous basalt flows containing sedimentary interbeds. Individual basalt flows range from 6 to 33 m (average 15 m) in thickness. Interbeds are composed predominantly of silts and clays, although sandy material and sporadic gravels

are also encountered. Interbed thicknesses range from 0.5 to 18 m (Fig. 1). The borehole was 45 m upgradient from an existing well which was cased and completed from 152.4 to 163.1 m. The existing well provided stratigraphic control for targeting borehole sample intervals and groundwater for water quality analyses. Depth to the water table in 1990 was 140.5 m.

Coring tools and procedures

Drilling and coring services were provided by P. C. Exploration of Bozeman, MT. Air rotary and dual wall reverse air rotary drilling techniques were used to advance a 14.6 cm borehole between targeted sample intervals [14]. Wireline coring techniques and tools (Christensen Mining Prod., Salt Lake City, UT) were used, with modifications, during actual sample collection. CP-sized (8.4 cm diameter) core was collected using either 1.5 m Lexan (clear polycarbonate) inner tubes or 1.5 m stainless steel split core barrels. Depending upon drilling conditions, a 1.22 – 1.52 m core was collected during each core run. Each core was aseptically handled using sterile gloves and placed in an Ar-filled glove box within 1 h of completing each core run and within minutes of arrival at the surface. Temperature-sensitive labels (Cole-Parmer, Inc.) were placed on the drill shoe and sample barrel and never exceeded 40 °C on core runs from which samples were distributed. This provided evidence that regions proximal to the freshly acquired core were not excessively heated.

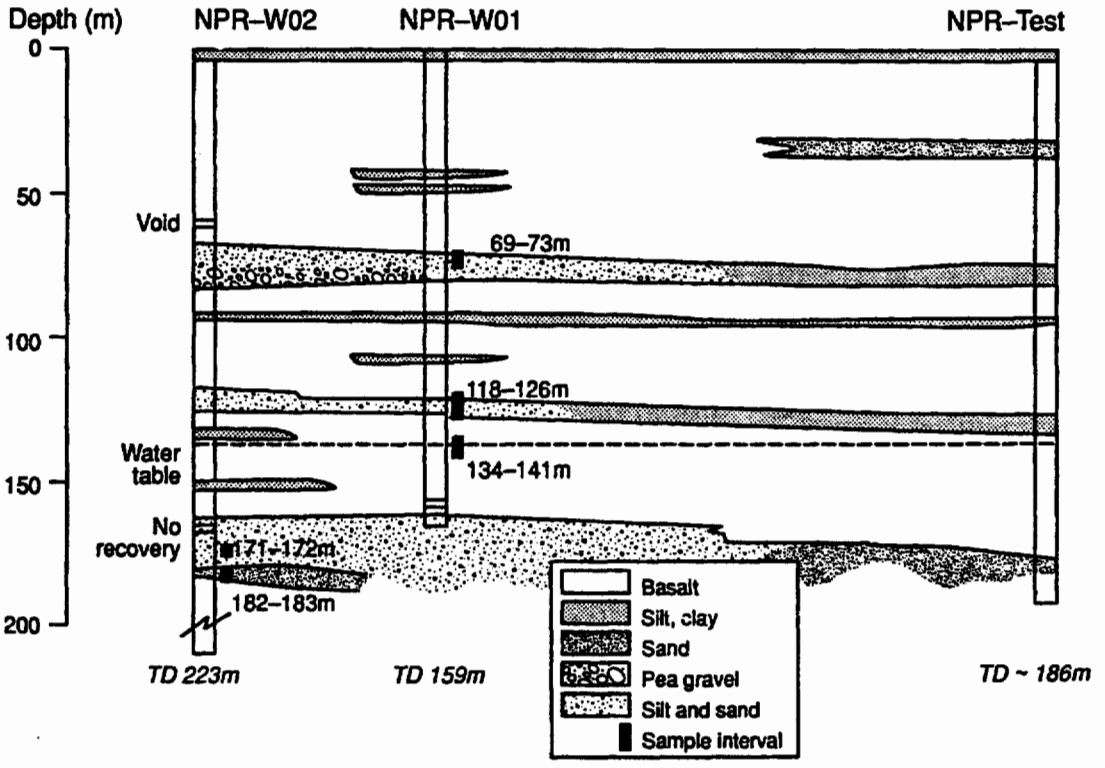

Fig. 1. Geologic cross-section of the INEL Deep Microbiology Site. Note the location of sample intervals and water table. TD, total depth.

Decontamination

To minimize introduction of contaminants to the borehole, strict cleaning procedures were implemented during drilling and sampling. An area around the drill rig (ca. 20 m diameter) served as the exclusion area during active drilling and sampling. Cleaning and decontamination was conducted upwind of the exclusion area. Assembly of coring tools and all tracer manipulation was done in a separate, upwind location using sterile gloves. Before arrival at the drill site, all drilling equipment (e.g., drill rig, drill pipe, bits, tools) was cleaned using a high pressure steam cleaner. Initial cleaning was done using potable water and biodegradable detergent followed by a potable water rinse. Upon arrival at the drill site, steam cleaning was repeated. During drilling and sampling, all downhole equipment was steam cleaned using deionized water immediately prior to placement into the borehole. Equipment not immediately used was wrapped in plastic and stored off the ground. Small transportable equipment was wrapped in foil, autoclaved at 120 °C for 20 min, and stored at the drill site.

Air and Ar drilling media

Air rotary drilling was used to advance the borehole between sample intervals. An Atlas-Copco oil-free compressor, with air filters capable of removing particles >17 μm, provided compressed air. Air was delivered to the bit face at 28 to 42 $m^3 \cdot min^{-1}$ and pressures between 690 and 1550 kPa.

Approximately 3 m above target sample intervals the air rotary system was removed from the borehole and coring equipment installed. Subsequently, vaporized liquid Ar (99.9% pure, 23 to 28 $m^3 \cdot min^{-1}$, 518 to 759 kPa) was used to advance the hole and acquire samples from the target interval. Liquid Ar was stored on site in a 22.7 m^3 double-lined steel vessel and approximately 2.3×10^4 m^3 of vaporized Ar were used during the project. Temperature and pressure in the tank were approximately -200 °C and 1553 kPa, respectively. During sampling, liquid Ar flowed through a vaporizer, equilibrated to ambient temperature and pressure, and then was directed to the drill bit – stratum interface. The required piping was a closed system reducing the possibility of contaminant introduction. Prior studies indicated fewer than 1 viable microbe $\cdot m^{-3}$ of vaporized liquid Ar (Colwell, unpublished data).

Tracer technologies

To determine the magnitude of infiltration and concomitant effects of pressurized gas and equipment operation on samples, three tracers were added during drilling: fluorescent microspheres, aqueous lithium bromide (Br), and gaseous perfluorocarbons (PFTs). The microspheres represented a surrogate microbial tracer, nonvolatile Br traced chemical infiltration during coring and gaseous, slightly soluble PFTs traced pressurized gas introduced to the subsurface during drilling and coring.

The microspheres (Polysciences Inc, Warrington, PA) were carboxylated, fluoresced yellow-green, and had a mean diameter of 0.9 μm. Five ml of concentrated microsphere solution were added to 100 ml of sterile water in a Whirlpak bag for a final concentration of 8.75×10^9 microspheres $\cdot ml^{-1}$. The Whirlpak bag was aseptically attached to the coring shoe at the end of each sample barrel and protected with a plastic lining (Fig. 2). When coring began, the impinging subsurface materials split

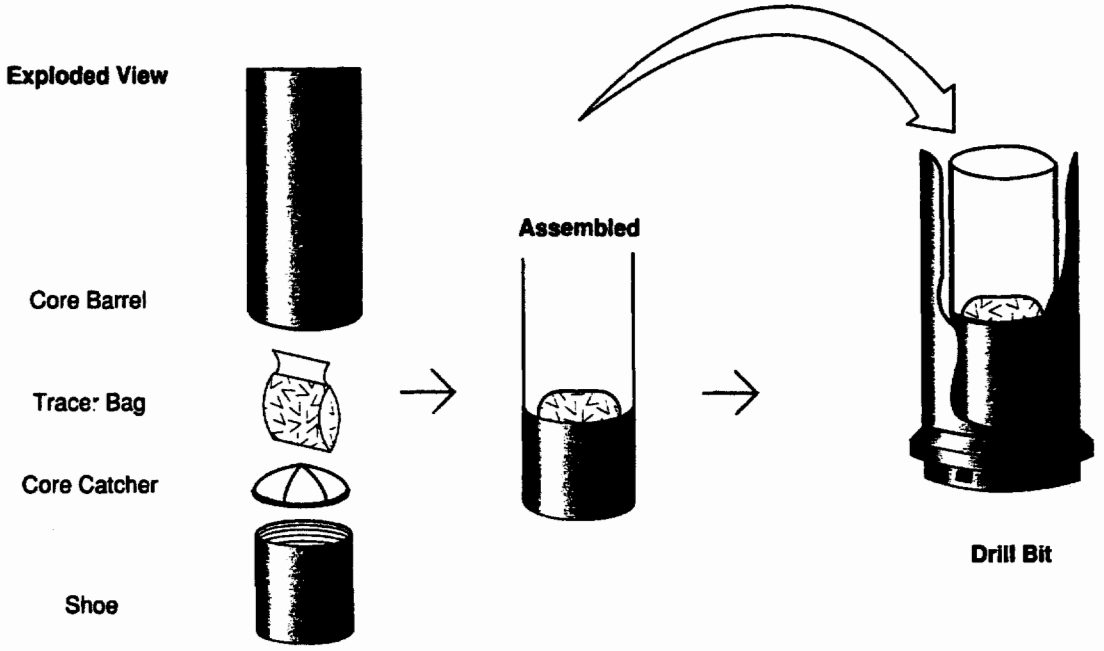

Fig. 2. Tracer bag assembly and location in coring and sampling tools. Tracer bag containing microsphere and Br^- tracers was broken open during coring and the contents spilled onto the nascent core. Subsequently pared samples were analyzed to assure several log decrease in concentrations of tracers.

the plastic lining and Whirlpak bag discharging the 100 ml suspension of microspheres in the vicinity of the coring bit.

Upon core retrieval, aliquots of the cored materials were subsampled, diluted 1:1 in 0.1% sodium pyrophosphate, vortexed and allowed to settle for 2 min. After settling, 10 μl aliquots of the supernatant were evenly spread (in triplicate) over 1 cm^2 circles etched on glass slides and allowed to dry. Microspheres were enumerated using a Zeiss Universal microscope (10× objective) equipped for viewing bacteria stained with acridine orange (50 W halogen lamp, 450–490 nm band-pass filter, 510 nm beam splitter, 520 nm barrier filter). Detection limits were 10^3 microspheres$\cdot g^{-1}$ sample.

Lithium bromide (44 g$\cdot$100 ml^{-1} sterile water) was added to the water in each Whirlpak bag used for the microspheres. Br^- was analyzed by weighing a recovered subsample, then leaching it with an equal mass of water and determining the Br^- concentration in the leachate using ion chromatography. A field-mobile Dionex ion chromatograph, including a Dionex AS4A column and Rainin automation system, was used to resolve and quantitate ions in solution. Detection limits for Br^- were approximately 0.5 mg$\cdot l^{-1}$.

To introduce PFTs, liquid PFT was pumped into a pressure vessel held at constant temperature (120°C), where it vaporized at a constant internal gas pressure approximately 345 kPa above the drilling gas pressure. The pressurized vessel was constantly flushed with Ar at a flow rate of 250 to 300 ml$\cdot$$min^{-1}$. Net (liquid equivalent) delivery of PFT to the drill-rig was 2 to 3 ml$\cdot$$min^{-1}$. In two instances, the PFT perfluorohexane (PFH) was injected during the final minutes of air-rotary drilling; a total (liquid) volume of less than 4 ml was injected in each case. During coring, the

PFT perfluoromethylcyclohexane (PFMCH) was injected into the Ar stream. Drilling gases traversed the hole then exited the drill rig 30 m downwind.

PFTs were extracted from subsamples of cores by equilibrating the subsample with 10 ml of methanol for 1 h. Samples were introduced onto a Tekmar model LSC-3 purge and trap concentrator and purged through a Tenex trap to remove possible organic impurities onto a Carbopak/Carbosieve trap. This trap was heated to 180 °C desorbing PFTs through a heated transfer line into a HP 5880 gas chromatograph equipped with a chrompack fused silica 50 m × 0.53 mm I.D. coated AL203/KCL capillary column and an electron capture detector. Column flow was 9 $ml \cdot min^{-1}$ of He carrier gas, with 22 $ml \cdot min^{-1}$ of P-10 (90% Ar, 10% CH_4) makeup gas. Column temperature was initially 100 °C, increased 10 °C $\cdot min^{-1}$ to 200 °C and held for 5 min; the electron capture detector was held at 250 °C. Retention times for the PFH and PFMCH were 5.74 and 7.99 min, respectively. PFT analyses were conducted on site. Limits of detection ranged downward from 0.9 ng PFT $\cdot g^{-1}$ sample and varied due to the absolute quantity of sample available for extraction.

Sample processing

To protect samples from exposure to oxygen after retrieval from the borehole, core barrels were immediately placed into an Ar-filled chamber (Fig. 3). The chamber was 5.5 m long and used multiple airlocks and entry ports to reduce Ar consumption and the risk of oxygenating the chamber. The first section, the core transfer tube, had a small volume (ca. 0.13 m^3) thus, 3 purge/evacuation cycles to replace atmospheric gas with Ar could be accomplished in < 5 min.

Sample logging and processing occurred in the fractionation glove box having a volume of ca. 1.6 m^3 (Coy Laboratory Products, Inc., Ann Arbor, MI). Sample

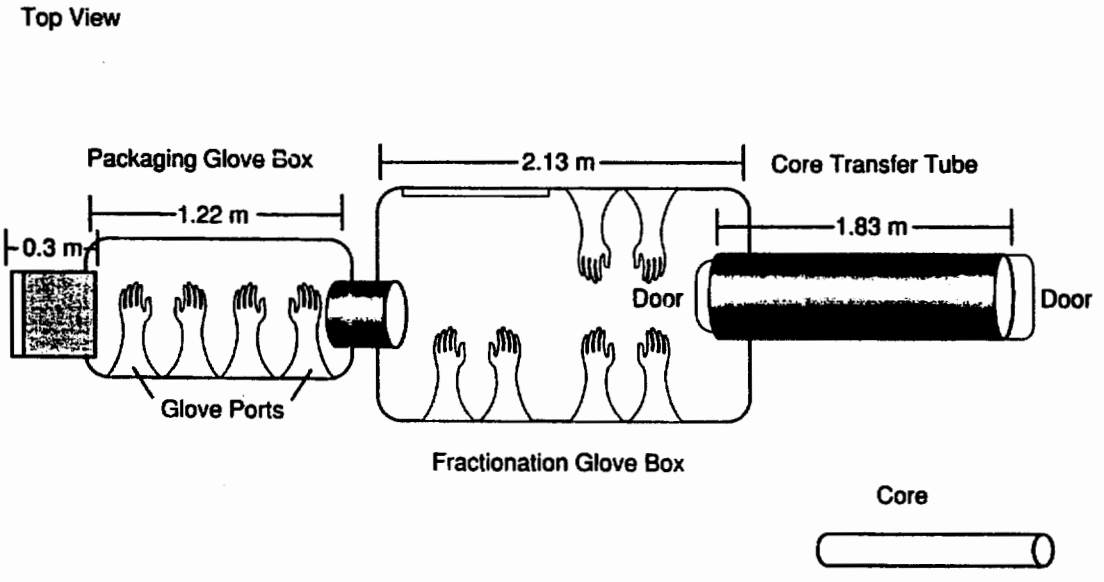

Fig. 3. Glove box array for sample processing. Entire assembly was 5.5 m long. Samples entered from the right into the core transfer tube where Ar replaced the outside atmosphere. Subsequently, the core was passed into the large glove box where samples were fractionated. Samples were weighed and labelled in the small glove box prior to exit, refrigeration and shipping.

processing was determined by the nature of the sample and the requirements of the recipient principal investigators. Concurrent with geologic logging of the samples, sample disbursal was determined and processing started. Processing usually involved 3 people working in the fractionation glove box.

The time required for processing a single 1.37 m core varied from 1 to 5 h for sediment and basalt samples, respectively. Sample handling in the chamber was minimized but when necessary was done using sterile surgical gloves placed over the butyl gloves of the chamber sleeves (Fig. 3). All consolidated materials (basalt) that were relatively intact were pared using a hydraulic core splitter (Sepor Inc., Wilmington, CA) (Fig. 4). The outer 1 – 2 cm of the core was split away and the inner portion placed into a Platner mill for crushing. Basalt samples were crushed to a nominal fragment size of 0.1 – 0.5 cm. Sediment materials were aseptically placed onto a sterile tray, homogenized, and subsequently distributed to investigators. Crushed basalt and sediment, as well as fracture infill materials and special samples (e.g., clay filled fractures or basalt/sediment interfaces), were placed directly into labelled Whirlpak bags and transferred to the packaging glove box.

In the packaging glove box (Fig. 3), two people weighed and placed samples into sterile canning jars that were sealed to maintain the Ar atmosphere. Samples were removed through the airlock adjoining the glove box and were refrigerated immediately. Within 1 – 5 h of sample retrieval from the borehole, samples were transported in coolers to a laboratory in Idaho Falls, ID. Within 24 h, samples were shipped by overnight courier to participating laboratories. At the end of each day that samples were processed, the inside of the entire sample processing array (glove boxes) was cleaned using 3% bleach, sealed and refilled with Ar. Small tools were autoclaved after use and large tools (core splitters and Platner mills) were cleaned with the bleach solution.

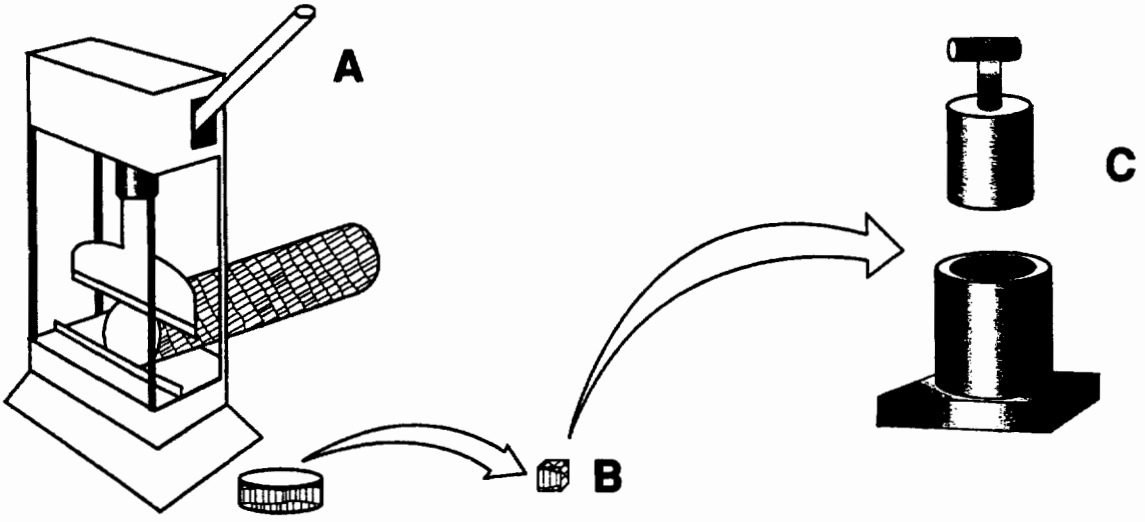

Fig. 4. Hydraulic core splitter (A) used to split sections from basalt cores and subsequently used to pare away outer, potentially contaminated layers yielding inner subcore (B). Platner mill (C) used to crush basalt samples to nominal size of 0.1 – 0.5 cm diameter.

Results and Discussion

Table 1 shows representative data for the concentrations of microspheres in samples obtained from the INEL boreholes. The mean concentration of spheres in the samples was log value 4.69 spheres $\cdot g^{-1}$ wet weight (range: 2.88 – 6.98). In all cases, concentrations of microspheres measured in the samples represented at least a 10^3-fold reduction from the original concentration of microspheres introduced to the core. Lithologic type (basalt vs. sediment samples) apparently did not influence microsphere concentrations. Conservative estimates indicated that if microspheres were evenly distributed in a 1.37 m core then this would yield log values of 7.68 and 7.84 spheres $\cdot g^{-1}$ of basalt and sediment, respectively. In all samples analyzed for microsphere tracers, the concentrations of spheres were lower than these values although concentrations varied considerably.

Fig. 5 indicates a trend towards higher microsphere concentrations at core tops compared to the middle and bottom sections of cores. Samples from cores that were <1.37 m long (denoted by arrows in Fig. 5), and therefore having had the same original concentration of microspheres distributed over a smaller volume, often exhibited higher microsphere concentrations in the middle and bottom sections. This pattern of microsphere distribution is probably due to the method of introducing the microspheres to the sample. The method, wherein a bulk quantity of microspheres was introduced to the top of a core, led to lower concentrations of microspheres as these particles adhered to the upper sections of a consolidated core. A better method of particulate tracer introduction would distribute particles evenly over the nascent core in the same manner that the drilling fluid contacts the core. Injection of the particulate tracer into the drilling fluid would be desirable because it provides tracer distribution by the same route as potential contaminants; however, the high cost of

TABLE 1

MICROSPHERE DISTRIBUTION IN REPRESENTATIVE SAMPLES FROM DIFFERENT LITHOLOGIES FROM THE INEL DEEP MICROBIOLOGY BOREHOLE

Core run	Depth (m)	Lithologic type	Log spheres $\cdot g^{-1}$
22	122.10	sediment	6.07
	122.10	sediment	5.43
	122.13	sediment	3.79
	122.68	sediment	5.96
38	137.77	basalt/silt	3.87
	137.89	basalt/silt	4.63
	138.07	basalt/silt	5.82
39	138.87	basalt/silt/clay	5.89
	139.02	basalt/silt/clay	6.16
	139.29	basalt	5.48

Fluorescent microspheres (8.75×10^9 ml^{-1}) were introduced near the drill bit durng coring and then washed from subsamples of the core, the supernatant dried on glass slides and the spheres enumerated using fluorescence microscopy. Detection limits were 10^3 microspheres $\cdot g^{-1}$ sample.

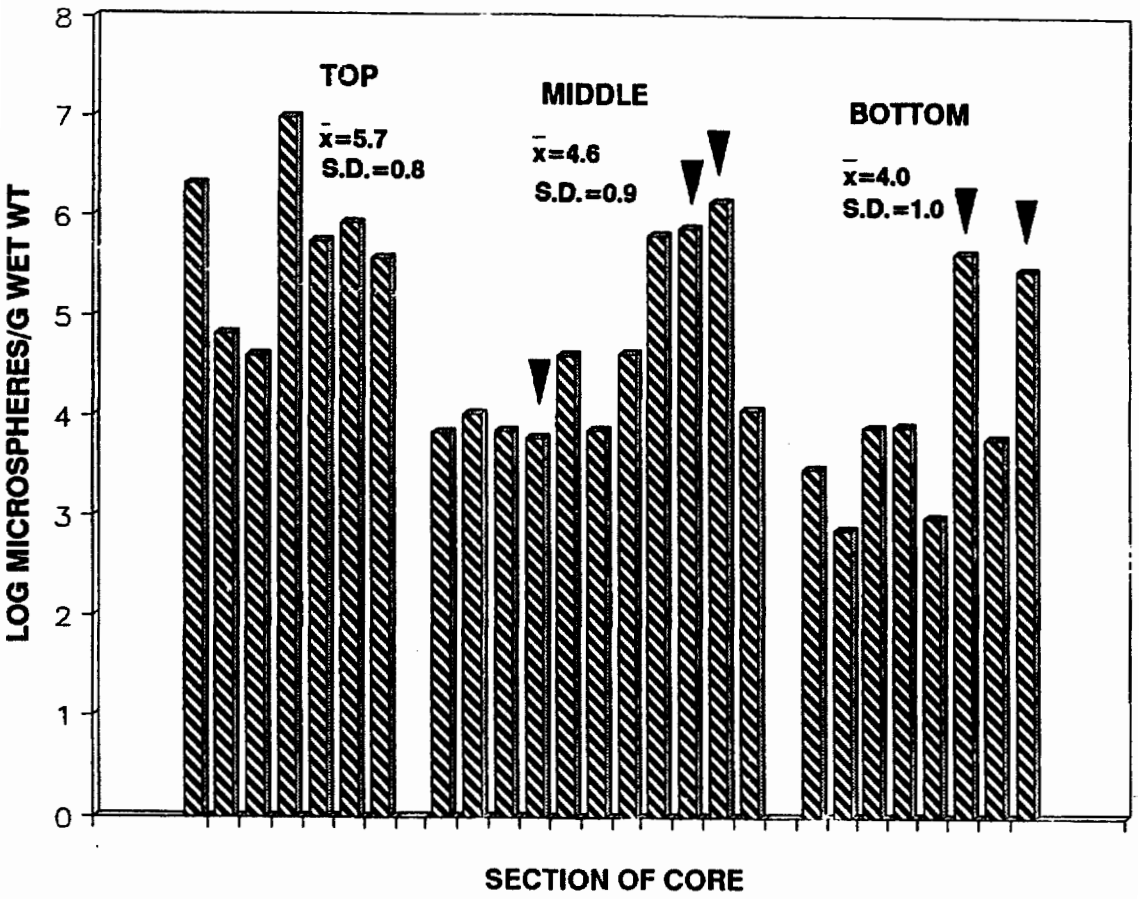

Fig. 5. Composite data for microsphere distribution within cores. Samples are grouped as to whether they were derived from the top, middle or bottom third of a given core. Bars noted with arrows represent samples obtained from cores that were less than 1.37 m in total length.

microspheres limits direct introduction into the drilling fluid.

Using microsphere distribution data and some assumptions, an estimate of potential contamination due to inadvertent introduction of microbes in the Ar gas stream may be obtained. Assuming 1 viable microbe·m^{-3} of Ar, a mean Ar flow rate during coring of 25 m^3 Ar·min^{-1}, 15 min of coring to obtain a core, and a dilution factor of 10^3 (as demonstrated by the microsphere data), an estimate of 0.375 viable microbes added per core is obtained. Most cores were 1.37 m long and 8.4 cm in diameter translating to a volume of 7560 cm^3. With densities of 2.7 g·cm^{-3} for basalt and 1.9 g·cm^{-3} for sediment, basalt and sediment cores had weights of 20.4 and 14.4 kg, respectively. Therefore the value for potential microbial contamination through introduction during use of Ar ranges from 0.018 microbes·kg^{-1} of basalt to 0.026 microbes·kg^{-1} of sediment. These values are within the confines of what most microbiologists would consider acceptable levels of possible contamination.

Lack of consistent trends in the concentrations of microspheres between consolidated and unconsolidated cores may be determined by factors that are unique to each core. The consolidation of the core (basalt vs. sediment) likely played a role in how evenly the spheres were distributed. In consolidated cores fewer spheres penetrated

from the outside to the center. Additionally, it is likely that spheres moved preferentially through fractured zones. Studies of microbial and microsphere transport in aquifers indicate that carboxylated latex microspheres imperfectly simulate the transport of bacteria in an aquifer [8]. To date, microspheres represent the most convenient, non-biological tracer applicable to trace the movement of bacterial-sized particles in subsurface materials.

Representative data for Br^- and tracer water in the samples is shown in Table 2. The average value for Br^- measured in 1:1 water extracts of samples was 5.05 μg $Br^- \cdot g^{-1}$ sample. The highest concentration of Br^- measured was 15.00 μg $Br^- \cdot g^{-1}$ sample. In all cases, concentrations of Br^- measured in the samples represented at least a 10^4-fold reduction from the original concentration introduced to the core. Lithologic type did not determine Br^- concentration. Even distribution of the Br^- tracer through a 1.37 m core was calculated to yield 2.2 and 3.2 mg $Br^- \cdot g^{-1}$ of basalt and sediment, respectively. Thus, the highest Br^- concentration measured was approximately 500 times lower than if the Br^- had been evenly distributed throughout a 1.37 m core.

The mean value for water added to the samples as a result of addition of a liquid tracer was 0.1% of the water already present in the formation (Table 2). The values for water in the cores due to the tracer solution never exceeded 0.5% of that already present and it is not likely that this quantity contributed significantly to the growth or activity of indigenous microbes.

Data from the PFT analyses provided evidence that air used during corehole advancement impinged on samples in both the 117 – 121 and 171 – 172 m sampling zones. This was indicated by the presence of PFH on samples from these depths which were below the last intervals to be drilled with air that contained PFH (Table 3). Even though air was not used for drilling or coring within 4.6 m of the planned core zone, the PFT used during air drilling (PFH) occurred at least 6.7 m ahead of its introduc-

TABLE 2

BROMIDE CONCENTRATIONS AND PERCENT WATER DUE TO TRACER ADDITION IN REPRESENTATIVE SAMPLES FROM DIFFERENT LITHOLOGIES FROM THE INEL DEEP MICROBIOLOGY BOREHOLE

Core run	Depth (m)	Lithologic type	μg $Br^- \cdot g^{-1}$	% Water as tracer
2	70.07	basalt	8.16	0.42
	70.65	basalt	3.14	0.37
	70.81	basalt	1.60	0.08
	71.17	basalt	1.34	0.04
22	122.10	sediment	8.78	0.13
	122.16	sediment	14.74	0.2
38	138.01	vesic. basait	0.94	0.01
	138.07	sediment	2.27	0.01
	138.14	vesic. basalt	1.83	0.02
	138.50	vesic. basalt	1.70	0.01

LiBr (44 $g \cdot 100\ ml^{-1}$ sterile water) was introduced near the drill bit during coring then leached from subsamples with water and the Br^- concentration in the leachate determined using ion chromatography. Detection limits for Br^- were approximately 0.5 $mg \cdot l^{-1}$.

TABLE 3

SELECTED PERFLUOROCARBON TRACER RESULTS FROM THE INEL DEEP MICROBIOLOGY BOREHOLE

Depth (m)	PFT added (g)		PFT detected ($ng \cdot g^{-1}$)		Comments
	PFH	PFMCH	PFH	PFMCH	
28.75			<0.2	<0.2	Basalt; before PFTs used
			<0.2	<0.2	Non-lithologic control (methanol exposed to air)
68.58		36	<0.9	15	Core top; good fluid circulation
70.41		6.3	0	0	Mid-core; obtained 3 h after coring; good circulation
71.32		6.3	0	<0.6	Core bottom; good circulation
114.00	3.5				
117.53		19.1	1.4	3.6	2.5 h after coring; mid-core
120.27		23.2	12	36	119.40 to 120.27; core bottom
120.60		7	18	55	Core top; after 2.5 h in glove box; poor fluid circulation
121.10		7	182	394	Core bottom; same core as 120.60, but processed immediately; poor circulation
167.64[a]	4				
171.91[a]		31.1	14	5	Poor fluid circulation

Quantities of perfluorohexane (PFH) and perfluoromethylcyclohexane (PFMCH) added to air and Ar drilling fluids, respectively, and detected after extraction of samples in methanol. Limits of detection varied due to the absolute quantity available for extraction. See text for details of addition and detection of PFTs.
[a] Sample completed in new borehole ca. 15.24 m from original hole.

tion. While the unsaturated and saturated subsurface environments at the INEL are aerobic [5], the effect of additional input of air is uncertain.

Most samples also showed evidence of impingement of Ar used during coring as determined by the presence of PFMCH on the samples. Previous use of PFTs as tracers during drilling and coring operations established their usefulness for these applications and also indicated the ability of the tracers to move into sediment samples from liquid drilling fluid [11]. Senum and Dietz [11] also demonstrated that PFTs could be transported in the subsurface via aqueous drilling fluids or groundwater between adjacent coreholes located 60 m apart.

PFT data suggests that the zone of influence of air during drilling extends at least 7 m and is probably determined by the number and extent of fractures in the subsurface within any given interval. In one stratum (68.58 to 71.32 m) where good circulation was noted (i.e., high return of drilling fluids from the subsurface to the surface exhaust), PFMCH measured in the samples was low (Table 3). Conversely, in strata where poor circulation was observed (120.27 to 120.60 m and 171.91 m), samples showed measurable concentrations of PFTs. This suggests that when good circulation exists, tracers circulate through the system and are less likely to enter sample strata. When a subsurface stratum yields poor circulation indicating numerous subsurface fractures and void zones, tracers are more readily forced into the sampling environment than directly to the surface in the exhaust flow. Elevated temperatures that may

occur at the bit – stratum interface would tend to maintain the PFTs in a vapor phase and cause further dispersal in the subsurface.

PFTs provide good qualitative evidence of drilling fluid movement and distribution in the subsurface. Quantitative evaluation of PFT concentrations is difficult in such studies when delays in sample retrieval lead to loss of PFT. It is also important to note that PFTs were measured at $ng \cdot g^{-1}$ sample concentrations, therefore significant reductions in PFT concentrations (and the carrier gas) can occur, yet PFTs can still be detected. Such reductions of PFH, and air as well, suggest that cored zones experienced introduced oxygen at concentrations well below levels that would be harmful to oxygen-sensitive microbes in an environment for which bulk measurements indicate an oxidizing atmosphere [5]. The presence of PFTs in most of the samples suggests drilling with forced air or Ar could have a drying effect on the samples. Unfortunately, the only alternative technology would utilize mud drilling fluids that can significantly increase microbial contamination of cores.

In summary, data from microsphere and Br^- analyses indicate that the cores were minimally impacted by chemical and particulate tracers used during sample collection. It may be concluded that, in samples provided to investigators, microspheres and Br^- introduced during the coring process were sufficiently dilute as to be insignificant. These quality control tracers were added at high concentrations and the significant reduction in concentration of these components provides assurance that any inadvertent microbial or chemical contaminants would have been reduced to insignificant values by dilution and as a result of sample selection and paring. The use of quality control tracers is essential in drilling operations seeking to acquire materials of high microbial and chemical integrity.

Extremely low concentrations of microbial phospholipid fatty acids in most of the samples (White/Ringelberg, personal communication) suggest that the reported handling and processing procedures successfully minimized potential microbial contaminants. It is unlikely that changes in the sample due to collection methods would cause such low numbers. For now, this validates the use of techniques employed in this study for providing uncompromised samples from an environment consisting primarily of consolidated basalt.

Sampling at the INEL was different than previous subsurface microbial sampling because the environment is primarily basalt and the aquifer exists 140 m below land surface. Newly introduced sample-related strategies included: (1) drilling with filtered air as a drilling medium (instead of muds), (2) coring with Ar (instead of air) for sample collection, (3) placement of the core into an Ar atmosphere within minutes of retrieval from the subsurface, (4) implementation of hard rock processing tools (core splitters and Platner mills), and (5) use of a customized, multi-component tracer system to assess sample integrity. While a filter capable of removing particles >17 μm worked well in this application, under some conditions a HEPA filter could be used as an added precaution.

The distinct subsurface conditions at different sites (e.g., unconsolidated sediments versus basalts) dictates the adoption of different methods of sample acquisition and quality control at each site. Ar was successfully used in this study as a lubricant, temperature controller, and cutting removal system while reducing exposure of subsurface formations to oxidizing conditions. While unique advantages are associated

with the use of gaseous drilling fluids versus liquid drilling fluids, use of a cable drilling tool to collect sedimentary material avoids the use of drilling fluid altogether. However, cable tools can be used only where samples are of unconsolidated material from relatively shallow depth (<200 m). The collective experience gained by investigators participating in sample acquisition at all sites represents significant advances in the repertoire of strategies available to future sample procurement endeavors.

Acknowledgements

This work was conducted through the Department of Energy contract to EG&G Idaho Inc. (DE-AC07-76IDO1570) and sponsored by the Subsurface Science Program, Ecological Research Division, Office of Health and Environmental Research, Department of Energy. Minimal support was provided by the Department of Energy, Office of Technology Development. Individuals that made this work possible include driller M. James of PC Exploration, L. J. Johnson, J. Lord, D. Blumhorst, C. Bishop, E. Johnson, and F. Roberto of EG&G Idaho Inc., P. Dirkmaat and I. Aoki of DOE-Idaho, T. Griffin of Golder Associates, Inc., T. Kieft of New Mexico Tech, J. Fredrickson of Pacific Northwest Laboratory and F. J. Wobber, Program Manager to the Subsurface Science Program.

References

1 Balkwill, D. L. (1989) Numbers, diversity and morphological characteristics of aerobic, chemoheterotrophic bacteria in deep subsurface sediments from a site in South Carolina. Geomicrobiol. J. 7, 33 – 52.
2 Balkwill, D. L., Fredrickson, J. K. and Thomas, J. M. (1989) Vertical and horizontal variations in the physiological diversity of the aerobic chemoheterotrophic bacterial microflora in deep southeast coastal plain subsurface sediments. Appl. Environ. Microbiol. 55, 1058 – 1065.
3 Benoit, R. E., Phelps, T. J. (1990) Microaerophilic bacteria from subsurface sediments. In: Proceedings of the First International Symposium on Microbiology of the Deep Subsurface (Fliermans, C. B. and Hazen, T. C., eds), pp 4-87 to 4-96. WSRC Information Services, Aiken, SC.
4 Chapelle, F. H. and Lovley, D. R. (1990) Rates of microbial metabolism in deep coastal plain aquifers. Appl. Environ. Microbiol. 56, 1865 – 1874.
5 Colwell, F. S. (1989) Microbiological comparison of a surface soil and unsaturated subsurface soil from a semiarid high desert. Appl. Environ. Microbiol. 55, 2420 – 2423.
6 Fredrickson, J. K., Garland, T. R., Hicks, R. J., Thomas, J. M., Li, S. W. and McFadden, K. M. (1989) Lithotrophic and heterotrophic bacteria in deep subsurface sediments and their relation to sediment properties. Geomicrobiol. J. 7, 53 – 66.
7 Garland, T., Murphy, E. and McFadden, K. (1990) Evaluation of core segment pore water contamination from tracers, well water sampling, and sediment extractions. In: Proceedings of the First International Symposium on Microbiology of the Deep Subsurface (Fliermans, C. B. and Hazen, T. C., eds), pp. 5-15 to 5-17. WSRC Information Services, Aiken, SC.
8 Harvey, R. W., George, L. H., Smith, R. L. and LeBlanc, D. R. (1989) Transport of microspheres and indigenous bacteria through a sandy aquifer: results of natural- and forced-gradient tracer experiments. Environ. Sci. Technol. 23, 51 – 56.
9 Jones, R. E., Beeman, R. E. and Suflita, J. M. (1989) Anaerobic metabolic processes in the deep terrestrial subsurface. Geomicrobiol. 7, 117 – 130.
10 Phelps, T. J., Fliermans, C. B., Garland, T. R., Pfiffner, S. M., White, D. C. (1989) Recovery of deep subsurface sediments for microbiological studies. J. Microbiol. Meth. 9, 267 – 280.

11 Senum, G.I. and Dietz, R.N. (1990) Perfluorocarbon tracer tagging of drilling muds for the asessment of sample contamination. In: Proceedings of the First International Symposium on Microbiology of the Deep Subsurface (Fliermans, C.B. and Hazen, T.C., eds), pp 7-145 to 7-158. WSRC Information Services, Aiken, SC.
12 Sinclair, J.L., Ghiorse, W.C. (1989) Distribution of aerobic bacteria, protozoa, algae, and fungi in deep subsurface sediments. Geomicrobiol. J. 7, 15 – 31.
13 Suflita, J.M., Jones, R.E., Liu, S. and Beeman, R.E. (1990) The distribution of strict and facultative anaerobic microorganisms in the terrestrial subsurface. In: Proceedings of the First International Symposium on Microbiology of the Deep Subsurface (Fliermans, C.B. and Hazen, T.C., Eds), pp 3-29 to 3-38. WSRC Information Services, Aiken, SC.
14 United States Environmental Protection Agency (1989) Handbook of suggested practices for the design and installation of groundwater monitoring wells. EPA 600/4-89/034. National Water Well Association, Dublin, OH.
15 Wilson, J.T., McNabb, J.F., Balkwill, D.L., Ghiorse, W.C. (1983) Enumeration and characterization of bacteria indigenous to a shallow aquifer. Ground Water 21, 134 – 142.

Abstract

Timo Ruskeeniemi, Lasse Ahonen, Markku Paananen, Shaun Frape, Randy Stotler, Monique Hobbs, Juha Kaija, Paul Degnan, Runar Blomqvist, Mark Jensen, Kimmo Lehto, Lena Moren, Ignasi Puigdomenech and Margit Snellman 2004. **Permafrost at Lupin: Report of Phase II**. Geological Survey of Finland, Nuclear Waste Disposal Research. Report YST-119, 89 pages, 49 figures, 1 appendix (delivered separately). ISBN 951-690-890-X, ISSN 0783-3555.

The aim of the project is to study the conditions and processes occurring in permanently frozen crystalline bedrock, with special reference to deep (*i.e.*, several hundreds of meters) bedrock conditions. The target of the study is the Lupin mine in Nunavut Territory, Northern Canada. The results may be utilized in assessing the long-term performance of deep underground constructions (*e.g.*, nuclear waste repositories) in cooling climatic conditions.

In Phase I of the project versatile background information was collected from the site *e.g.,* on climate, geology and on hydrogeological and hydrogeochemical conditions. During Phase II a broad range of research was conducted including i) electromagnetic soundings to investigate the distribution of permafrost in the surroundings of the mine; ii) drilling of three research boreholes at the base of the permafrost for groundwater research; iii) application of borehole video surveys to study the distribution of open fracturing and iv) sealing of several boreholes to regain the natural hydraulic conditions in the bedrock. Subsequently, gas and water were sampled, pH, redox and dissolved oxygen were measured and monitoring of hydraulic heads is on-going. Some preliminary cross hole hydraulic tests were also conducted.

In addition to the field research, crush and leach tests of drill core samples to investigate the salinity in the rock matrix, and freezing experiments using selected Canadian and Fennoscandian groundwaters were carried out at the University of Waterloo, Canada.

This report describes the methods used in the research, presents the results and discusses the results to date. Some of the subtasks are reported separately and only reviews are presented here. Finally, an attempt is made to conceptualise some of the effects of deep permafrost on the groundwater conditions in crystalline bedrock at Lupin using the knowledge gained from the Permafrost Project and from the literature.

Keywords: permafrost, crystalline bedrock, groundwater composition, gas composition, fracturing in bedrock

Tiivistelmä

Timo Ruskeeniemi, Lasse Ahonen, Markku Paananen, Shaun Frape, Randy Stottler, Monique Hobbs, Juha Kaija, Paul Degnan, Runar Blomqvist, Mark Jensen, Kimmo Lehto, Lena Moren, Ignasi Puigdomenech and Margit Snellman 2004. **Lupinin ikirouta: Raportti II tutkimusvaiheesta**. Geologian tutkimuskeskus, Ydinjätteiden sijoitustutkimukset. Tiedonanto YST-119, 89 sivua, 49 kuvaa, 1 liite (rajoitettu jakelu). ISBN 951-690-890-X, ISSN 0783-3555.

Hankkeen tarkoituksena on tutkia pysyvästi jäätyneenä olevan kallioperän olosuhteita ja siinä tapahtuvia prosesseja, erityisesti syvän kallioperän olosuhteissa (s.o. useiden satojen metrien syvyydessä). Tutkimuksen kohteena on Lupinin kaivos Nunavutin Territoriossa Pohjois-Kanadassa. Tuloksia voitaneen hyödyntää arvioitaessa syvien maanalaisten tilojen pitkäaikaiskäyttäytymistä (esim. ydinjätteen loppusijoitustilat) kylmenevissä ilmasto-oloissa.

Hankkeen I vaiheessa keskityttiin keräämään perustietoa mm. tutkimuskohteen ilmastosta, kvartäärigeologiasta, geologiasta sekä hydrogeologisista ja hydrogeokemiallisista olosuhteista. Hankkeen II vaiheessa jatkettiin tutkimuksia varsin laajalla rintamalla. Elektromagneettisten SAMPO luotausten avulla selvitettiin ikiroudan esiintymistä kaivoksen ympäristössä. Pohjavesiolosuhteiden tutkimusta varten kairattiin kolme uutta tutkimusreikää välittömästi ikiroudan alapuolelle. Kairanreikien avorakoilua tutkittiin reikävideolaitteistolla. Useita kairanreikiä suljettiin läpivienneillä varustetuilla tulpilla ja niissä tehtiin kaasu- ja vesinäytteenottoja, fysikaalis-kemiallisia mittauksia ja mitattiin hydraulisia korkeuksia. Myös joitakin alustavia hydraulisia reikä-reikä testauksia suoritettiin.

Varsinaisten kenttätutkimusten lisäksi Waterloon yliopistossa (Kanada) tehtiin kairausnäytteillä crush and leach -tutkimuksia, joiden tarkoituksena on selvittää kivien huokosissa olevan suolan määrää ja alkuperää. Lisäksi tehtiin jäädytyskokeita Kanadasta ja Fennoskandiasta otetuilla pohjavesinäytteillä.

Tässä raportissa kuvataan käytetyt tutkimusmenetelmät ja saadut tutkimustulokset sekä pyritään vetämään yhteen tähän asti saatua aineistoa. Eräät osatehtävät on raportoitu erillisinä raportteina ja niistä esitetään keskeisimmät tulokset.

Lopuksi pyritään konseptualisoimaan ikiroutaolosuhteiden vaikutuksia kiteisen kallioperän hydrogeologisiin olosuhteisiin Lupinista saadun tutkimusaineiston ja kirjallisuuden perusteella.

Avainsanat: ikirouta, kiteinen kallioperä, pohjaveden koostumus, kaasun koostumus, rakoilu kallioperässä

Preface

This PERMAFROST project is a co-operative international undertaking jointly funded by participants from Finland (Geological Survey of Finland and Posiva Oy), Sweden (Svensk Kärnbränslehantering, SKB), Great Britain (UK Nirex Ltd) and Canada (Ontario Power Generation and University of Waterloo).

This Phase II Report is the third in the series "Permafrost at Lupin". The continuously up-dated Geochemical Database has the status of an internal document until completion of the research at Lupin, after which time the partners will jointly make a decision regarding the release of the data. References to articles utilizing the Lupin data, or otherwise related to the ongoing project, are given below.

In parallel to this report is published a companion report has been published by S.K. Frape, R.L. Stotler, T. Ruskeeniemi, L. Ahonen, M. Paananen and M.Y.Hobbs 2004. Hydrogeochemistry of groundwaters at and below the base of the permafrost at Lupin: Report of Phase II. Ontario Power Generation, Supporting Technical Report No. 06819-REP-01300-10047-R00, April 2004.

The Lupin mine was operated by Echo Bay Mines Ltd. until the year 2004, after which Kinross Ltd. took over. Both these companies have not only provided access to their property, but have also been extremely collaborative and have shown great hospitality towards the Permafrost project. Numerous persons have contributed to our work at the practical level and we wish to thank all our friends at Lupin for their invaluable assistance.

Paananen, M. and Ruskeeniemi, T. 2003. Permafrost at Lupin: Interpretation of SAMPO electromagnetic soundings at Lupin. Geological Survey of Finland, Report YST-117, 22 p. + 4 app.

Ruskeeniemi, T., Paananen, M., Ahonen, L., Kaija, J., Kuivamäki, A., Frape, S., Moren, L. and Degnan P. 2002. Permafrost at Lupin: Report of Phase 1. Geological Survey of Finland, YST-112. 59 p. + 3 app.

Ruskeeniemi, T., Ahonen, L., Paananen, M., Blomqvist, R., Degnan, P., Frape, S. K., Jensen, M., Lehto, K., Wikström, L., Morén, L., Puigdomenech, I. and Snellman, M. 2003. Groundwater under deep permafrost conditions. In: Haeberli, W. & Brandová, D. (eds.) 8th International Conference on Permafrost, Zurich, Switzerland, 20-25 July 2003: extended abstracts reporting current research and new information. Zurich: University of Zurich, 141-142.

Stotler, R.L., Frape, S.K., Ruskeeniemi, T., Ahonen, L., Blomqvist, R., Degnan, P., Jensen, M., Lehto, K., Morén, L. and Snellman, M. 2003. Hydrogeochemistry of crystalline bedrock under deep permafrost conditions. In: Geoscience horizons, Seattle 2003: GSA Annual Meeting and Exposition, November 2-5, 2003. Geological Society of America. Abstracts with Programs 35 (6), 573.

Zhang, M. and Frape, S.K. 2003. Evolution of shield brine groundwater composition during freezing. Ontario power Generation, Report No: 06819-REP-01200-10089-R00, 49 p.

Contents

APPENDIX 1, Table of Chemistry (Delivered separately)

1 Introduction

According to the geologic disposal concept in Finland and Sweden, spent nuclear fuel will be sealed in corrosion-resistant and watertight canisters, and then emplaced either in holes drilled at the bottom of tunnels excavated into the crystalline bedrock or in long horizontal holes (deposition drifts). In Finland and Sweden, the depth of high level nuclear waste repository is to be approximately 500 m below ground surface. When the canisters have been emplaced, all the tunnels are to be filled, *e.g.*, with a mixture of bentonite and crushed rock, and the shafts leading to the repository will be closed. In Canada and UK, disposal concepts are still being debated. Nevertheless, it is possible that the deep geological disposal in a crystalline host rock may be chosen as the preferred disposal route.

In assessing the safety of the geologic disposal concept, it is essential to assess what physical and chemical conditions could evolve within the repository and surrounding environment. The objective of performance and safety assessments is to demonstrate the long-term safety of a repository for long-lived radioactive waste and most management agencies consider scenarios up to 1 million years (My) into the future.

During at least the past 2 My, repeated cycles of glaciation have occurred in the Northern Hemisphere. At present, a major part of the area to the north of latitude 60°N is under permafrost conditions, although within Fennoscandia at the same latitudes, temperate conditions prevail. Climate models based on astronomical forcing predict a cold period after approximately 60 000 years (Berger *et al*. 1993). Cold, dry periods favour the formation of periglacial conditions and the development of deep permafrost is expected to reoccur in northern and central Europe and North America.

In order to evaluate the long-term performance of a geologic repository, the influence of periglacial and glacial conditions must be considered. A key goal of this research project is to enhance the scientific basis for safety and performance assessment and to derive constrained permafrost scenarios relevant to the evolution of crystalline groundwater flow systems.

Based on an earlier literature study and theoretical considerations (Ahonen 2001), a number of issues were identified as possible targets of study: 1) Freezing rate and depth extent of permafrost in crystalline bedrock; 2) Cold saline water segregations (cryopegs) and their role in transport processes, 3) Role of non-frozen areas (taliks) as pathways for groundwater flow, 4) Aggregation of solid methane hydrates (clathrates), and 5) Effects of freezing on bedrock stability.

All these aspects are related to the long-term stability of hydrogeological and hydrogeochemical conditions. Some of these phenomena are reviewed in length in the literature and much is known about their role in shallow systems or in sedimentary environments. However, much less has been published regarding cryogenic processes and hydrogeology in crystalline rock under deep permafrost conditions.

During the studies in Phase I (Ruskeeniemi *et al.* 2002) a moderate understanding was achieved on the general geological, structural, Quaternary geological and the permafrost features of the Lupin Mine area. Preliminary characterisation of the deep groundwaters and the dissolved gas phase was also carried out. However, very little was known about the natural groundwaters within or just below the permafrost or at median depths. All

samples collected from the upper part of the mine seem to be more or less contaminated by the mining activities.

It has been a common view that it is important to identify and characterise the permafrost water, an end-member water type, at Lupin (and potentially in Fennoscandia). Therefore, the temporal priority in Phase II was given to activities aiming to sample water, or activities giving support for a better understanding of the distribution of groundwater and permafrost. Some hydrogeological research (geophysics and hydraulic measurements) and complementary gas sampling were also carried out. In parallel to the work at Lupin, freezing experiments were conducted at the University of Waterloo on assignment from Ontario Power Generation.

First, this report presents the data obtained from Lupin during Phase II and describes the applied research methods (Section 2). Secondly, the information obtained during Phase I and II is summarized (Section 3), and the first conceptualisation of the site is provided in Section 4.

2 Phase II activities

2.1 Sampo soundings

The SAMPO wide-band electromagnetic method (Soininen and Jokinen 1991) has shown potential for locating salinity differences in studies of deep groundwaters. The method has also been successfully applied to determine the depth of saline water bodies below the Antarctic ice sheet (Ruotoistenmäki and Lehtimäki 1997, 1999).

The starting point of the geophysical interpretation is that the frozen rock matrix (permafrost) is highly resistive (>10000 ohmm), whereas fractures or fracture zones saturated by saline or brackish waters are much less resistive, but still act s poor electrical conductors. Their resistivity values are highly dependent on porosity and water salinity, having typical values of some hundreds of ohmmeters. Surface conductors, such as the highly moist active layer and the surrounding lakes and ponds also have their own effects on the measurements, usually decreasing the measured resistivity values. Furthermore, mine construction and mineral (sulphide) conductors (typical resistivity less than 1 ohmm) may occasionally dominate the results, masking possible indications of saline or brackish waters.

SAMPO is a frequency domain wide-band electromagnetic sounding system that provides information on electrical properties of the ground. The system consists of a transmitter loop and three perpendicular receiver loops (Fig. 1). The transmitter and receiver are connected by a radio link. The system operates at 81 fixed frequencies within a band width of 2 – 20000 Hz. The maximum investigation depth is about the same as the coil separation (*i.e.* the distance between transmitter and receiver loops). In the interpretation it is assumed that the sounding information is obtained from the midpoint between the transmitter and the receiver.

The primary measured parameters are three perpendicular components of the total electromagnetic field (vertical, horizontal radial and horizontal tangential components). To visualize the results, apparent resistivity versus depth (ARD) can be calculated from the relations of the vertical and radial components B_z/B_x for each frequency. The interpretation, based on the B_z/B_x ratios, is done by a layered model program. In undisturbed natural conditions, the one-dimensional layer model interpretation produces satisfactory results.

The Geological Survey of Finland performed field measurements using SAMPO in the Lupin area between the 11th and 23rd of June 2002 (Paananen and Ruskeeniemi 2003). The locations of the sounding lines are shown on Figure 2. Two different sounding geometries were applied, broadside (transmitter and receiver moving along parallel lines) and in-line (transmitter and receiver moving one after another along the same line). The field conditions, mainly the availability of space and the form of the sounding area, determined the geometry used. The coil separations were typically 675 – 800 m. In addition, in-line soundings with a 100 m or 200 m coil separation were carried out at 6 profiles. For long coil separations, the transmitter was a square coil with a side 50 m in length. For 100 m and 200 m coil separations, a circular loop with a diameter of 20 m was used as a transmitter.

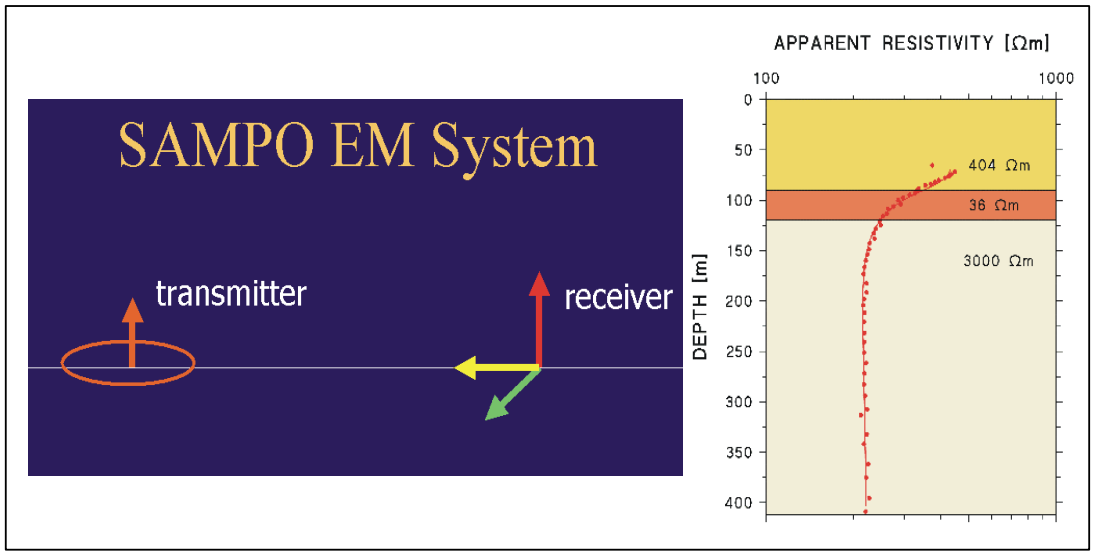

Figure 1. The principle of the SAMPO-method and an interpreted ARD curve.

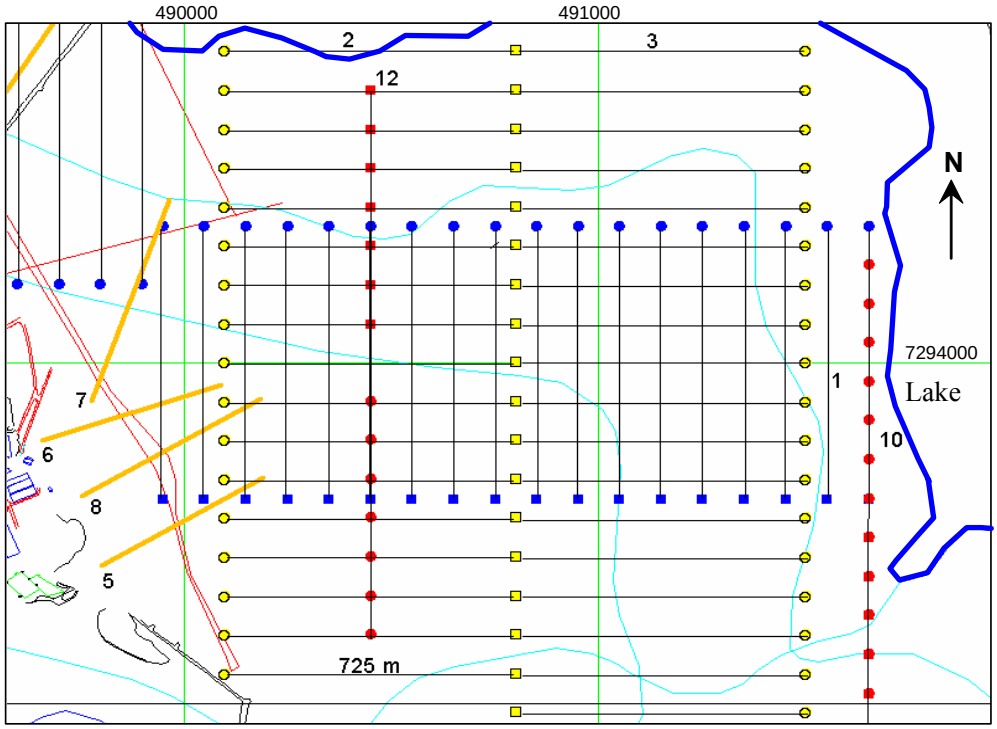

Figure 2. Locations of SAMPO soundings at Lupin between the mine (on the left) and Lake Contwoyto, survey lines 1 (blue, broadside), 2 and 3 (yellow, broadside), 5, 6, 7, and 8 (orange, in-line), and 10 and 12 (red, in-line). Square = transmitter, circle = receiver. The locations of transmitter and receiver are not marked for lines 5 – 8, crossing the assumed V1 structure (red, tabular form on the left) due to a small coil separation (100 m).

The main sounding lines were positioned to cover the area between the mine and Lake Contwoyto in the east and north (Lines 1-3, 5-9, 10 and 12, Fig. 2). This is the area where most of the geological and geophysical surface information is available. It is known that the local bedrock in this area is similar to that in the mine proper. Additionally, it was possible to make continuous lines from the mine. Lines 5-9 were conducted specifically to study a previously assumed fracture zone, termed V1, while the aim of the others was to locate the base of the permafrost. Different sounding configurations and line orientations were used to analyse possible effects of the sounding geometry.

In addition, other separate sounding lines were measured to provide information on specific situations: Two lines on the headland, 3 km east from the mine, were surveyed to investigate whether signs of permafrost could be detected below an area surrounded by the water basin. One 2.4 km long line, NW from the mine, represents an in-land area far from the lake. The line extends from an area of schist close to the contact of a major granodiorite formation. Other two lines about 4 km to the SW from the mine were in-land reference profiles to test the potential disturbances caused by the mine construction and activities. Finally, one line crosses the contact between the schists and an outcropping granodiorite approximately 5 km SW from the mine.

For every sounding point, an ARD-curve was calculated, and they were printed as profiles for every sounding line. Furthermore, colour sections of apparent resistivity were compiled for each line. The interpretation was done using the layer-model inversion program developed at the Geological Survey of Finland (Fig. 3). Normally a two-layer model was used, where the upper layer represents highly resistive permafrost and the lower layer corresponds to unfrozen bedrock, possibly saturated by saline or brackish waters enriched from the permafrost. In some cases, a three-layer model was applied, where the third layer includes mineral conductors or bedrock saturated by strongly saline groundwater.

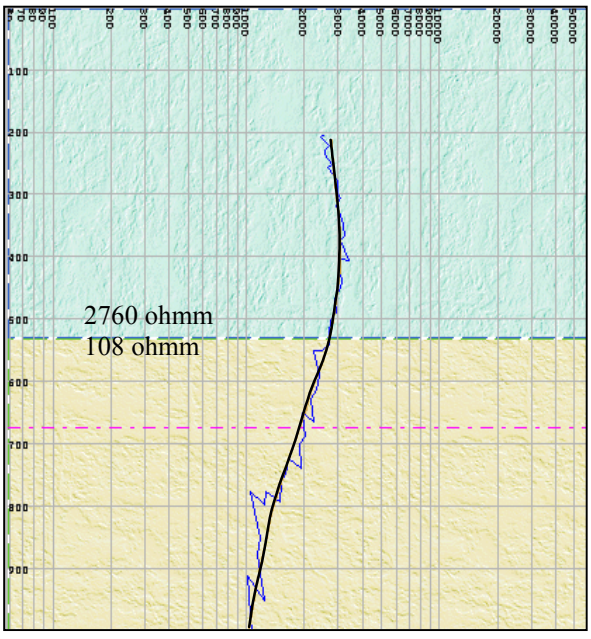

Figure 3. ARD-curve of sounding point 5 in survey line 1 and the layer model interpretation with two layers as an example. The serrated curve is the data and the smooth black curve depicts the curve-fit related to the model. The thin dashed line at c. 680 m presents the investigation depth of the method.

The error in the interpretation depends on several factors: accuracy of the measuring device, tilt correction of the data, suitability/unsuitability of the layer model and the interpretation procedure itself (number of layers, accuracy of the curve-fit etc.). Therefore it is not possible to give an unambiguous error estimate for the interpretation. However, within the selected model, the accuracy of the interpretation can be examined. The sensitivity analysis of sounding point 5 in survey line 1, for example, indicates that the error in the depth interpretation at this point is less than 50 m using a two-layer model.

Data obtained from the survey lines were interpolated to a 3D depth model of the conductor between the mine and the lake (Fig. 4). A general trend is that the conducting layer is at higher levels in the western part around the mine, apparently at a depth of about 500 ± 30 meters, deepening toward the north, east and southeast to about 630 ± 30, approaching the maximum investigation depth.

The numerous local highs in the conductor elevation may indicate saline inclusions within the permafrost whereas the lows probably indicate deepening of the permafrost or, at least, deepening of the saline groundwater table to greater depths. Near the mine, the effects due to anthropogenic constructions cannot be ruled out.

Paananen and Ruskeeniemi (2003) modelled the salinity of the low-resitivity layer. The model is based on the porosity and resistivity contribution of different components of the system. Using 0.5 % as fracture porosity, 30000 ohmm as dry rock matrix resistivity and 100 and 1000 ohmm as formation resistivity (typical interpreted values), typical in-situ electrical conductivity values of saline/brackish waters below the permafrost would be 200 – 2000 mS/m. Based on the electrical conductivity data obtained, salinity of the water below the resistivity contrast was further estimated (Fig 5).

The main results of the survey are:

- A weak, subhorizontal conductor was observed at numerous sounding points irrespectively of the measurement configuration.
- These sounding anomalies form a subhorizontal layer at the depths between 400 and 700 m, in contrast to the vertical orientation of the geological units in the area.
- The conductor gets weaker or deeper close to Lake Contwoyto and seems to be absent below the lake.
- There seems to be a lithological control: the conducting layer is not observed in granodiorite.
- It is assumed that the conducting layer represents saline or brackish waters at the base of the permafrost, the calculated TDS-values (total dissolved solids) are in a realistic range for such waters observed at Lupin.

The outcome of the possible implications are discussed more in Section 3.2.

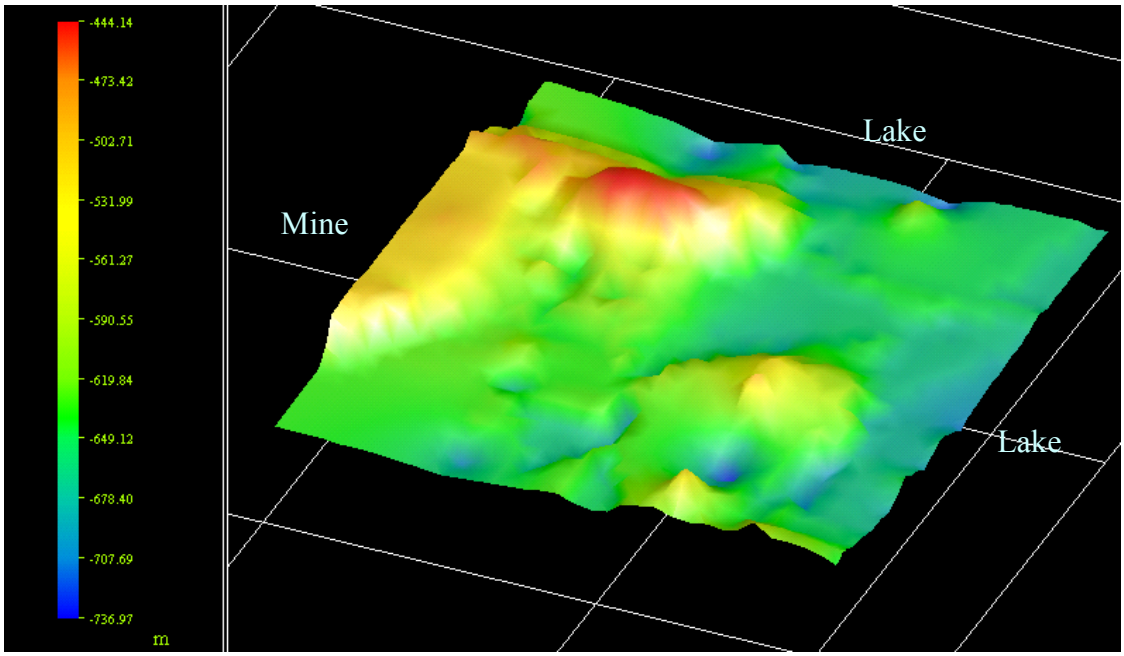

Figure 4. Interpolated depth of the conductor, 3D view from SE.

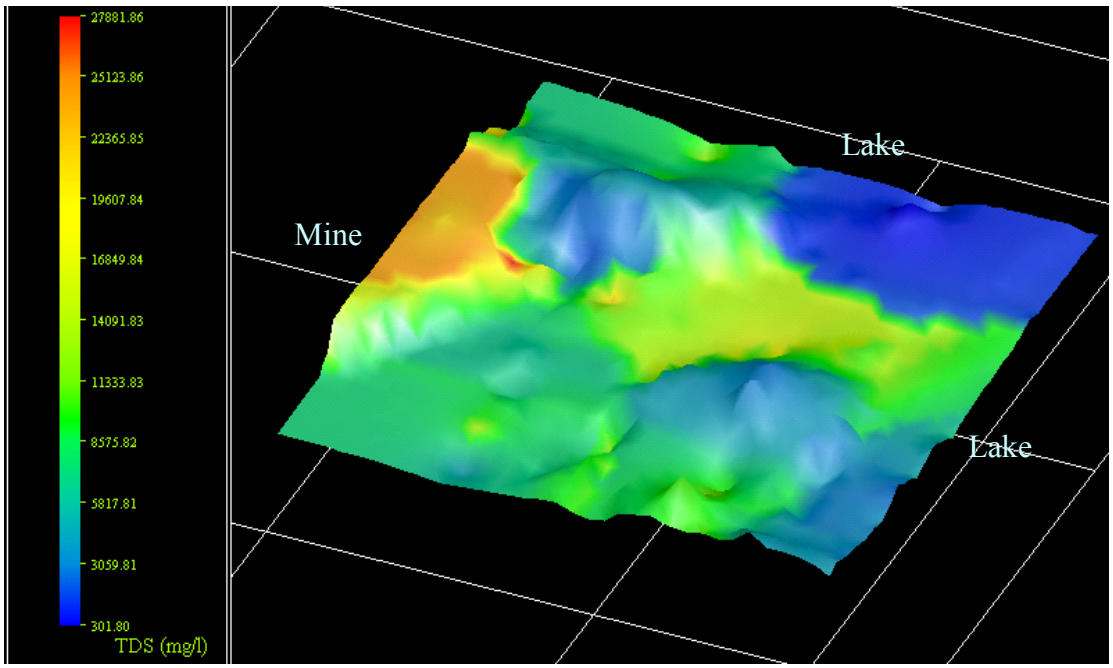

Figure 5. The depth of the conductor (elevations) and interpolated TDS values (colours), 3D view from SE.

2.2 Diamond drilling

2.2.1 General

The aim of the permafrost project was to drill research boreholes below the base of the permafrost (540 m below ground surface) to obtain groundwater samples, which are likely to show indications of the freezing out process. In addition, the boreholes were needed for research on the prevailing hydraulic conditions and gas accumulations below the permafrost.

It was known from the borehole video surveys (Phase 1) that the bedrock between hydraulic zones is relatively sparsely fractured and will most likely yield only small amounts of water. Therefore, it was suggested that drilling should attempt to intersect the interpreted vertical fracture zones in the east (V1), where the volume of water is expected to be larger and where the signs of the freezing processes, if any, should be detectable. At the same time the borehole would provide an opportunity to take samples from less fractured bedrock considered more representative of repository conditions. However, it must be emphasised that the amount of water expected from the sparsely fractured sections may be very small and difficult to sample.

The most favourable levels for the drilling campaign are those close to the base of the permafrost , *i.e.* levels at 490 m and 570 m. Both of these levels provide good drifts for drilling stations and access to what was regarded as the pristine bedrock area in the east. The latter level is already in unfrozen bedrock and the targeted structure, V1, can be reached with shorter boreholes from this level.

After discussions with the mining personnel and checking the potential sites for drilling stations the 570 m level was chosen for the following reasons:

- the ground conditions from a mine safety point of view are good and there is enough space for the planned activities
- rock temperature is above zero
- power lines and ventilation are available after some renovation
- there is a sump for the flushing water spills close to the station
- the ramp provides easy access to the area

During a subsequent trip to the mine, the field party attempted to drill a number of shorter (<30 m) holes at 550 m depth, slightly above the 570 m level. The station chosen was slightly below the permafrost, and due to time constraints, only one borehole (550-112) could be completed (section 2.2.7).

2.2.2 Technical description

Boreholes 570-105 and 570-106 are located at level 570 in the Central Zone about 50 m NE from the ramp (Fig 6.). Both holes are drilled into the E wall of the drift and their vertical distance apart is about one meter, borehole 570-105 being higher in the wall. The azimuth of both boreholes when the drilling commenced was adjusted to be close to 090 in the local coordinate system and the inclination for borehole 570-105 was set +2° (up-handed) and for 570-106, -25° (down handed), respectively. The wall of the drift was selected for the 0-point for the length measurements.

The drilling rig LM37 was used, applying a wire-line technique where the core barrel is retrieved with the aid of water pressure. The diameter of the boreholes is 60 mm (BQ) and the diameter of the recovered core sample is 40.7 mm. The drilling was carried out using a 3-m core barrel until about the 200 m hole length after which a 6-m barrel was applied. A 3-m steel casing was sealed with resin at the collar of both holes to facilitate the installation of a valve or any other instrumentation. The inner diameter of this casing is 60 mm. The drilling of borehole 570-105 was terminated at 515 m and borehole 570-106 was extended to 387 m. The coordinates and the technical characteristics of the boreholes are given in Table 1.

After completing the drilling, borehole 570-105 was cleaned using spiked flushing water. About 2.5 m^3 of water was pumped through the slowly rotating drilling rods to the end of the hole. At first the outflow was muddy, but it soon cleared up. No special cleaning measures were applied to borehole 570-106. The borehole video survey showed that the walls of the holes are clean down to 280 m. Only a narrow muddy streak was observed on the floor of the hole. It is likely that the flat lower end is not as well flushed.

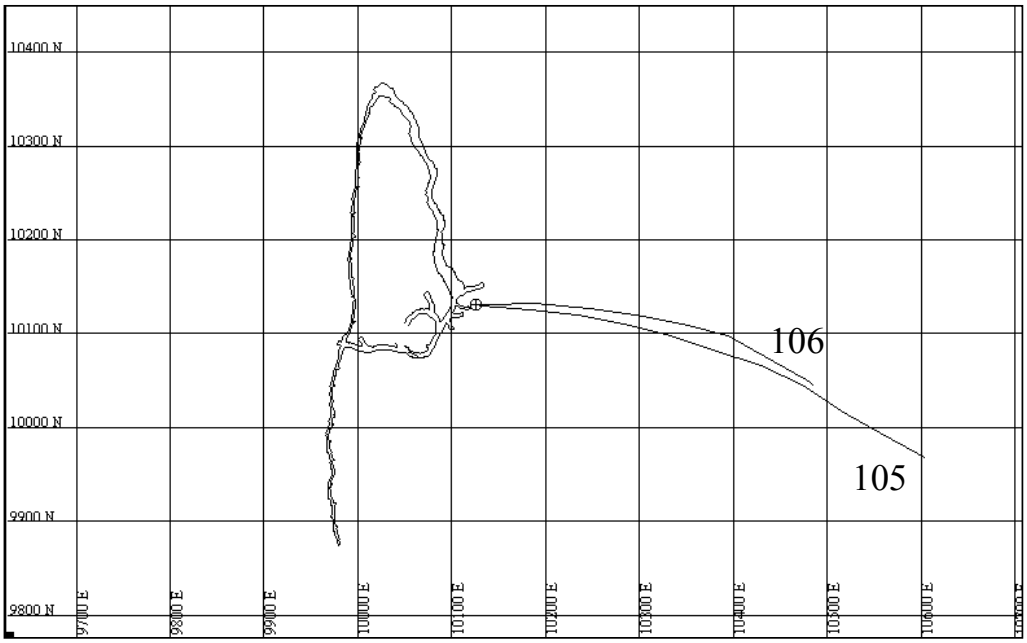

Figure 6. An aerial view of locations and the true traces of boreholes at the 570 m level.

Table 1. Coordinates for the collar and technical characteristics of the boreholes. The coordinates given are local. The zero-point for the elevation in the mine coordinates is level 2000 m.

	570-105	570-106
Northing	10130.88	10130.88
Easting	10125.86	10125.86
Elevation	1433.57	1432.57
Azimuth (º)	087	070
Inclination (º)	+2	-25
Length (m)	515	387
Diameter (mm)	60	60

An acid test method was used to follow the change in the inclination (dip) during drilling. Every 50 m, a glass ampoule filled with hydrofluoric acid was put in a specific holder at the rear end of the core barrel. The rods were pushed into the borehole again and were allowed to be at rest for half an hour. The inclination was obtained by measuring the angle between the horizontal line etched by acid and the axis of the ampoule. To determine the horizontal deviation a drill-operated survey tool (Reflex EMS) was also applied. The measuring interval was 50 m.

Both holes turned up and to the right, because even in a homogeneous rock boreholes often tend to turn towards the direction of rotation of the drilling rig (clock-wise). However, planar discontinuities, like foliation, fracture surfaces, and the change in the hardness of the rocks when the lithological contacts are passed, all have an effect on the trace of the hole. If these structures are cut perpendicularly, no bending is expected, but the lower the angle between the hole axis and the feature, the more it affects the borehole trajectory. In the case of boreholes 570-105 and 570-106 the vertical and the horizontal angel between the foliation and the core axis was 70 – 85 degrees.

The vertical bending of both holes was much more than expected. The dip for borehole 570-105, which was +2 degrees at the beginning, was +14.5 degrees at the end of the hole. A similar effect was observed in the other borehole as well. The drilling was started with a dip of -25 degrees in order to intersect the vertical V1 structure near a depth of 700 m at 500 m of hole length. Since the inclination was only -2 degrees at 380 m it became obvious that we could not reach the target depth and drilling was terminated.

However, the bending also had beneficial effects. The upward bending in 570-105 resulted in the intersection of the base of the permafrost at around 340 m of hole length (Fig. 7). According to the temperature measurements in the mine, it is assumed that the rock temperature at the end of the hole is -0.5ºC. Hence, the hole provides an opportunity to sample water and drill core both from frozen and unfrozen ground. Borehole 106 revealed the depth of the unsaturated zone at the time of the drilling. A couple months after the completion of the hole the lower part of the hole started to fill

with water. Because no significant inflow has been observed in the upper part of the hole, filling of the borehole is due either to a rise in the water table from depth or to lateral seepage in the lower part of the hole.

Attempts were also made to measure the rock temperatures in the hole. The method frequently used in sites where frozen ground is known to exist entails pushing a probe to the measuring point using compressed air. A pre-set timer allows the probe to adjust to the prevailing temperature prior to retrieval and observation of the readings. However, the results obtained clearly show that the 2.5 minutes time used for the equilibration was not enough under dry hole conditions.

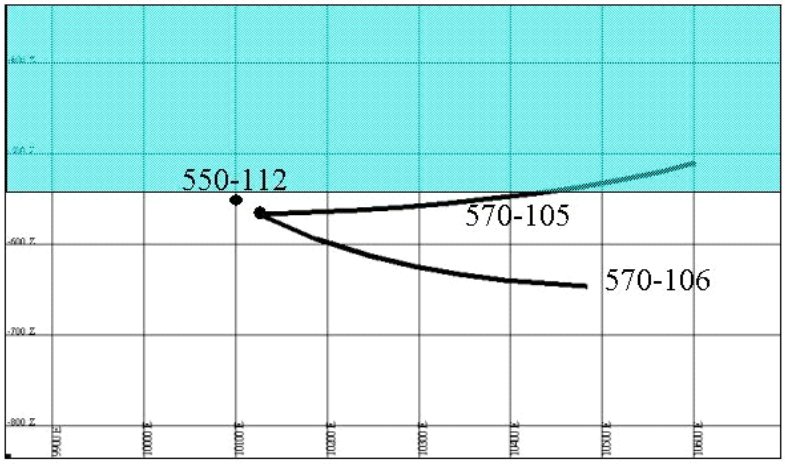

Figure 7. Cross-section (E-W) showing the true traces of the boreholes 570-105 and 570-106, and the location of borehole 550-112. The base of the permafrost at 540 m depth is also shown.

2.2.3 Borehole activities

Flushing water

Water has two main functions in a drilling operation: cooling of the drilling bit, and flushing of rock debris from the hole. Both of these effects are necessary when drilling in hard rocks. The estimated flow of flushing water was 45 L/min during active drilling.

The water ordinarily available close to the 570 m level is re-circulated brine used for mining operations. To avoid contaminating the borehole, it was necessary to make arrangements to bring down sufficient amounts of fresh water from the surface. All the fresh water for the mine camp and the mill is taken from Lake Contwoyto. The lake water is fresh, dilute and contains only insignificant amount of organics. No significant changes in the chemistry are expected despite the large amount of pumping. The 2” fresh water pipes taking water underground did not have the capacity to cover the water demand during drilling. Therefore, the only possibility was to transport the water from surface down to the drilling level. A steel tank on a forklift, a scoop or a trailer was used to bring down the water tank. It was estimated that one trip along the spiral ramp would take 2 – 4 hours. This was clearly too slow to satisfy the water demand and, therefore, it was necessary to re-cycle the flushing water. This was arranged by installing a tee to the

casing at the collar of the hole and leading the return water into a two-tank system (Fig. 8). Two 5 m^3 plastic tanks were purchased for this purpose. The return water drained into the first tank where the drilling debris was allowed to settle. The overflow was lead to the second tank, from which the water was pumped back to the drill. Despite the use of this collection system continuous replenishment of flushing water was necessary. One person was engaged for most of the shift on this task.

Figure 8. Arrangement to collect return water from the hole. The water is transported through the blue hose to a settling tank, from which the overflow is directed to a second tank. At the end of the shift, the hole was allowed to drain to recover most of the return water and the hose was then disconnected. After about three hours the next shift observed the outflow.

The total amount of water consumed during the drilling was 89 m^3 for borehole 570-105 and 69 m^3 for borehole 570-106, but due to substantial loss of return water during core retrieval, it was not possible to obtain meaningful numbers for the amount of water possibly intruded into the bedrock. The average water consumption was about 170±5 L/drilled meter.

Figure 9 shows the water consumption as a function of the propagation of drilling. As a rule, water consumption increases with advancing drilling. A special feature observed in the drilling of 570-106 was the relatively sharp deflection in the water consumption curve at the borehole length of about 270 m, where the average water consumption doubled. A similar, but less clear, deflection point may also be observed in 570-105 at a borehole length of about 460 m. The anomaly in borehole 570-106 can be related to a hydraulic zone.

The flushing water was labelled with uranine (sodium fluorescein). The target concentration was 500 µg/L. At replenishment, a pre-measured amount of dye solution was added and mixed into the tank. Samples were taken to control the uranine concentration, which turned out to vary within an acceptable range (Table 2). The observed variation was obviously due to the imperfect mixing of uranine prior to the sampling. The average uranine concentration in the flushing water during the drilling of

borehole 570-105 was 514 µg/L. This value was used to estimate the amount of flushing water in the hydrogeochemical samples, and to correct their chemistries. Because the spiking procedure was successful, it was used with small practical improvements during the drilling of borehole 570-106 as well. It was considered unnecessary to collect control samples for uranine analyses.

Table 2. Flushing water samples and their characteristics from the drilling of borehole 570-105. Samples were taken from the drilling water tanks after replenishment and mixing of the uranine solution. The fresh water sample FW0 is from a tap at the mill. The tap water is pumped from Lake Contwoyto. In the table nm. means 'not measured'.

Code	Hole length (m)	Uranine ug/L	EC mS/m	Note
FW0			2	Fresh water
FW1	17	nm.	15	Flushing water
FW2	104	505	5	"
FW3	161	380	12	"
FW4	215	495	15	"
FW5	311	655	14	"
FW6	368	480	62	"
FW7	440	560	20	"
FW8	472	530	11	"
FW9	505	510	11	"
FW10	512	510	8	"
FW11	515	nm.	5	Cleaning water

Chemistry of the flushing water

The Lake Contwoyto water used for the drilling has been sampled three times: in October 2000 (Lu/GTK/17) from the pumping station, in June 2002 from the harbour (Lu/GTK/S17), and finally, the fresh flushing water sample (FW0) was taken from the tap at the mill in November 2002. There was no obvious change in the chemistry between the samples. The water is very dilute, TDS 0.01 g/L. Na, Ca and Mg are the dominant cations, while SO_4, HCO_3 and Cl are the major anions. The stable isotopes show a narrow range ($\delta^{18}O$[1]: -19.1 – -20 ‰ and $\delta^{2}H$: -157 – -160 ‰), but the two available tritium measurements range from 15.8 TU to 20 TU (tritium units). The lower value was measured from FW0 and is considered more representative as it more closely resembles other values from the area. The pH values measured in the laboratory vary from pH 5.6 to pH 6.1, but as was determined from the in situ measurements from some boreholes, the laboratory values may be too low.

[1] $\delta^{18}O$ indicates the deviation of the abundance ratio of the isotope ($^{18}O/^{16}O$) of that of the reference VSMOW (Standard mean ocean water of the Vienna convention), while $\delta^{2}H$ is defined analogously to the isotope ratio $^{2}H/^{1}H$. The Ratio is normally given in per mil (‰). The same notation is used later in the text for isotopes ^{13}C and ^{37}Cl, having references Pee Dee Belemnite (PDB) and Standard mean ocean chloride (SMOC), respectively.

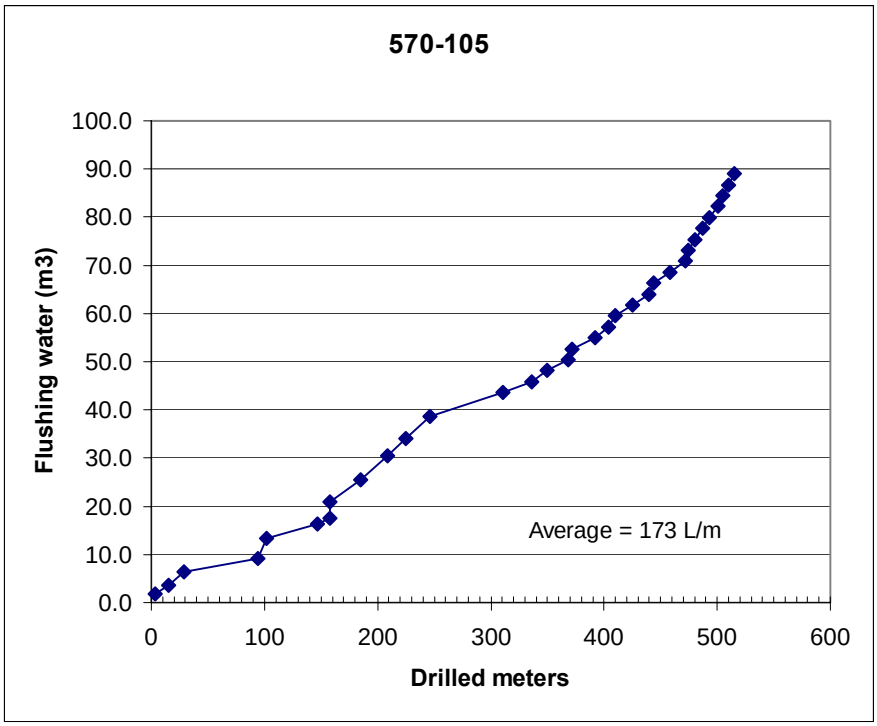

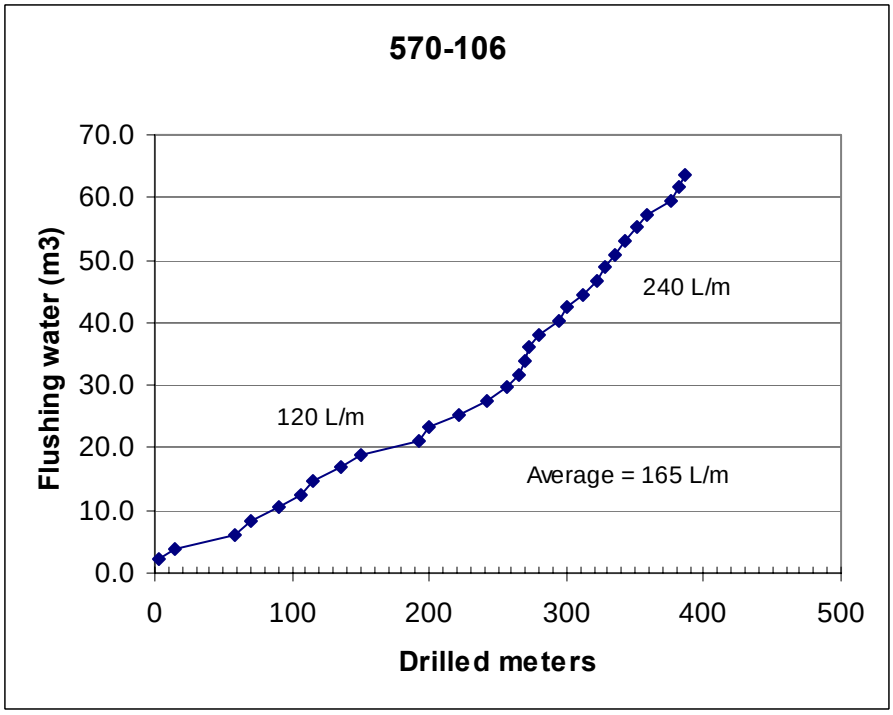

Figure 9. The consumption of flushing water vs. hole length in boreholes 570-105 and 106 based on the recorded water replenishments.

Monitoring of the return water during drilling

Return water monitoring was conducted to obtain preliminary information on the presence of any potential water conducting and water bearing sections, as the drilling penetrated the rock section. The reasoning behind this was that there might be a saline and/or pressurised waterfront at the base of the permafrost. It was assumed that saline flow into the hole would create an observable anomaly in the electrical conductivity and/or the rate of outflow. This information could then be used when planning the location of plugged sections for geochemical sampling.

The monitoring procedure with return water and flushing water samplings was fully applied in the drilling of borehole 570-105. A less structured approach was adopted for borehole 570-106, partly due to the different conditions in a down-dip inclined hole and partly due to the experience and information already available from the previous drilling.

Borehole 570-105

Both the amount and quality of the return water was monitored during drilling of borehole 570-105. The *outflow rate* was monitored at every shift change. The re-circulation hose was disconnected from the collar tee and the hole was drained for about three hours to remove excess flushing water. The amount of outflow and electrical conductivity of water (EC) was measured and samples (RW1–RW6) for chemistry and uranine determinations were collected. It was expected that the outflow rate would increase with the increasing length of the hole as more fractures were cut, but this was not the case. There was some variation, but the flow rate remained below 150 ml/h for the duration of drilling. The first observation of scarce, but continuous outflow after the draining period was recorded at 209 m. The samples taken prior to this depth were taken from the return water during drilling.

Electrical conductivity was measured on a regular basis. The EC for the fresh, clean water was below 10 mS/m. However, due to the re-circulation and continuous mixing with the muddy return water, the EC of the water pumped into the hole was generally around 20 mS/m and had a tendency to increase when the amount of the water in the tanks decreased. At replenishment, the EC again decreased depending on the amount of added water. This and some unfortunate quality problems with the transported water make it difficult to interpret the outcome, but certain conclusions can be drawn. Figure 10 presents the measured electrical conductivity values vs. borehole length.

The following anomalies can be observed in Figure 10:

1. At 212 m hole length the drilling rods were accidentally filled with contaminated water, but no actual drilling was done. The transported flushing water replenishment turned out to be brine. The reason for the problem was either technical breakage or misuse of the valves at the mill's water lines, which resulted in leakage and mixing of brine into the fresh water line. The contaminating brine was a NaCl solution used for drilling in frozen ground. The hole and both tanks were drained and washed with fresh water. The electrical conductivities of the return water recovered quickly and dropped down to normal level.

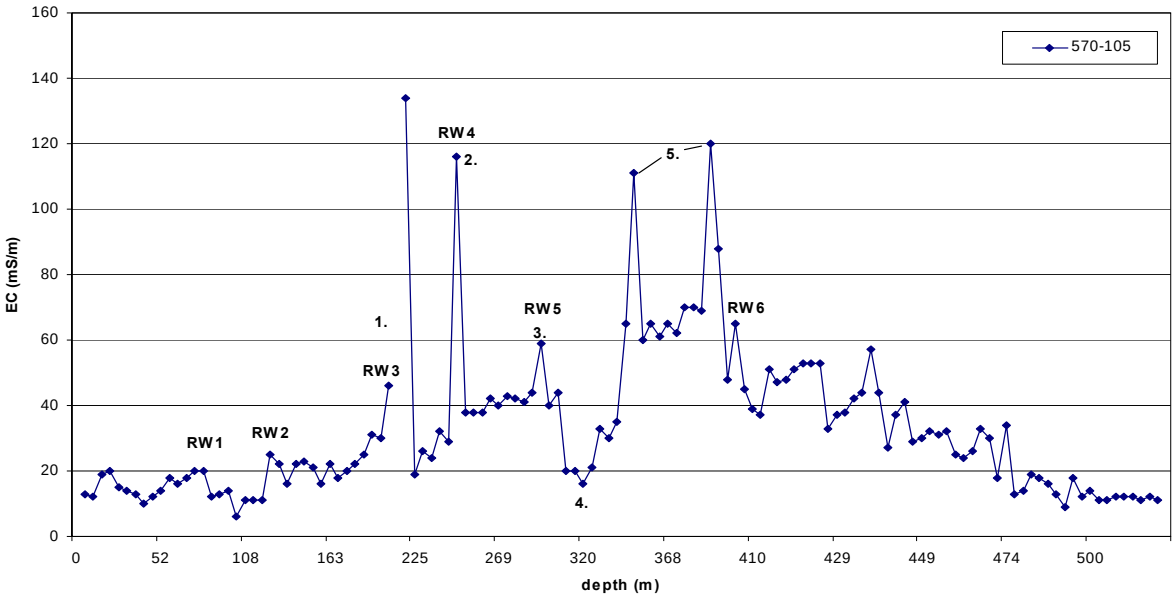

Figure 10. Electrical conductivity of the return water vs. depth during the drilling of borehole 570-105. The base of the permafrost was intersected at the hole length of 340 m. See text for the numbered incidents.

Before this episode, a steady increase of the EC values had been observed. The highest recorded value was 46 mS/m, which was two fold the EC measured from the flushing water used at this point. This may indicate water seepage into the hole from a more intensely fractured rock around 200 m. Return water sample RW3 represents this water. The out-flow rate was 40 ml/min. As mentioned above, this was the very first instance when a continuous outflow was recorded. According to the uranine measurement RW3 contains 14 % formation water. The tritium content of RW3, 13 TU, was also clearly lower than that of the flushing water (15.8 TU).

2. After the brine contamination, 8.5 m^3 of fresh water was used to reach the length of 246 m. The EC of the return water ranged from 19 to 32 mS/m, until it suddenly jumped to 116 mS/m. At 246 m the outflow rate was 125 mL/min. Three hours later it decreased to 44 mL/min. It is assumed that the observed salinity increase may be of natural origin. Sample RW4 is taken from this zone. The tritium content was 12 TU, again lower than that of the flushing water. Nothing exceptional was observed in the core.

3. When drilling further, the EC remained somewhat elevated, slightly above 40 mS/m, until around 310 m. The next sample, RW5, was taken at hole length 302 m. At this point the outflow was 100 mL/min and the EC 59 mS/m. Based on the uranine level this sample has almost 40% formation water.

4. At 314 m hole length the drilling was started using clean, fresh water tank, which clearly shows in the EC values. After about 10 m drilling, the EC starts to increase again due to the mixing of return water.

5. Major problems occurred with obtaining flushing water. The Mine department was short of manpower and, especially, transport vehicles. Consequently, both day and night shifts had difficulties with water transport. At 336 m and again at 350 m hole length 2.3

m^3 (500 imperial gallons) of slightly contaminated water (EC 61 mS/m) was brought down. In order to continue drilling, this had to be accepted.

The measured EC values for the return waters were between 35 – 65 mS/m until 357 m where a sudden increase to 111 mS/m was observed. After drilling four meters, the EC was returned to the level of the flushing water (60 mS/m). The reason for this anomaly remains uncertain due to the quality problems. However, mixing of a natural component can be suspected, because the observed EC was almost twofold compared to the drilling water.

After abandoning one contaminated water load, a third, still contaminated replenishment had to be accepted at 372 m hole length. The EC of the drilling water was as high as 90 mS/m when drilling from 372 m to 392 m. The clean water replenishment after 392 m lowered the EC down to 60 mS/m and at 410 m the EC of the flushing water was 35 mS/m.

The EC in return water between 372 and 392 m was relatively high, the highest value being 120 mS/m at 379 m. This was again higher than any measurement from the flushing water. The sampling was delayed to reduce the effect of the possible contamination and a chemistry sample RW6 was taken at 407 m hole length. Tritium content in this sample was 14 TU. The outflow was 80 mL/min, EC 65 mS/m and uranine level indicated a mixture of about 40% formation water.

In summary, the outflow from the borehole was low throughout the 515 m drilled. The highest measured rates after the major load of flushing water had drained from the hole were about 100 mL/min at 302 m. The first occurrence of constant outflow was recorded at 209 m indicating that either the open fracturing is sparse within the first 200 m or the mine has drained the bedrock. On three occasions it appears that water-conducting systems were intersected and natural waters were introduced into the hole. At hole lengths of roughly 250 m, 300 m and 400 m, elevated EC's were observed and the collected samples turned out to contain 14 – 39 % formation water. Figure 11 compares the return water samples with the other Lupin waters based on their Br and Cl contents. Mixing of the Na-Cl brine tends to shift the composition to the right in the diagram due to the salt's extremely high Cl/Br ratio. The plot suggests that samples RW1 and RW4 may be affected by the brine, while the others seem to represent a natural component. The chemistry of the waters at the base of the permafrost is discussed in Section 3.3.

The apparent, steadily decreasing trend in EC values after 400 m may reflect the cleaning of the hole after the contamination from the drilling fluids. However, there are other aspects of the data that need to be explained. All replenishment after 410 m was dilute water with EC well below 10 mS/m. The recovery should have been quicker, especially because the hole is deviating upwards (at the end of the hole the dip is +14 degrees). In addition, the water consumption/run clearly increased adding to the flushing of the hole. A "steady state" was reached only at 475 m and the return waters showed similar EC values as at the beginning of the drilling. One possible explanation for this slowly decreasing trend might be that the frozen rock matrix contains saline fluids inherited from the passing saline waters, possibly relating to a freeze-out process. This salinity was then released during drilling. The increasingly upwards-deviating hole intersected the base of the permafrost, assumed to be at 540 m depth, at around 340 m of hole length. To test this hypothesis and to gain information on the composition of the

rock matrix fluids, a number of core samples were collected from boreholes 890-188, 570-105 and 570-106 for crush and leach experiments to be carried out in the University of Waterloo. The latest borehole, 550-112 drilled in May 2003, was also sampled both for core and for water analysis (see Sections 2.2.7 and 2.3.). The crush and leach experiments are discussed in Section 2.6.

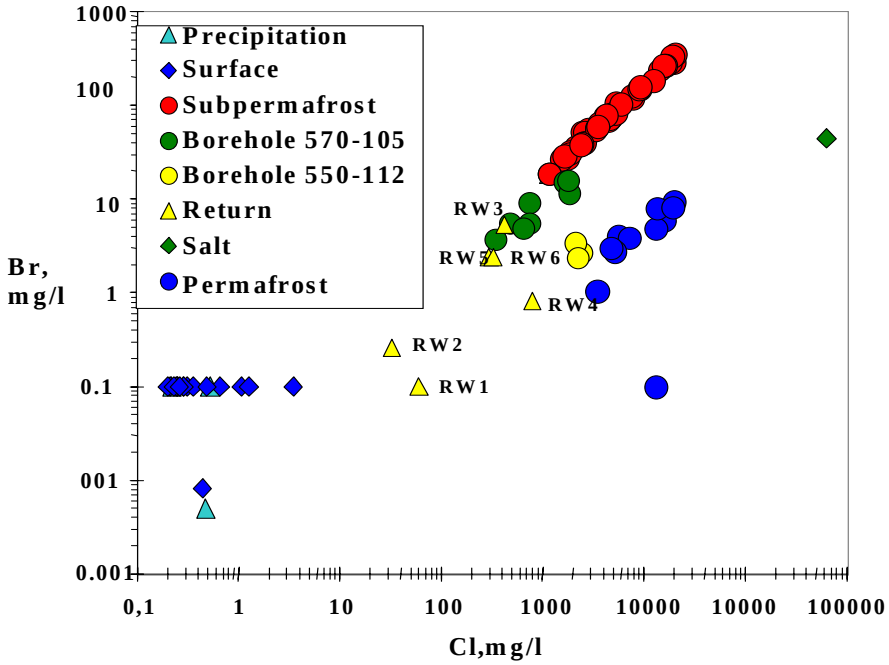

Figure 11. Br vs. Cl plot of the various waters at Lupin showing two different trends, salt-water contaminated waters from permafrost levels and subpermafrost waters representing the natural deep groundwaters. The compositions of the return water samples (RW1-RW6) are corrected based on their uranine contents. It is noteworthy that the waters from 570-105 group together with the deep groundwaters, while borehole 550-112 has more common with the permafrost waters (for discussion see section 3.3).

Borehole 570-106

The return water monitoring during the drilling of the inclined borehole 570-106 was based on the EC measurements. Because the hole was not overflowing, it was not possible to obtain any outflow rates. In fact, the water level slowly decreased when drilling water was not being pumped into the hole.

The measured range of EC was narrow compared to the first borehole (Fig. 12). This implies that the quality of the flushing water was under control, but it may also suggest that there was no significant inflow of formation water with elevated salinity into the hole. However, because the hole was filled continuously with fresh water it may be that possible inflow from formation water was effectively masked by the overwhelming amount of flushing water. Most of the observed variation in the EC of the return water, for example, the elevated values at 120 m and 357 m, can be directly correlated with the quality of the replenishment water.

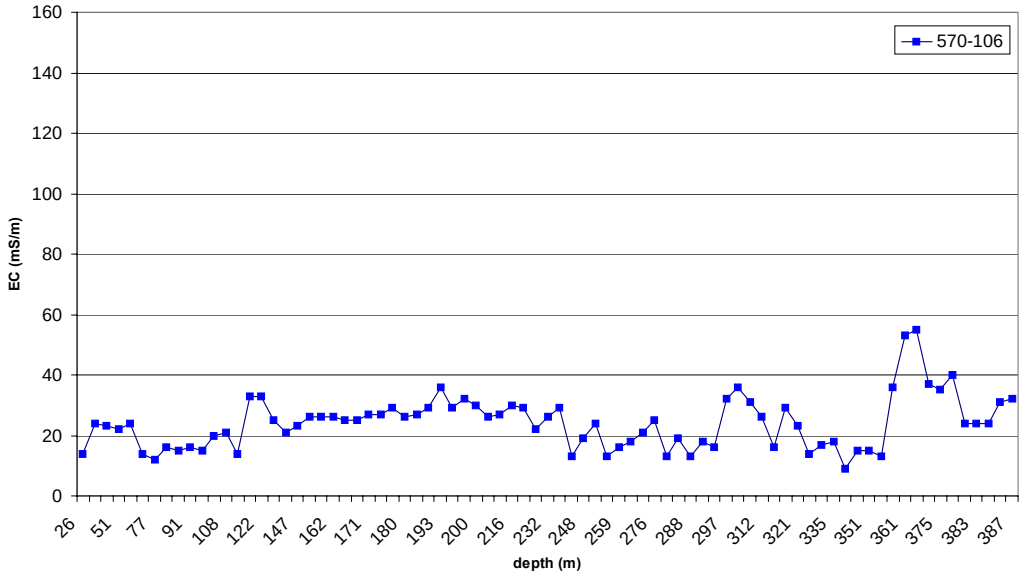

Figure 12. Electrical conductivity of the return water vs. depth during the drilling of borehole 570-106.

Cross hole monitoring

In November 2002, after completing the drilling of 570-105, a packer system was installed in the borehole for water sampling. Two packers divided the hole into three sections (0 – 45 m, 45 – 160 m and 160 – 515 m). During the drilling of 570-106, pressure monitoring was carried out in the packed-off sections of borehole 570-105 to observe possible indications of hydraulic connections between these holes. As borehole 570-105 is up-handed, there was practically no water in the hole at the start of drilling 570-106. Consequently, the original head in 570-105 was set to zero (atmospheric). If flushing water from borehole 570-106 (feed pressure about 1.4 MP) intruded connections to the plugged borehole 570-105, it could thus be observed as a slight increase in hydraulic head in some of the monitored sectors. Results of head monitoring in borehole 570-105 are summarized in Figure 13.

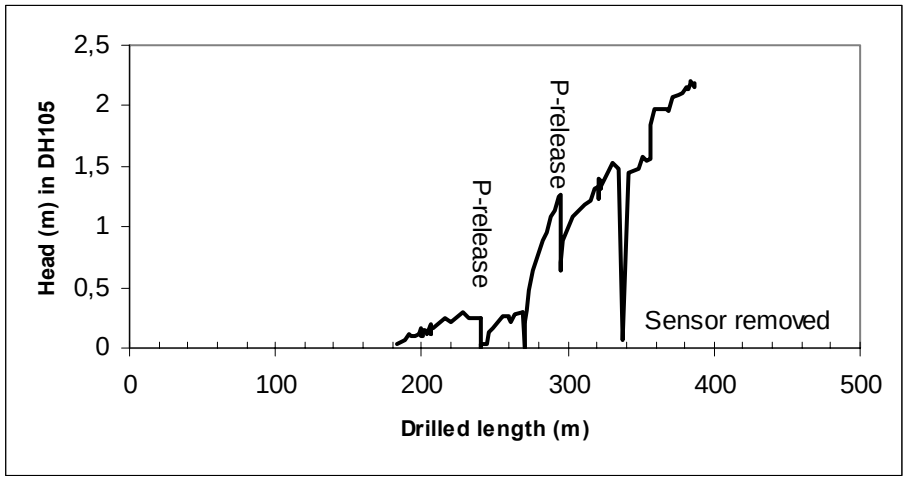

Figure 13. Head monitoring of borehole 570-105 during drilling of 570-106.

During the drilling of the first 160 meters of borehole 570-106, section 45 – 160 m was monitored in 570-105, but no indications of hole-hole interaction were observed. The first indications of interaction were observed when the drilling reached a length of about 190 m. The pressure above the sensor was sporadically released to check if it would build up again. The most pronounced interaction (possible water intrusion) into 570-105 was observed when drilling of borehole 570-106 had propagated to a depth of 270 m. The consumption of the flushing water was also observed to increase at this hole length (Fig. 9). Any head anomalies thereafter may be due to interaction via this zone. However, one additional interconnected hydraulic conductor may have been intersected at a length of about 360 m.

2.2.4 Geological description

Lithologies

The research boreholes intersect all the major rock types at Lupin (Fig. 14). Due to the large fold structure in the area the mineralised iron formation-type amphibolite was intersected three times. Occasionally, the rock is laminated by alternating amphibole and chert (SiO_2) bands, but massive types are more typical. In highly mineralised sections the dissemination and lamination of sulphides (pyrrhotite and arsenopyrite) may constitute a considerable proportion of the rock. The thickest ore-type intersection was nine meters. Conformable and/or cross-cutting thin quartz veins are common. Variably chloritised garnet amphibolite horizons are commonly associated with the iron formation.

The acid wall rocks are commonly rather fine-grained and, although they contain large amounts of mica, the schistosity is often difficult to observe. Clearly schistose types are called phyllites and the coarse varieties are named as mica gneisses. Small amounts of graphite are frequently observed, especially on fracture surfaces. More coarse-grained brownish varieties are called greywackes or quartzites if quartz is clearly the major mineral. Locally these rocks may have a sandy appearance demonstrating their sedimentary origin. Dark cordierite spots (ϕ 5 – 25 mm) are common both in phyllitic rocks and in graywackes. Both these major rock units are heterogeneous and different varieties alternate randomly. All kinds of intermediate types exist and it is difficult to maintain a systematic classification. This also implies that it is practically impossible to correlate these rock types from one borehole to another.

A homogenous, 4 – 7 m thick muscovite granite vein was observed in both boreholes. The rock is grey and the grain size is 2 – 4 mm. A similar vein is reported in many of the boreholes deeper in the mine, but it is not certain if it is the same vein.

Fracturing and fracture infillings

Amphibolitic rocks are usually intact and in general the coarse-grained rock types are less fractured than the fine-grained rocks. Fracturing is very common in the fine-grained phyllitic rock. Most of the fractures are parallel to the schistosity, which makes it very difficult to distinguish between the true brittle fractures and slipping along bedding planes due to folding. Both similarly result in chlorite and/or graphitic surfaces, but have a different impact on the bedrock properties. Oblique directions, both vertical and

subhorizontal, are also encountered, but rarely. Another problem related to the deformation is that the rocks liable for brittle behaviour (mica-poor, hard rocks) have fractured badly during the early phase of deformation, but have healed during later stages. This means that these healed fractures tend to open during drilling and result in apparently highly fractured zones which have nothing or very little to do with the groundwater flow. This was clearly seen when the fracture logs were compared with the borehole video survey record.

However, certain highly fractured zones are marked in Figure 14. The zones at 270 m and 360 m in borehole 570-106 have been shown to have connections to borehole 570-105, but a more precise correlation between the boreholes remains uncertain (see section 2.2.3).

Fracture infillings are very scarce and mineralogically very monotonous. Thin calcites are the only true infillings, because the other encountered coatings, graphite and sulphides, may have been remobilised from the rock. Platy, white or clear calcite is the typical type. Some clearly hydrothermal calcite-sulphide veinlets, with some crystal morphology, have been observed. Both calcite types have been collected for fluid inclusion studies being carried out by the University of Waterloo.

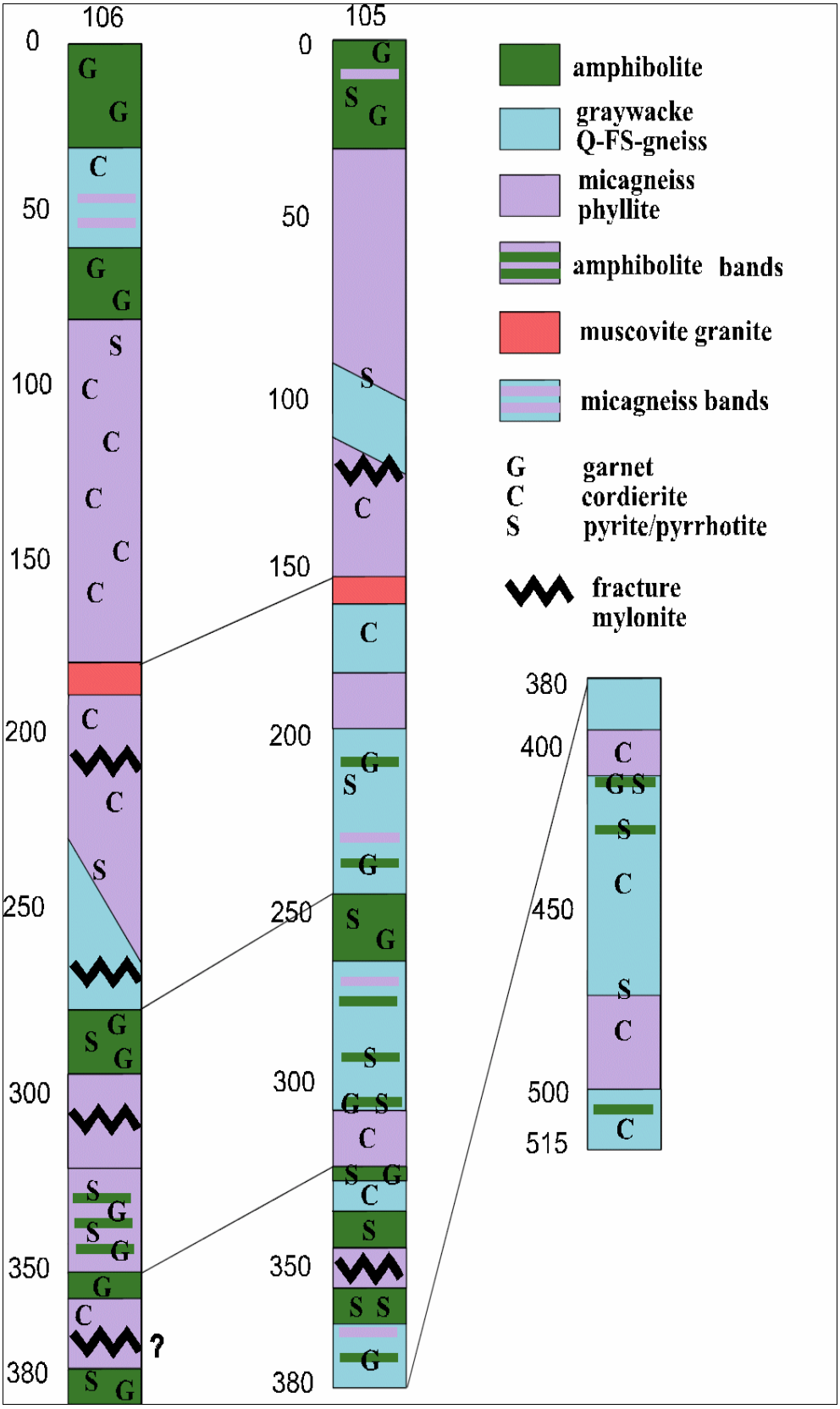

Figure 14. Lithologies vs. borehole length encountered in boreholes 570-105 and 570-106.

2.2.5 Geochemical water sampling in the new boreholes

After completing the drilling activities for borehole 570-105 on 30th of October 2002, the hole remained open till 2nd of November when the packers were installed into the hole. During this period the outflow was collected, the rate was measured and samples were collected for standard chemistry, stable isotopes and tritium.

The packer system consisted of two one meter long rubber packers, which were inflated with water. A 10 bar pressure was applied. The packers were installed into the hole using 3 m long aluminium rods, 13 mm in diameter. Water from each section was collected in 3 L plastic canisters (Fig. 15). During the drilling of borehole 570-106 the packed-off sections were used for pressure monitoring and finally, the packers were removed on the 9th of December 2002 prior to the deviation measurements. No outflow from the hole was observed prior to the removal. Both holes were left open for the forthcoming video survey. The hole remained open until 25th of May 2003, when one packer was installed at 150 m and a sample collection was rearranged. Table 3 gives a summary of the collected samples.

Figure 15. Sampling arrangement at the packed-off borehole 570-105. The packers were inflated with water. The pressure was set at 10 bars. One-way escape of air from the tightly sealed sample bottles was facilitated through simple water seals.

Table 3. Hydrogeochemical samples from borehole 570-105. FW denotes flushing water and the corresponding percentage indicates the amount of the flushing water in the sample based on the uranine concentration. The average uranine level in flushing water was 514 µg/L and the isotope composition was: $\delta^{18}O$ -19.64 ‰ and $\delta^{2}H$ -157.2. The tritium level was 15.8 TU. Samples Lu/GTK/47, -48 and -62 represent the open-hole situation (O.H.), where the outflow is a mixture of the waters introduced into the hole. Samples Lu/GTK/49 – 52 and -79 were collected from packed-off sections.

Code	Section (m)	Sampling date	Uranine µg/L	$\delta^{18}O$ (VSMOW)	$\delta^{2}H$ (VSMOW)	^{3}H (TU)	Note
Lu/GTK/47	0-515 (O.H.)	31.10.2002	350	-20.0	-159.0	13.7	67% FW
Lu/GTK/48	0-515 (O.H.)	2.11.2002	330	-20.1	-160.6	13	63% FW
Lu/GTK/49	0-45	2 -29.11.2002	14	-21.2		8	3% FW
Lu/GTK/50	45-160	2 -29.11.2002	165				32% FW
Lu/GTK/51	160-515	2-16.11.2002	375	-20.0	-158.6	16.1	73% FW
Lu/GTK/52	160-515	16-29.11.2002	330	-20.0	-156.6	11.7	64% FW
Lu/GTK/62	0-515 (O.H.)	27.2 - 20.5.2003	3	-22.4	-175.03	1.5	0.6%FW
Lu/GTK/79	0-120	25.5 - 12.6.2003					

Empty = not analysed

Open hole sampling

The monitoring of the borehole began 26 hours after the drilling was completed on the 31st of October 2002. The outflow rate was considerably lower than during drilling (160 mL/h), but the EC, 65 mS/m, was higher than observed at the end of the drilling (11 mS/m). The pH was 8.12. The water was distinctly greenish, due to uranine, but otherwise clean. Sample Lu/GTK/47 was collected and a water collection system was installed at the collar of the hole.

After 22 hours, the outflow had decreased to 98 mL/h. The EC had increased slightly to 82 mS/m. The next sample, Lu/GTK/48 was taken on the 2nd of November representing the flow of the past 20 hours. The flow rate had further decreased to 56 mL/h, but the EC was again a bit higher, 91 mS/m. The water was greenish as before and there was some rust sediment derived from the casing at the collar of the hole. Immediately after the latter sampling was complete, the installation of the packers began.

A third open-hole sample Lu/GTK/62 was collected on the 20th of May 2003. The volume was 1.25 L and it represents the outflow after 27th of February 2003. EC was considerably higher than in the previous samples, 658 mS/m.

Packer sampling

The original plan was to divide borehole 570-105 in three sections to be able to collect separate samples from the frozen ground between 330 – 515 m and the section below

the permafrost, 190 – 330 m, and to separate the dry, potentially contaminated part of the bedrock from the casing at the collar, 10 – 190 m. Unfortunately it turned out that the friction in a dry, slightly up-handed hole was too high to allow the implementation of this plan. Instead, the following three sections were separated: 0 – 45 m, 45 – 160 m and 160 – 515 m. The installation was completed on the 2nd of November 2002.

The last measured outflow rates from the open hole suggested that, if maintained, the bottles would fill up within a few days. Therefore, it was arranged that a local worker would attend to the filling of the sample bottles. He reported that most of the water was coming from the section 160 – 515 m. The other two sections produced very little water. It soon became clear that the outflow was decreasing quickly and after two weeks (16th of November 2002), when the canister was changed, there was about 2 L of water (Lu/GTK/51). The flow further decreased and was very low by the end of November (29th of November 2002), when our team returned to the site and the preparations for the drilling of borehole 570 – 106 begun. During the second two-week period about 1 L was collected from the section (Lu/GTK/52). In addition, during the one month the packers were in place, a small amount of water was collected from the other two sections. Samples Lu/GTK/49 (0 – 45 m) and Lu/GTK/50 (45 – 160 m) were barely large enough for standard chemistry and uranine measurements.

After collecting the open-hole sample Lu/GTK/62, one packer was installed at 150 m of hole length in 25th of May 2003 to locate roughly the spot of the water seepage. It turned out that the water was coming from the bedrock section 0 – 150 m. A local worker collected the sample Lu/GTK/79. About 0.5 L of water was accumulated during the period of three-week.

The chemistry of the water samples collected from borehole 570-105 is discussed in Section 3.3.

2.2.6 Hydraulic testing in borehole 570-106

During the field trip in February 2003, borehole 570-106 was surveyed with a video camera and the hole was seen to be dry down to 240 m of hole length. A simple hydraulic test was carried out by filling the hole with water and following the lowering of the water level with the help of the video camera. The hole was filled up to 270 m hole length and the behaviour of the water level was observed using the video image. No change was observed within 45 minutes.

Next, the hole was filled up to the collar and the drawdown was monitored using a water table logger (EC-sensor). The result of the log is shown in Figure 16. The test carried out was considered as a slug test.

In a typical slug test a volume of water or a metal bar is added to the well and relaxation of the water level is monitored. The average hydraulic conductivity (K) of the borehole was coarsely estimated using the Hvorslev method, commonly used in interpreting slug tests (*e.g.*, Fetter 2001).

$$K = \frac{r^2 \ln(\frac{L}{R})}{2Lt_{37}} \qquad (1)$$

Where R is the effective radius of the well, and r is the radius of the monitoring pipe or casing (in this case r = R). The well-depth is denoted by L, and t_{37} is the time required for 37% recovery of the water table (reducing the time-related logarithmic expression to 1). Graphical solution of the t_{37} –value can be done from a lin-log graph of time vs. head ratio h/h_0 (where h = momentary head and h_0 is the initial disturbance compared to the original head). In the present case, the original (equilibrium) head was measured to be at the depth of 56 meters below the borehole collar (221 meters of bore length), where the zero-level of h was set. Graphical interpretation of the measurements is given in Figure 17.

The t_{37} value can be estimated at about 250 000 sec from Figure 17. By assuming that the "well-depth" equals the borehole length (390 m) and by using the borehole radius of 0.03 m (r = R), average hydraulic conductivity (K) of the borehole can be estimated to be about $2 \cdot 10^{-8}$ m/s.

It must be noted that many of the assumptions used in deriving the Hvorslev-solution are not strictly valid in the current case, causing uncertainty in the interpretation. However, the value obtained gives an estimate of the average K-value of the bedrock studied. There is clear evidence that the water flow was concentrated within a few conductive zones. Thus, a more appropriate parameter describing the hydraulic conditions of the system studied would be the borehole transmissivity (T), defined as T = K·L, and having a value of about $8 \cdot 10^{-6}$ m^2/s. This value approximates the transmissivity of the most conductive zones.

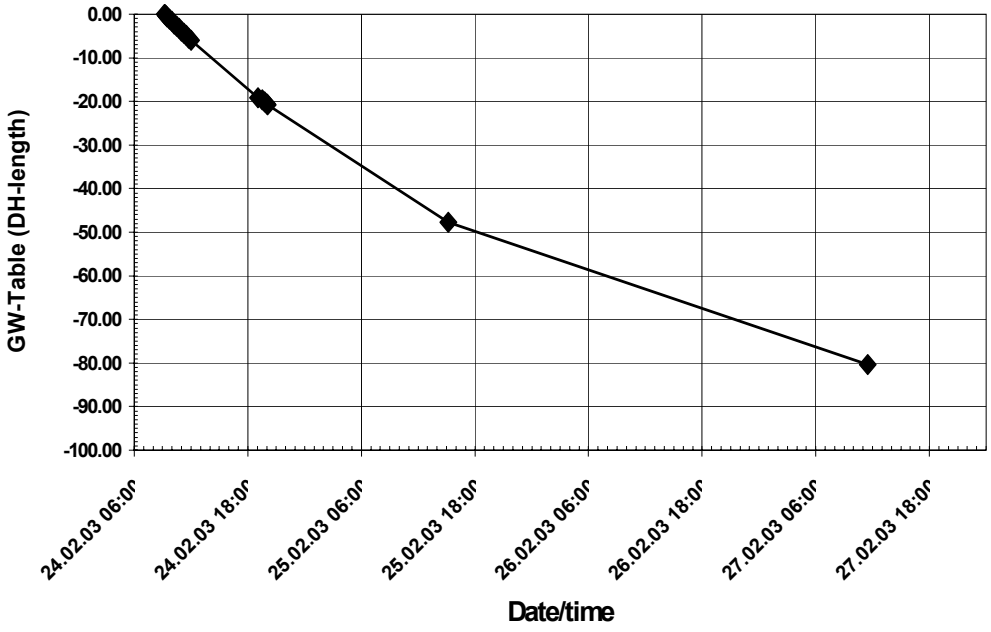

Figure 16. Lowering of the groundwater level in the water-filled borehole 570-106 as a function of time.

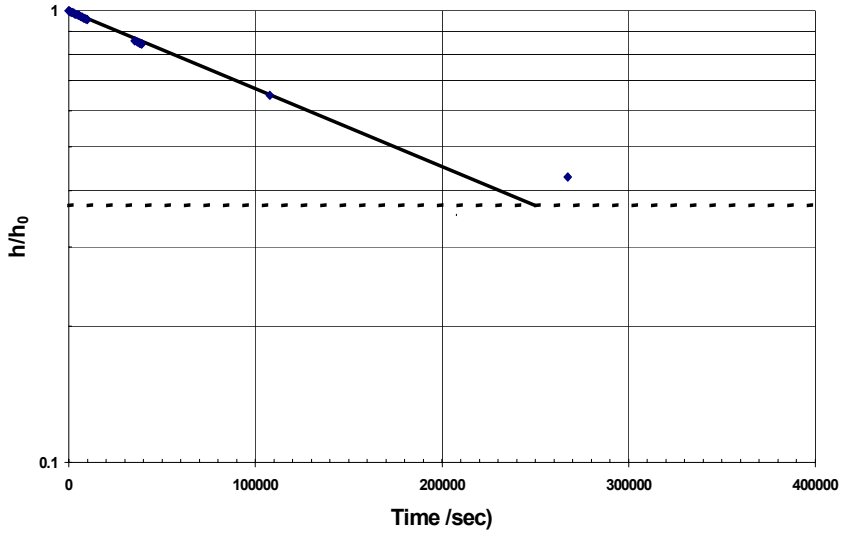

Figure 17. Graphical interpretation of the slug test done in borehole 570-106. For h/h_0 see the text.

2.2.7 Borehole 550-112

Borehole 550-112 was drilled using a Bazooka drill rig. This rig is a lightweight, portable unit that was ideal for operations in this section of the mine. The rig is limited to 30 meter long holes, but the core recovered is suitable for lithological and geochemical studies. The 550 m station will be available for additional drilling operations during subsequent trips.

The 550-112 hole is located approximately 15 meters from the main ramp, in a short drift used for storage. The elevation of the collar of the hole is 549 m. The hole was drilled with a dip of +15°, and is shown on Figure 7 in approximate relation to the 570 boreholes. The hole was drilled with an angle of roughly 60° against the strike for a length of 23.8 m. The change in elevation was 6.15 m, reaching 543 m, just short of the base of the permafrost at 540 m. The hole intersected rather fine-grained phyllites/mica gneisses. Occasionally, thin quartz veins are encountered. Flushing water from the lake was spiked with uranine solution.

The drilling and core recovery went quickly and efficiently for the first 10 meters of operation. The electrical conductivity of the return water was very constant at approximately 18 mS/m during the initial phase. At 10.5 meters, a fault or crush zone was encountered, which had a total length of approximately 1.5 meters. The zone was recognized by poor core recovery, broken and weathered rock chips, iron-rich water and precipitates, and a slight rise in conductance to 22 – 27 mS/m. Inspection of the ramp along the suspected strike of the fault revealed a very thin (10 – 30 cm wide) zone that was producing saline waters similar to solutions found elsewhere in the ramp fault and suspected of containing considerable contamination.

During continued drilling, excellent core was recovered. Return water conductivities varied between 22 and 30 mS/m. At approximately 22 meters depth, the conductivity increased abruptly to a high of 38 mS/m. This zone would have been directly below the suspected permafrost boundary. At completion, the borehole was flushed with the uranine-spiked flushing water. The hole was quickly plugged, and water samples were

taken periodically over the next 24 hours. Soon after the completion of the drilling, the hole produced water at the rate of 2 L per hour. One of the first observations was that the green uranine colour of the flushing water disappeared very soon after drilling. Although a contaminated water component must be associated with the fault zone, the more highly saline water from deeper in the borehole seems to have some impact on the samples taken (the chemistry of these waters is discussed in a later section).

Finally, borehole 550-112 was sealed with a Margot plug and equipped with a pressure gauge. No pressure was recorded in the first 6 weeks of installation and unfortunately, no one has been able to re-enter that portion of the mine in the past seven months to monitor the pressures in the borehole.

2.3 Hydrogeochemical studies

The hydrogeochemical studies in Phase II included: 1) characterisation of surface waters, 2) characterisation of the groundwaters at the base of the permafrost and 3) detailed characterisation of the deep groundwaters. The chemistry of these waters and the previously sampled permafrost waters are discussed in more detail in section 3.3.

2.3.1 Surface waters

The research area, like other permafrost areas, is characterised by a large number of smaller and larger lakes and ponds. Most of them are probably shallow and are likely to freeze down to the bottom during winter. The ice starts to melt in early June and most of the lakes are open by late June. Water in lakes has three main sources: 1) melt water in springtime, 2) meteoric precipitation and 3) melting ground ice/permafrost.

The snow cover is rather thin and its contribution to the water budget is small due to the dry and cold climate. However, strong winds tend to build up thick snowdrifts in sheltered slopes where the melt water finds its way into local depressions. Only a small portion of the melt water percolates into the soil, because the ground is frozen and the active layer is still very thin. Most of the annual rain falls in August – September. The moisture predominantly originates either from the Pacific Oceans or the Arctic Ocean, which may result in a considerable variation in the isotopic composition of the rainwater (IAEA/ISOHIS 2001). Melting ground ice provides an extensive and continuous water source during the warm summer months. The typical silt moraines in the area are saturated by a mixture of rainwater and water from the melting ground ice prior to freezing. The next summer this water is released by the advancing active layer, which may extend to a depth of about two meters. Some of the observed springs are assumed to be dependent on this type of water source.

A fourth, still hypothetical water type might be discharging deep groundwaters. This situation might be experienced in a talik structure related to a major fault. Artesian aquifers are known to occur in permafrost areas.

During Phase I of the project samples were taken from Lake Contwoyto, which represents the major water body in the area. In order to further characterize the meteoric waters a number of small lakes and ponds were sampled in the vicinity of the mine in June 2002. An effort was also made to find and sample springs. A chain of lakes related

to a regional structure called the Norma Fault were sampled as well for evidence of deep, potentially saline discharge. The fault is located about 7 km S from the mine (Fig. 18). In contrast to groundwater samples the code Lu/GTK/S# was used for surface samples collected in 2002.

Water samples Lu/GTK/S1-S2, S4-S5 and S7-S9 are from small pools assumed to be springs. A constant flow and a soil-covered bottom without vegetation were used as indications for a "never" drying pool. Sample Lu/GTK/S18 is a rainwater sample and Lu/GTK/S19 is a snow sample collected from a thick drift. The sample represents a 70 cm thick profile. All the other samples are lake waters. Sample Lu/GTK/S17 is from Lake Contwoyto. Note that sample S3 was not collected at all, because the intended sampling area turned out to be connected to the already sampled S2-area.

Spring was late in 2002 and there was still melting snow on the terrain. Thus melt water may have diluted some of the samples. All sampled surface waters, except the lake S16, which turned out to be contaminated by the mine waters, are very dilute (TDS 0.006-0.022 g/L). No indications of deep discharge were observed. The major cations are Mg, Ca and less commonly Na and K, while major anions are SO_4 and HCO_3 (see Fig. 40).

Only the snow, rain and Lake Contwoyto samples were analysed for stable isotopes and tritium. The two snow samples Lu/GTK18 (from October 2000) and Lu/GTK/S19 show slightly deviating $\delta^{18}O/\delta^{2}H$ values (-25.7 ‰/ -195 ‰ and –29.2 ‰ /-226 ‰), which reflect differences in precipitation temperatures. The latter sample represents the snow accumulation formed during the coldest season of the year. As expected, the rainwater has somewhat heavier isotope composition, $\delta^{18}O$ –20.3 ‰ and $\delta^{2}H$ –156 ‰, compared to the snow. The tritium values for the snow and rainwater samples are almost identical, 11 TU and 12 TU, while the snow from 2002 shows a lower value, 6.5 TU.

The first sample from Lake Conwoyto (Lu/GTK/17) was taken from the fresh water pumping station in 2000. This and the flushing water sample (FW0) represent water pumped up from a depth of 7 m, while Lu/GTK/S17 was collected from the surface of the lake. The stable isotopes show a narrow range ($\delta^{18}O$: -19.1 – -20 ‰ and $\delta^{2}H$: -158 – -160 ‰), but the two available tritium measurements range from 15.8 TU to 20 TU. The range of results from several years may be typical of seasonal or long-term trends in the area. Considering all the available tritium data for precipitation samples and surface waters, there is a trend to decreasing values with time. However, the values may simply reflect slight changes in the source of air mass and not enough data exists to say anything more definitive.

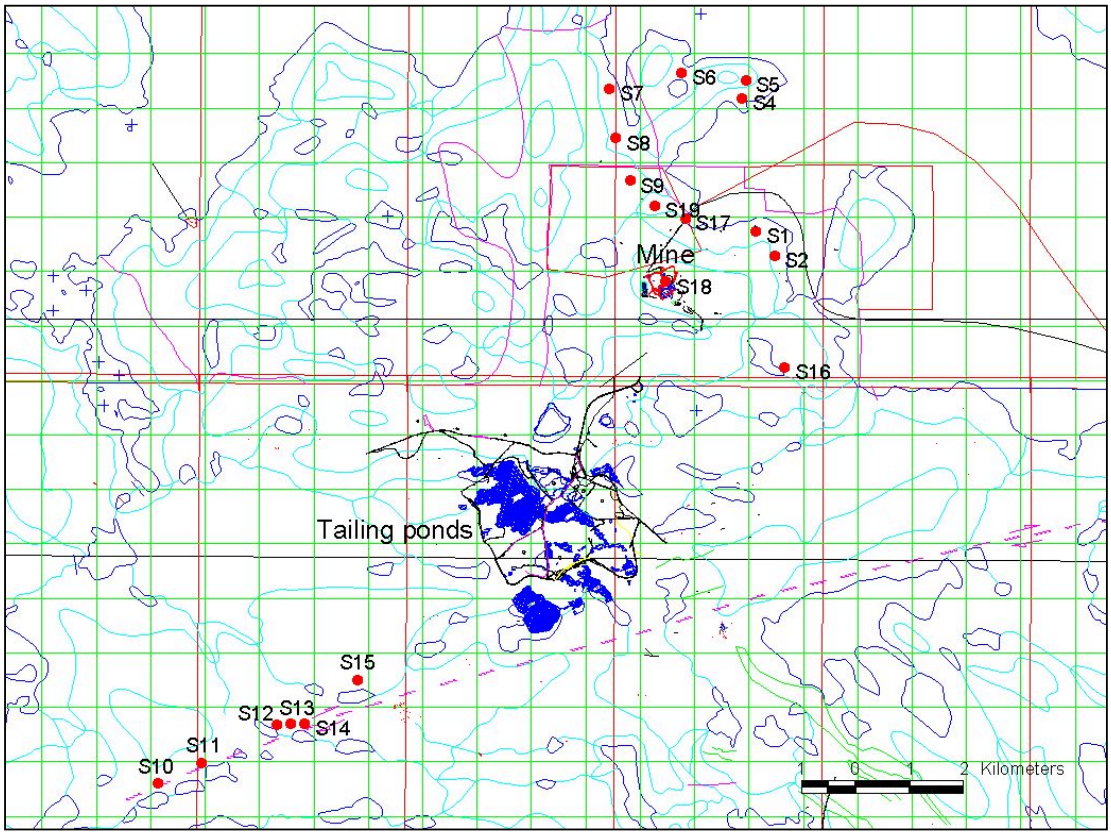

Figure 18. The locations of the surface samples collected in June 2002. Note that sample S3 was not taken. The trace of the Norma Fault, S from the tailing ponds, is indicated by a dashed, violet line.

2.3.2 Water at the base of the permafrost

The characterisation of waters at the base of the permafrost is based on samples collected during and after the drilling of the boreholes at 570 m level (see section 2.2.5). Although the samples were relatively small and contained considerable amounts of flushing water, certain conclusions can be drawn from the uranine-corrected results and the flow rates since the completion of drilling.

There is clearly very little water available close to the base of the permafrost. No pressurised water or gas flow was observed in the boreholes drilled to date (550-112, 570-105 and 570-106). The slightly up-grade borehole 570-105 yields some water. According to the uranine determinations the amount of flushing water was high and rather constant in most of the samples collected soon after the completion of the drilling. However, after six months the flushing water component was reduced to insignificant level (see Table 3). The down-handed borehole 570-106, which extends to about 640 m in vertical depth was also dry after drilling. However, three months later, the water level had risen and was observed at 630 m depth. It may be that sealing of the flowing holes deeper in the mine has an affect on the groundwater table at higher levels or that other local conditions have changed the levels in this hole. The salinities of the retrieved waters are below 4 g/L.

Comparable information is obtained from the short borehole 550-112 drilled upwards at 550 m level. The 23.80 m long borehole was drilled in May 2003 with a dip of +15° and is assumed to extend very close to the base of the permafrost. Soon after the completion of drilling, the hole produced water at the rate of 2 L/h. The hole cleaned up very quickly in that the uranine disappeared and the flushing water component was insignificant (< 4 %) in the first samples (Lu/GTK/76 and 78). The EC's around 1000 mS/m indicate that the water is rather saline, maybe about 15 g/L. A fault exposed to the ramp, was intersected half way along the hole. It is possible that it introduces contaminated water into the hole. A third sample from the hole was collected in Mid-June 2003. The chemistry is discussed in section 3.3.

A pressure gauge was installed in the hole, but it turned out that the hole is not pressurised. This may also be due to the presence of a fault. Pressure measurements at different levels below the permafrost were motivated by the fact that hydraulic head distribution around the mine could be outlined from the pressure data. The information could then be used to evaluate the reason (natural vs. artefact conditions) and the consequences of the observed unsaturated zone. For example, unsaturated conditions would favour the accumulation of gas under the impermeable permafrost provided pathways exist for gas migration.

2.3.3 Characterisation of the deep groundwaters

The detailed hydrogeochemical studies concentrated on the characterisation of the deep groundwaters at levels 890 and 1130. The relationship of these waters to the fluids within and under the permafrost must be understood in order to assess possible groundwater geochemical evolution at potential repository depths.

To obtain representative samples and physico-chemical measurements it was considered necessary to pressurise the holes and let the natural outflow clean the holes. There are clear indications that the gas samples were affected by the open-hole situation (see Ruskeeniemi *et al.* 2002, p. 42). For the packer installations see section 2.5.2.

Redox and oxygen concentrations were measured from six boreholes using a flow-through cell. A platinum electrode with a combined Ag/AgCl reference was used for redox measurements. The obtained values were converted to Eh-scale according to the operation manual of the electrode. The outflow rate from the borehole was set to around 1-1.5 L/min. The monitoring time varied from 20 to 55 hours. Therefore, about 1 – 5 m^3 of water was removed from the holes during the monitoring cycle, which means that in principal the water volume in the holes was changed at least 1 – 5 times. The pH and electrical conductivity values were recorded after the oxygen and redox values had stabilised (Table 4). Dissolved oxygen concentration decreased to value 0.0 mg/L (reading accuracy) in all cases. There were indications that Eh-values may have decreased further, if the timetable would have allowed lengthening of the monitoring time. Gas samples were collected prior and after the redox measurements to observe trends possibly related to the cleaning of the hole. Isotope and chemistry samples were collected after redox measurements.

Table 4. Final redox (Eh) and dissolved oxygen values measured in flow-through cell.

Borehole	Date	Eh mV	O_2 mg/L	pH	EC mS/m
890-118	21.2.03	24	0.0*	8.3	545
1130-192	22.2.03	18	0.0	8.2	4430
1130-217	24.2.03	-16	0.0	8.6	1370
1130-192	25.2.03	-11	0.0	8.5	1410
1130-181	27.2.03	-10	0.0	8.4	1230

* Detection limit

The field-measured *pH-values* are rather uniform in all boreholes on the two levels monitored. The pH values measured from the previous samples in laboratory are uniformly about two units lower than these *in situ* results. Possible reasons to that include undersaturation of samples from depth with respect to atmospheric CO_2, if gas diffusion into the sample can occur during transportation. The DIC/bicarbonate content of the deep samples is low (5 to 15 mg/L). In contrast, the change in the pH of samples at 570 level is almost insignificant and, if anything, is towards higher values. Further discussion of CO_2 /DIC may be found in Section 3.3.

At first glance, the sealing of the holes had little effect on the *chemistry* of the samples. Figure 19 provides the Ca/Na vs. Br/Cl diagram in which data from the available samples are shown. The observed shift is usually rather limited and the trends are random and minor from one hole to another. The salinity has remained the same or decreased slightly. The change in stable isotopes and tritium are also insignificant, possibly with the exception of borehole 1130-191, where the tritium has increased slightly from < 0.8 TU to 1.5 TU. Finally, as will be discussed shortly, the isotopic composition of the hydrocarbon gases (CH_4) shows little change between sealed and unsealed borehole samples.

The second sampling round from the pressurised holes in May 2003 revealed that the salinity in boreholes 1130-191 and 1130-217 had increased distinctly since February 2003. The shift in TDS in borehole 191 was from 5.7 to 13.7 g/L and in borehole 217 from 8.5 to 15.5 g/L, respectively. These holes are drilled only about one meter apart with a small difference in the azimuth and they are also almost of the same length (see Section 2.5.1/Level 1130). Therefore, they intersect the same geological units and their salinity difference is somewhat unexpected. The abrupt change in the salinities indicates that a new kind of water has started to flow into the holes. The latter sample was taken after redox monitoring during which the hole 1130-217 was allowed to flow.

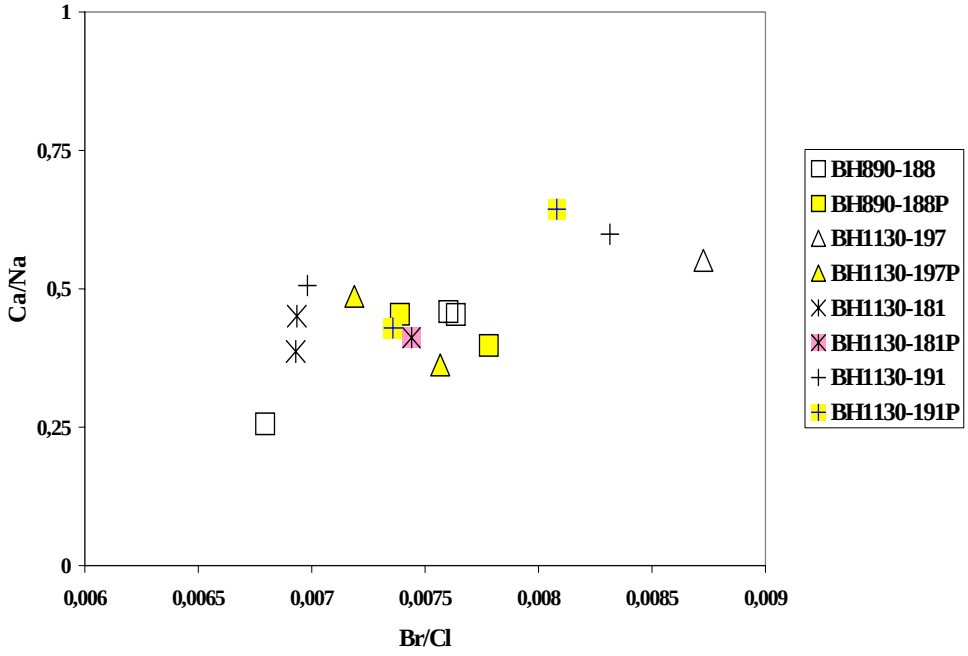

Figure 19. Comparison of the open-hole (clear symbol) and pressurised samples (coloured symbol) from boreholes at 890 and 1130 level.

A new exploration tunnel at 1130 m level was drifted towards the east in April 2002 (see Fig. 27). This drift provides an opportunity to sample groundwaters further away from the mine than any other location. There were a number of new, short boreholes in May 2003 and more were planned to be drilled for exploration purposes in this area. Many of the boreholes are dry, but others are producing some water. Several narrow (10-50 cm) faults with variable orientations are exposed in the drift. They seem to be tight, usually graphite bearing shear zones with polished slickensides. None of them are clearly leaking, however, at the far end of the drift is there some water dripping from the ceiling.

It is remarkable how variable the waters are that are encountered within the 150 m of the drift. The electrical conductivities vary from 476 mS/m to 2490 mS/m. The most dilute waters are leaking from a bolthole and from a 40-m long uphanded borehole and dripping from the ceiling at the end of the drift indicating that the source of water is somewhere above, but not very far from the drift. The flow and electric conductivity has remained constant since February 2003, when the bolthole was sampled for the first time. The tritium content of these dilute waters was <0.8 TU. The waters from the flat boreholes are distinctly more saline, the EC ranging from 1040 mS/m up to 2490 mS/m. The most saline water is coming from a short hole drilled SE from the end of the drift.

2.4 Gases associated with deep groundwaters

In February 2002, five boreholes in the 1130 m exploration drift were sampled for gas. Sampling conditions were not ideal, because the boreholes were generally open in the case of the horizontal holes 1130-191, -192 and -197, or situated in shallow standing pools of water in the case of the near vertical holes 1130-175 and -176. Therefore, new sampling rounds were carried out in February and May 2003 after sealing and

pressurising the boreholes (for sealing dates, see Table 9). In addition to the boreholes listed above, borehole 890-188, 1130-217 and 1130-219 were also sampled in May 2003. Samples were collected to analyse the chemical and isotopic compositions of the gas, and a team from Carleton University, Canada sampled the noble gases. Water samples were taken simultaneously to achieve total geochemical characterisation of the groundwater.

The gas volumes released from a unit volume of water were estimated using the following arrangement. The packer valve was partly opened and adjusted to achieve a steady flow rate, water pressure at the collar was recorded. The gas was collected in a water-filled glass bottle submerged upside down in a bucket. When the gas volume, the flow rate and the collection time are known, the volume-volume ratio (approximating NPT, i.e., 1 bar, 25^{o}C) can be calculated. The results are presented in Table 5. The highest amount of gas, 0.5 L_{gas}/L_{water}, was observed in borehole 1130-192, which also has the highest salinity and the highest pressure. The other holes at this level had volume-volume ratios from 0.14 to 0.33 L_{gas}/L_{water}, while the borehole at the level 890 (890-188) produced only 0.09 L_{gas}/L_{water}. Volumes of gas per kg of water are, as expected, very comparable to those reported in Sherwood-Lollar *et al.* (1994) at a number of other crystalline shield sites.

Table 5. Gas volumes measured during the gas sampling at levels 890 m (borehole 890-188) and at 1130 m.

Borehole	Gas vol. (L)	Flow (L/min)	Coll. time (min)	Water vol. (L)	Gas vol. L_{gas}/L_{water}	pH	Pressure (bar)
890-188	0.4	0.62	7.3	4.53	0.09	-	-
1130-217	1.0	0.91	4.1	3.73	0.27	8.13	32
1130-191	0.7	0.47	4.5	2.12	0.33	8.18	32
1130-197	0.7	0.54	6.5	3.51	0.20	8.36	37
1130-192	0.4	0.27	3.0	0.80	0.50	8.4	50
1130-219	0.4	0.45	6.1	2.75	0.15	8.28	19

The volume percentages of component gases measured in gas samples from the 1130 m and 890 m level are given in Table 6. The hydrogen and carbon isotopic signatures of methane (C1), ethane (C2) and propane (C3) were also measured (Table 7). In Table 8, the chemical and isotopic compositions of the gases from Lupin are compared to those of gases measured for other Shield sites.

Table 6. Volume % of selected gases from several boreholes in the Lupin Mine. Samples collected in May 2003. ND = not detected.

Borehole	Methane	Ethane	Propane	Iso-Butane	Butane
	Volume-%				
890-188	74.38	0.547	0.0136	ND	0.000244
1130-175	86.73	1.894	0.0942	0.0067	0.00663
1130-176	84.68	1.604	0.0885	0.00754	0.00726
1130-191	80.81	1.486	0.08	0.004	0.00398
1130-192	85.72	2.053	0.1239	0.006	0.0063
1130-197	72.70	0.934	0.033	0.00116	0.000889
1130-217	85.90	1.613	0.083	0.0041	0.0043
1130-219	83.03	1.267	0.046	0.00116	0.000784

Table 7. Hydrogen and carbon isotope signatures of methane, ethane and propane of the Lupin Mine gas samples. ND = not detected.

Borehole	^{2}H			^{13}C		
	Methane	Ethane	Propane	Methane	Ethane	Propane
890-188	-359	ND	ND	-54.57	-37.79	ND
1130-175	-347	-249	ND	-44.73	-35.23	-32.11
1130-176	-344	-243	ND	-44.73	-35.69	-32.30
1130-191	-350	-253	ND	-45.72	-35.29	
1130-192	-329	-234	ND	-42.41	-35.53	-32.97
1130-197	-349	-231	ND	-48.65	-36.06	
1130-217	-349	-251	ND	-40.52	-35.69	
1130-219	-349	-228	ND	-47.73	-35.45	

Table 8. Comparison of Lupin gas with other Canadian and Finnish (*) Shield gases.

	CH_4	N_2	Ar	H_2	$^{13}C_{CH4}$	$^{2}H_{CH4}$
Lupin	NA	NA	NA	NA	-44	-321
Sudbury	12.5	72.2	3.9	NA	-27	-180
Thompson	52.2	43.2	0.52	NA	-55	-280
Matagami	87	8.53	0.13	NA	-50	-425
Outokumpu/Juuka*	78.9	6.32	<0.05	12.8	-25	-200
Ylivieska*	NA	NA	NA	NA	-45	-350
Enonkoski*	75.9	11.4	<0.05	0.04	-65	-350

In Figure 20, the $\delta^{13}C$ results for hydrocarbon gases associated with the deep groundwaters at Lupin (from the 1130 level) are compared to other gas data of both thermogenic and abiogenic origin from Sherwood Lollar *et al.* (2002). Based on the trend of $\delta^{13}C$ towards more positive values with increasing carbon number, and a comparison to other gases from shield environments, the gases collected at the 1130 level are predominantly thermogenic in origin. As in most Shield sites, there may also be a very old bacterial component.

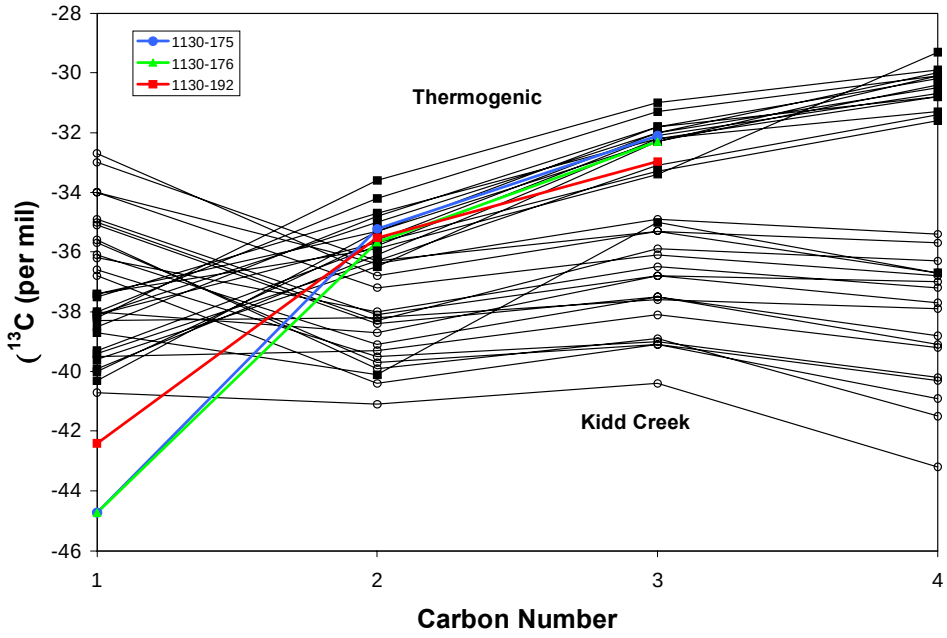

Figure 20. $\delta^{13}C$ Values of individual hydrocarbons versus carbon number for gas samples from the Kidd Creek mine, for thermogenic gases from southwest Ontario natural gas fields, and for gases associated with deep groundwaters (1130 m level) from the Lupin site (shown in colour). Modified from Sherwood Lollar *et al.* (2002).

In Figure 21, the isotopic compositions of methanes from Lupin are compared to other Shield sites in Canada and Finland. On this figure, the well-established fields for bacterial and thermogenic methanes are shown. Many of the sites have methanes outside or partially outside these fields. These methanes are thought to be abiogenic (high temperature, even mantle) in origin (Sherwood Lollar *et al.* 1989, 2002). The Lupin methanes would be classified as a mixture of abiogenic and biogenic, if only the bulk hydrocarbon $\delta^{13}C$ and $\delta^{2}H$ values were considered.

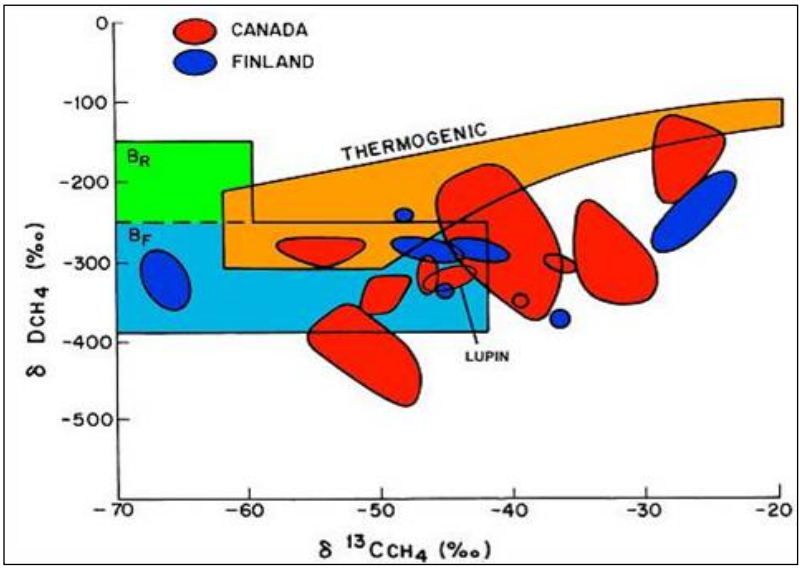

Figure 21. Isotopic Compositions of Methanes from Lupin Compared to Selected Canadian and Finnish sites. Modified from Sherwood-Lollar *et al.* (1989). B_R is the potential field of bacterial methane attributed to CO_2 reduction and B_F is the field of potential methanes attributed to acetate fermentation.

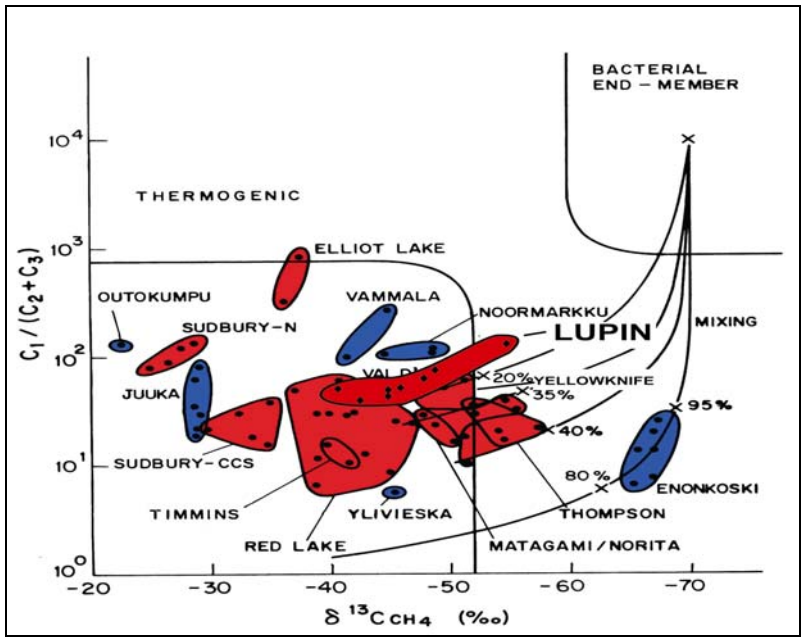

Figure 22. $\delta^{13}C_{CH4}$ versus C1/(C2 + C3) ratios for Canadian and Fennoscandian Shield gases. Adapted from Sherwood-Lollar *et al.* 1994.

Figure 22 attempts to further classify the Lupin hydrocarbon gases. The proportional volumes of C1/(C2 + C3) are plotted against the bulk ^{13}C value of the gases. Methanes from Lupin fall in a field dominated by many of the other shield sites, which are believed to be mixtures of abiogenic and biogenic gases. However, Lupin is the extreme (<10 %) of biogenic mixing. The ^{13}C of the dissolved inorganic carbon (DIC[2]) suggests that the enriched DIC may be derived from bacterial conversion of methane to CO_2. This in turn suggests that a small bacterial component of gas (< 1 %) with an unknown age may be present in some samples. Samples have been collected for dating the deep waters and the dissolved gas phase (^{36}Cl and ^{14}C). However, the isotopic signatures indicate that the gas is primarily thermogenic and most likely originates from depth.

Additional carbon isotope analyses (both ^{13}C and ^{14}C) on the dissolved inorganic carbon component show indications that much of the DIC may have resulted from degradation of the methane after initial thermogenic methane formation. The CO_2 produced for example, by acetate fermentation, can be incorporated into the dissolved carbon pool. Three boreholes 890-188, 1130-181 and 1130-192 gave ^{14}C pmc-values (percent of modern C) of 8.72, 2.78 and 16.2, respectively. However, the ^{13}C values were –8 ‰, -15 ‰ and +2 ‰, respectively. The enriched value for borehole 1130-192 (one of the most concentrated saline fluids), coupled with the holes higher than normal HCO_3 concentration, may indicate bacterial reduction/oxidation of methane. As well, very recent ^{13}C results on methane gas shows small (2 ‰) but consistent isotopic shifts in the gas signature of several boreholes. Further work will be concentrated on determining if the methane to DIC link is real, or if it is a modern present day borehole bacterial situation, or a palaeophenomenon.

In Figure 23, the $\delta^{13}C$ values are plotted versus their $\delta^{2}H$ values, and compared to abiogenic gases from Kidd Creek, and to thermogenic gases from southwest Ontario. Although $\delta^{2}H$ values for C1 – C3 components are available for gas samples from Lupin, $\delta^{13}C$ values are available only for C1 and C2 gas components. This increases the uncertainty of any interpretation of the trends in the $\delta^{13}C$ values as a function of $\delta^{2}H$. However, although the absolute $\delta^{2}H$ values of the Lupin gases are different from the other Shield gases plotted in Figure 21, it appears that there is a positive correlation between $\delta^{13}C$ and $\delta^{2}H$. This is an established trend for thermogenic gas reservoirs worldwide (Sherwood Lollar *et al.* 2002), and is significantly different from the trend observed for hydrocarbon gases from Kidd Creek (abiogenic).

The age of the bacterial methane and the DIC is not easily determined, because the ^{14}C component is most likely derived from a carbon pool older than the dating method (>60 000 years). As a result, measured ^{14}C values will be close to 0 pmc. The thermogenic component is most likely derived from metamorphic heating of the original ocean bottom sediments (turbidites) into the metaturbidites and amphibolitic gneisses at the Lupin site. In this case, the majority of the gas component could be billions of years in age.

---

[2] Within the considered pH-range, DIC is practically equivalent to HCO_3^-

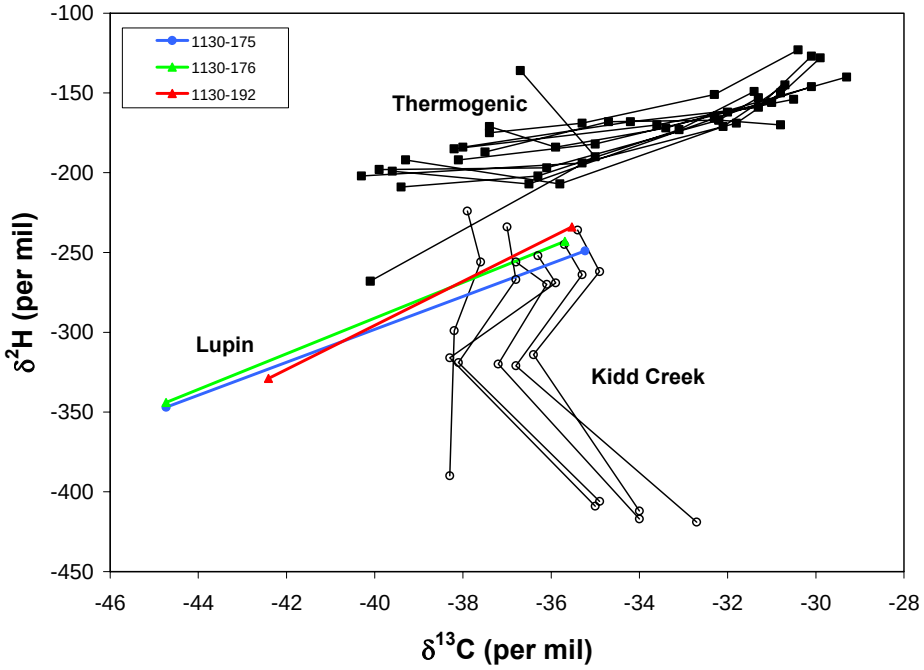

Figure 23. Plot of $\delta^{13}C$ vs. $\delta^{2}H$ values for C1 – C4 for samples from Kidd Creek, thermogenic gases from southwest Ontario, and from Lupin (Colour). Modified from Sherwood Lollar *et al.* (2002).

2.5 Hydrogeological studies

2.5.1 Video surveys

A video survey of the boreholes was continued during Phase II. Three existing boreholes reopened at 1130 level were recorded, as well as the new holes at the 570 m level. Currently the database includes information on the open fracturing from 13 boreholes from levels 250, 570, 890, 1105 and 1130.

Level 570

Due to the friction in boreholes 570-105 and 570-106 the survey was limited to 137 m and 281 m, respectively. Only a few minor fractures were encountered in these boreholes (Fig. 24).

It is known that a small amount of water is seeping into borehole 105 between the section 0 – 45 m. (see section 2.2.5). The video survey revealed 2 or 3 partially open vertical fissures and some minor channels in broken rock. None of them was observed to produce any water. It was very much the same in the next sampling section 45 – 150 m, as far as it was recorded. In borehole 106 the survey extended deeper, but only a few additional fractures were observed. As before, they are vertical and cut the schistosity (i.e they are not conformable). The hydraulic anomaly observed at 270 m of hole length during drilling seems to be due to a few fissures between 264 m and 280 m.

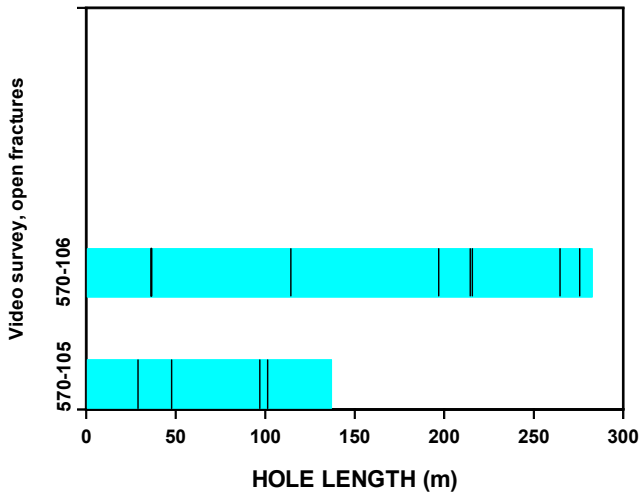

Figure 24. Open fracturing in boreholes 570-105 and 106 based on video survey. Thick line indicates several closely spacing fractures.

Level 1130

Borehole surveys at the level 1130 provides an opportunity to correlate open fracturing from one borehole to another. Boreholes 1130-219, -197, -192, -217 and -181 are located within 330 m in the same drift (Fig. 27). They are all drilled towards the east, and with the exception of borehole 219, they produce considerable amounts of water and gas. The latter hole is 330 m long, while the others are 440 – 570 m long.

It was possible to carry out video logging in boreholes 1130-197, -217 and in the first 100 m of borehole 1130-181. Boreholes 1130-192 and -219 had been surveyed earlier.

Boreholes, 1130-192 and -197, which have the highest hydraulic pressures have abundant, relatively evenly distributed open fracturing. Both vertical and subhorizontal sets are present. There are some fractures, which have apertures 1 – 2 mm, but a large majority have apertures well below 1 mm. Only rarely do these fractures appear in swarms. Usually, there are tens of meters or sometimes even a hundred meters of intact rock before the next open fracture is observed. Frequently the open fracturing is related to fine-grained, relatively homogenous cordierite bearing phyllite or greywacke. Typically the gas production is related to the minor fractures or shattered rock containing randomly oriented cracks.

An interesting comparison can be done between two of the boreholes, 1130-197 and 1130-219. The collars are 3 m apart and the longest distance between these holes is 70 m (Fig. 27). The first mentioned hole is 570 m long and the other is 330 m long. Both holes have been surveyed with the video camera. Within the common 330 meters, borehole 1130-197 intersects almost 30 open fractures, while the number in borehole 1130-219 is only 15. Further, in the latter only two larger fractures were observed. Most of the other fractures are only partially open. No gas was observed in this hole, but in 1130-197 several fractures were seen to produce gas. It is obvious that most of the fractures may be only poorly connected or not connected at all from one hole to another. This is demonstrated by the fact that the borehole 1130-219 was almost “dry” (<< 0.5

L/min) compared to the hole 197 (4.5 L/min) until the latter was pressurized. When the pressure in 197 was increased to over 30 bars the flow from 219 increased.

A similar comparison would be interesting between holes 1130-191 and 1130-217, which start basically from the same point and their azimuth differ by only 3 degrees. As a result, their maximum divergence is only 23 m at 440 m. The hydraulic tests and the pressure monitoring show that the holes have hydraulic connections (see sections 2.5.2). Unfortunately, it was not possible to remove all the plugs from 1130-191 and therefore the video log is available only from 1130-217.

Borehole 188 at level 890 is in a comparable position to hole 1130-197. These holes are assumed to intersect the same geological units. However, hole 188 has a distinctly different fracture pattern (Fig. 26). While open fracturing is relatively evenly distributed along the whole length of borehole 1130-197, in 890-188 most of the fractures are observed after 420 m and the mid-part of the hole is relatively intact rock.

Beyond 350 m distance to the east in this area of the mine, the existence of a major structure as speculated in Ruskeeniemi *et al*. 2002 is possible. In two long boreholes, 890-188 and 1130-192, the video survey terminated at a fragmented zone through which strong gas and water flow was observed. Borehole 1130-197 is also long enough (570 m) to intersect the same zone, but the video survey extends only to 423 m. However, the observed hydrogeological and hydrogeochemical compartmentalisation seems to provide evidence for a discontinuous hydraulic regime rather than laterally continuous planar hydraulic structures.

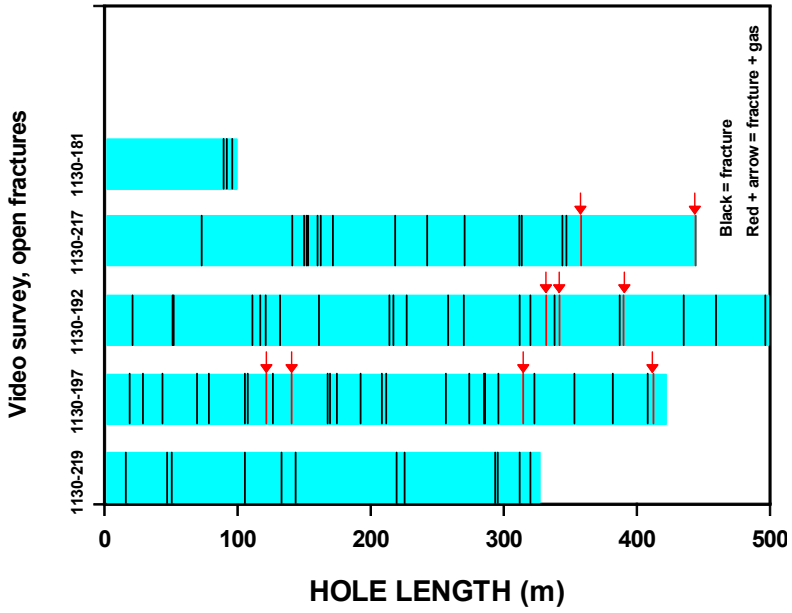

Figure 25. Open fracturing in certain boreholes at 1130 m level. Black lines indicate open fractures and the arrows show locations, where gas emanation is observed. For the relative locations of the boreholes see Figure 27.

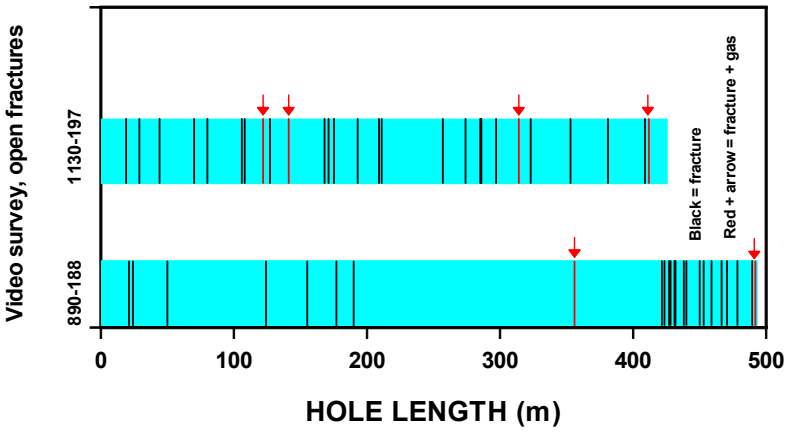

Figure 26. Open fracturing in boreholes 890-188 and 1130-197. For explanations, see Figure 25.

2.5.2 Pressure measurements in the mine

Hydraulic pressure measurements were included in the Phase II programme in order to obtain information on the prevailing hydrogeological conditions and to test whether accurate measurements could provide indications of connections between the subpermafrost regime and the surface. However the unexpectedly low water production of the new borehole 570-105 at the base of the permafrost forced a somewhat modified plan. The first priority became determining the depth of the groundwater table to assist the planning of the second borehole to be drilled at 570 m level. At the time only two water-producing boreholes, 1130-192 and 890-188, were available. All others more or less leaking boreholes had irremovable plugs. However, four other holes were later opened for research.

The project purchased mechanical margot-type plugs, which facilitated the sealing of a hole 3 m from the collar. This depth was assumed to be enough to avoid the interference of artificial fissuring generated by the mining activities. The margot-plugs have a half-inch lead-in. A valve and a standard, industrial pressure gauge were installed at the end of the plugs for long-term monitoring. The reading accuracy of the standard gauges range from about 20 kPa to 100 kPa (0.2 – 1 bar) and of the more accurate digital pressure gauges from 9 to 17 kPa (0.09 – 0.17 bar), respectively, depending on the scale of the gauge.

Hydraulic pressures have been measured in seven boreholes at levels 890 and 1130. All the monitoring holes, except borehole 1130-219, are drilled eastwards and they all produce water and gas. Borehole 1130-219 is about 330 m long and produced hardly any water before the nearby 1130-197 was plugged. All the other holes are roughly parallel, 400 – 570 m long and are all drilled within 250 m along the NE trending exploration drift. Figure 27 gives the location of the monitoring holes at 1130 m level. Borehole 188 at 890 m level is about 50 m shorter, but in a comparable position to 1130-197. The distance between the collars is 256 m. All the monitoring holes are horizontal (dip 0 degrees).

As mentioned above, the first measurements were carried out in the two available boreholes, 890-188 and 1130-192, during late 2002. In both holes the pressure increased to a certain level in a matter of hours and stabilised after a couple of days. Over time,

only a slow increase has occurred. The first results showed that the groundwater table has declined considerably below the permafrost, but also that there is a significant difference between the two holes (Table 9). The hydraulic head for borehole 1130-192 was at a depth of 672 m, while in borehole 890-188 it was 73 m lower. These results motivated the rehabilitation of five additional boreholes (1130-181, -191, -217, -192 and -197) at level 1130 in February 2003. At the same time it was found that the plug had popped out of 1130-192 and had to be reinstalled. One more borehole (1130-219) was rehabilitated and plugged in May 2003.

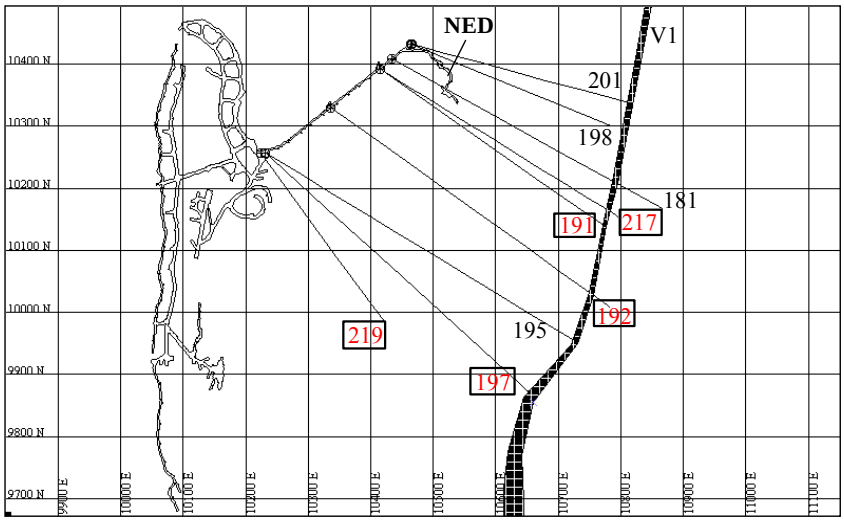

Figure 27. Monitoring boreholes (labels in boxes) at 1130 m level (Ruskeeniemi *et al.* 2002). The coordinate grid is shown with 100 m spacing. NED denotes for the New Exploration Drift completed in April 2002.

Table 9 and Figure 28 give the available readings. Borehole 1130-181 is producing water, but it is not pressurised, because the new drifting activity almost cuts the hole at the 100 m mark. Water and gas are bubbling from the floor of the drift through fractures, which likely intersect the borehole. The hole was clearly pressurised prior to the drifting on April 2002.

Boreholes 130-191 and 1130-217 start practically from the same point with only a small difference in the azimuth. They intersect the same fractures for most of their length and it is not surprising that they clearly interact and show similar pressures. However, slight differences in their vertical deviations result in preferential gas accumulation in borehole 1130-191. One badly leaking plug remained deep in borehole 1130-191 and it could not be removed. It prevented the video logging of the hole, but the hole was open long enough in front of this plug to allow the installation of the margot-type plug.

The pressure readings in borehole 1130-197 are probably lowered by the nearby borehole 195, which is plugged, but leaking through fractures cutting the hole behind the plug. This may explain why the analogous borehole 188 at level 890 has 116 m higher head than borehole 197. This is somewhat unexpected since they are assumed to intersect the same geological units. An increased outflow from borehole 1130-219 was observed after sealing borehole 1130-197 and, therefore, this hole was closed in late

May 2003. Nevertheless, hole -197 shows the highest heads after 1130-192. Boreholes 1130-195, 1130-197 and 1130-219 are located close to each other, but because their azimuths are different, they deviate quickly from one another.

Table 9. Hydraulic pressures in six boreholes and corresponding depths of the groundwater table assuming that 1 bar equals 10 m of water. The sealing dates of the holes are also given.

	Level 1130										**Level 890**	
	bh.197		**bh.192**		**bh. 217**		**bh.191**		**bh.219**		**bh.188**	
Observation date	bar	gw level	bar	gw level	bar	gw level	bar	gw level	bar	gw level	bar	gw level
6.12.2002			45,8	672								
9.12.2002											14,5	745
27.2.2003	26,0	870	46,0	670	20,0	930	20,0	930			18,0	710
25.3.2003	34,1	789	47,9	651	26,2	868	26,6	864				
28.3.2003											19,2	698
5.4.2003	34,5	785	48,3	647	27,6	854	28,3	847				
20.5.2003											20,4	686
21.5.2003	35,3	777	51,1	619	32,7	803	32,4	806				
25.5.2003									19,3	937		
24.8.2003	35,2	778	51	620	34,5	785	34,5	785	21,7	913	22,8	662
Sealing date	**25.2.03**		**3.12.02/ 22.2.03**		**24.2.03**		**24.2.03**		**24.5.03**		**5.12.02**	

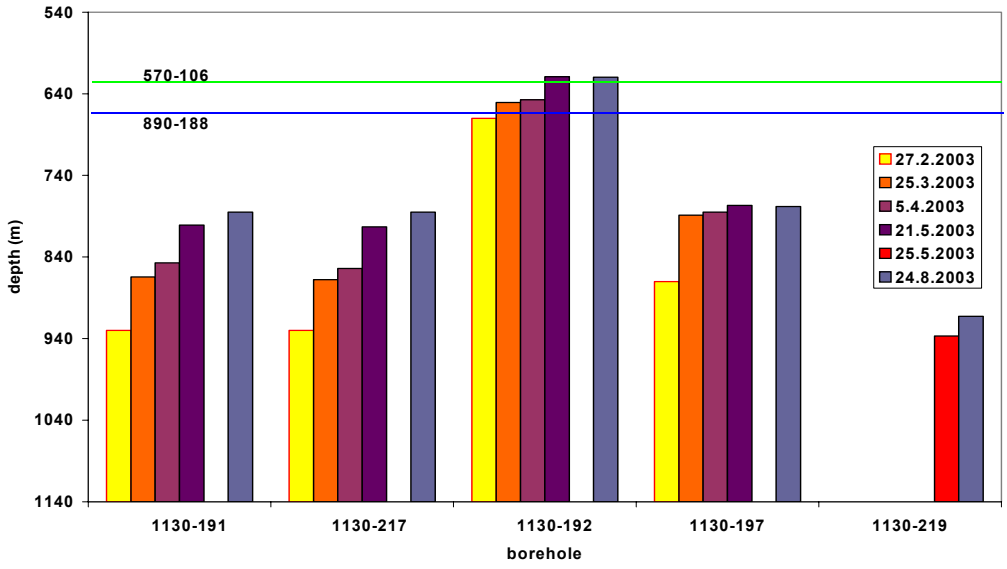

Figure 28. Change in the hydraulic head as a function of time. The depth is based on the hydraulic pressure observations in five boreholes at 1130 m level and in borehole 188 at 890 m level (see Table 9). For borehole 890-188 is given the depth based on the pressure reading from 24th of August 2003, which corresponds for the depth of 662 m (blue line). The green line at 631 m shows the water level observed in borehole 570-106 on 21st of May 2003. The base of the permafrost is at 540 m depth.

Although equilibrium has not yet been achieved, the results suggest that there is a considerable unsaturated zone below the permafrost ranging from 90 m to about 300 m in thickness. The hydraulic field is heterogeneous and nearby holes give different values, which may indicate that they are either not interconnected or only poorly connected. The connections between boreholes 1130-191/217 and -192 are especially poor. Although the distance between them is only around 100 m the heads differ by 165 m. Similar observations were made for borehole 890-188. Sealing of the borehole 1130-192 appears to have little effect to borehole 890-188. As mentioned above, borehole 1130-192 had become unplugged between Mid-December 2002 and Mid-February 2003. During this same period, the pressure in 890-188 had increased by 3.5 bars.

It should be noted, and will be discussed in later sections that the chemistry and dissolved solids (TDS) show considerable variation between the different boreholes. In May, 2003 an initial round of hydraulic tests between the various boreholes was attempted.

2.5.3 Hydraulic testing

Hydraulic testing on the 1130 m level was conducted with two goals: (a) to gain information on hydraulic parameters of the aquifer in the immediate area of the borehole being tested and (b) to gain physical evidence of borehole interconnectedness (or lack thereof) through fractures. For hydraulic testing, the existing pressure gauges were augmented by higher accuracy digital pressure gauges, with reading accuracies of between 9 and 17 kPa (0.09 – 0.17 bar), depending on the scale of the gauge.

Testing was conducted by opening the valve on a borehole. Flow was measured by filling a 16-liter bucket throughout the test, and then interpolating data for the intermediate times (Fig. 29). Drawdown was monitored on the digital gauges throughout the test. Boreholes were tapped for between 40 and 180 minutes. After shutting of the valve, borehole pressure recovery was monitored (as permitted by mining operations) until it had fully recovered to pre-test levels, typically less than 24 hours.

The first response test was conducted on borehole 1130-192. The valve was fully opened, until it appeared that the borehole would fully depressurize. As geochemical samples were to follow the testing, the valve was eased back to maintain pressure throughout the test. As such, only recovery data is available from this particular borehole.

Pumping and flow data are shown in Figures 29 and 30. Several researchers have shown the slope of a borehole response curve to be useful in the interpretation of data (Kruseman and de Ridder 1994, Horne 1995). The slopes of the borehole response curves in both wells at early time are equal to 0.5. This is typical for the linear flow period with a well parallel and perpendicular to a fracture (Kruseman and de Ridder 1994). As response trends towards late time, pseudo-radial flow becomes more pronounced. At late time, the slope does not trend towards 0.25; this indicates the fractures are of infinite conductivity (Kruseman and de Ridder 1994). Also, the lack of a slope of one at early time indicates negligible wellbore storage (Horne 1995).

Several curve-fitting approaches were tried in interpretation of the Lupin data. However, the drawdown and recovery curves did not match the solutions presented by the various methods. Ultimately, the data was analysed using the Cooper-Jacob straight-line method (Cooper and Jacob 1946). This method may be applied to fractured rock situations with the presumption that the medium is approaching homogenous continuum. Further, the method is applicable for long pumping time (straightening of the slope on the drawdown vs. log-time graph) and – finally – the method applies in describing the hydraulic conditions near the pumping well.

To solve for transmissivity using the Cooper-Jacob approach, drawdown is plotted against time on a semi-log scale (Figure 30). The early curve is attributed to skin effects. Once the curve straightens, slope is calculated over one log cycle and transmissivity is calculated using the equation:

$$T = \frac{2.3Q}{4\pi\Delta s} \qquad (2)$$

where T = transmissivity (m^2/s), Q = flow rate (L/min), and Δs = change in drawdown over one log cycle of time for the straight line portion of the curve.

As each borehole was tapped, pressures in nearby boreholes were monitored. Within the accuracy of the pressure gauges, no response was recorded on any test, except between boreholes 1130-217 and 1130-191, where pressures were the same in 1130-191 as in 1130-217 during the test on 1130-217. Further, comparing borehole response and recovery (Figures 30 and 31), the physical data collected from these tests suggest the fractures are disconnected or poorly connected.

Transmissivity values estimated from eq. (2) were $2.2 \cdot 10^{-6}$ m^2/s and $1.1 \cdot 10^{-6}$ m^2/s for boreholes 1130-197 and 1130-217, respectively.

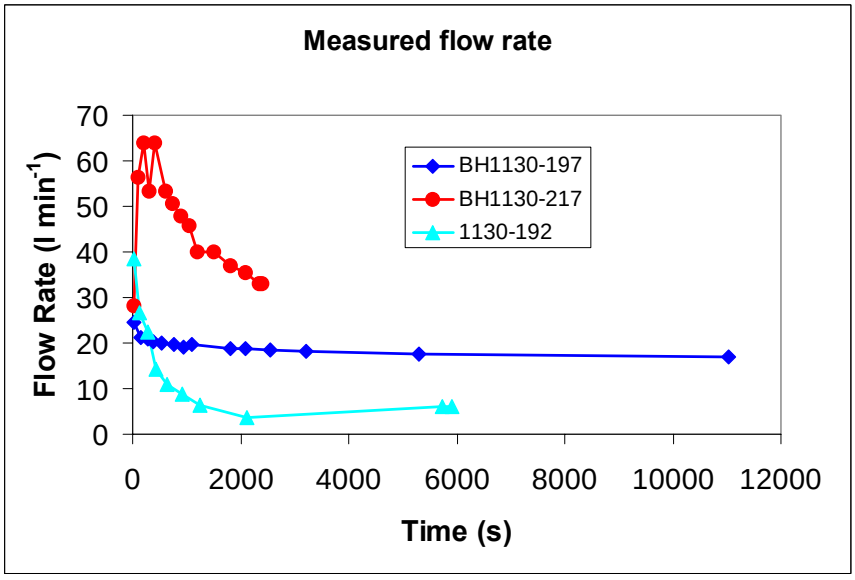

Figure 29. Measured flow rate in three of the test boreholes.

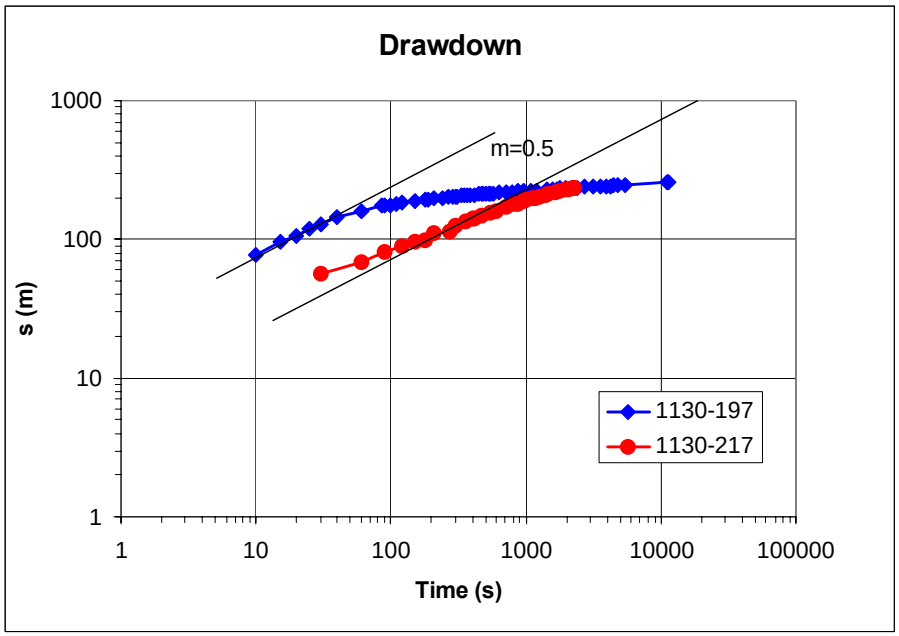

Figure 30. Drawdown vs. logarithmic time in boreholes 1130-197 and -217.

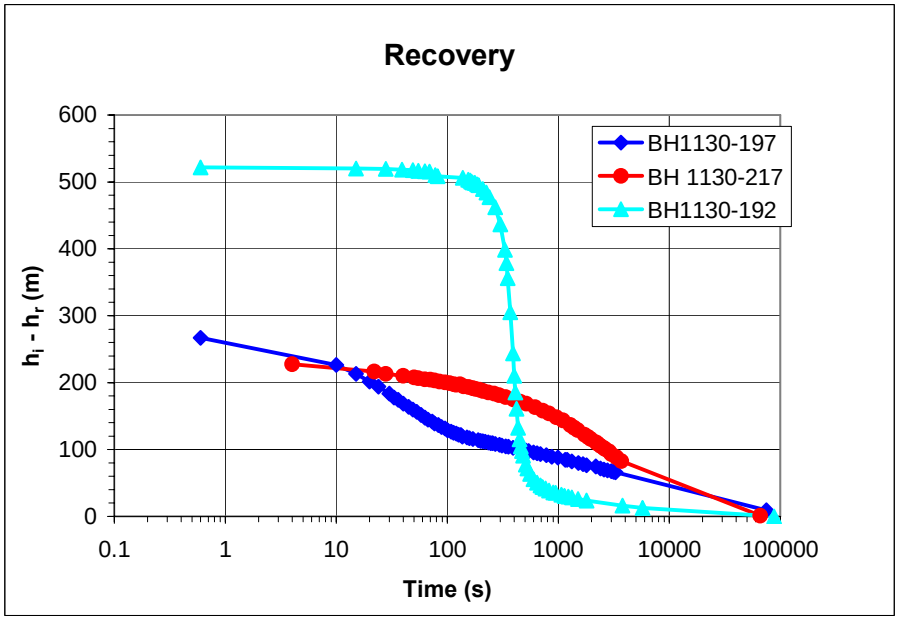

Figure 31. Recovery of the test boreholes.

2.6 Water-rock interaction studies

2.6.1 Crush and leach

The considerable chemical differences observed between waters from various boreholes prompted the development of a geochemical program to determine the rock matrix chemistry. It was felt that valuable geochemical and isotopic data, particularly across the permafrost boundary, could be extracted. Sections of core from an exploration borehole (890-188) and holes drilled by the Permafrost project (550-112, 570-105 and 106) have been chosen to represent the various rock types, subpermafrost and permafrost areas of the rock mass.

The core is photographed, and a small section (2 cm) is set aside for reference purposes. The remainder of the core is crushed coarsely in a jaw crusher, and then powdered in a shatter box for 3 minutes. The powdered solid is weighed, placed in a HDPE bottle, and an equal volume of doubly-deionized water is added. These slurries are then mixed continuously on a flat-bed shaker (side-to-side motion). After 24 hours of reaction, the slurries are filtered through a 0.2μm filter. If there is sufficient filtrate, an aliquot is reserved for stable chlorine-37 analysis, and the remainder is sent to the Geological Survey of Finland (GTK) for major ion analysis.

Concentrations of B, K, Li, Mn, Sr, Cl and Br are analyzed by ICP-MS; Ca, Fe, Mg and Na are analyzed using ICP-AES; Sulphate was determined by ion chromatography, and alkalinity is determined by titration. Leachates with sufficient total Cl^- (> 3.5 mg) are analyzed for stable chlorine isotopes using the CH_3Cl procedure modified from Long *et al.* (1993) at the University of Waterloo Environmental Isotope Lab (EIL). The analytical precision is 0.15 ‰ (1 σ), based on repeated measurements of Standard Mean Ocean Chloride (SMOC).

The results for the first eight crush and leach samples are presented in Tables 10 and 11. Leachates from the remaining 3 crush and leach tests performed to date (from borehole 550-112) are currently being analyzed.

The concentrations of the major ions in the rock are calculated as shown in the following example for core from borehole 570-105. From the chemical analyses, the Cl^- concentration of the leachate is 24 mg/L (Table 10). The crushed core was leached at a water:rock ratio of 1:1, using 504.86 grams of solid, and 0.504 L of doubly-deionized water.

- Mass of Cl^- released from the rock = (24 mg/L) · 0.504 L = 12.1 mg
- Cl^- concentration in rock = 12.1mg/504.86 g · 1000 g/kg = 23.96 mg/kg of rock (ppm)

In these calculations, it is assumed that all available chloride was released into the leachate during the 24 hour reaction period.

$\delta^{37}Cl$ signatures

To date, a total of 11 core samples have been crushed and leached. Of these, only five samples had sufficient chloride for $\delta^{37}Cl$ analysis. The results are presented in Table 11. In the on-going crush and leach experiments, larger quantities of rock material are used in an effort to increase the total mass of Cl^- available for stable chlorine isotopic analysis.

The results presented in Table 11 are very preliminary, but do present some interesting aspects for speculation. First, a review of Figure 46 shows the relationship between the $\delta^{37}Cl$ of the rock and groundwaters from the site. The rock samples from boreholes 550-112 and 570-105 at or near the permafrost boundary are quite positive and the 550-112 sample is very similar in value to the groundwaters taken from that borehole. The chloride released during the crush and leach is assumed to be from sources such as fluid inclusions and bound matrix salts. However, the absolute amount of chloride in many of these samples is very small, so a process involving Cl^- mobilization and freezing close to the permafrost contact can not be ruled out.

The $\delta^{37}Cl$ signatures of leachates from the rock matrix in boreholes 550-112 and 570-105 are more positive than SMOC (0 ± 0.15 ‰). In contrast, leachates from the 570-106 borehole which is angled downward, and from the deeper 890 m borehole have signatures that are essentially SMOC and slightly negative, respectively. A similar range of $\delta^{37}Cl$ signatures (between +0.1 and -0.3 ‰) were measured for the deeper groundwaters from the 1130 level (Fig. 46). This would suggest (based on a very limited data set), that there may be strong rock control on the source of chloride and the isotopic signature with depth (*i.e.* salts present in the deep groundwaters have in part been released from porewater from within the rock matrix). Additional measurements of the chlorine isotopic signatures of rock matrix fluids are required to verify these preliminary results.

Table 10. Chemical composition of leachates and calculated concentrations of major ions in rock (below).

Borehole	Depth (m)	B µg/l	K mg/l	Li µg/l	Mn µg/l	Sr µg/l	Cl mg/l	Br µg/l	Ca mg/l	Fe mg/l	Mg mg/l	Na mg/l	SO_4 mg/l	Alk mmol/l
570-105	32.10-32.28	55.6	66.3	111	1.99	29.8	24.0	224	9.98	<0.03	0.96	44.9	37.9	2.48
570-105	155.40-155.56	56.9	31.9	21.8	4.18	103	41.4	332	14.9	<0.03	0.78	62.5	33.6	2.17
570-106	99.10-99.25	25.0	19.3	0.65	0.141	4.25	9.46	98.1	0.54	<0.03	0.91	14.8	2.1	0.74
570-106	128.22-128.39	36.0	71.5	22.7	2.26	6.26	14.6	157	0.42	<0.03	0.48	42.9	13.6	2.43
570-106	179.63-179.87	45.1	53.5	3.71	3.84	23.3	71.7	947	3.63	<0.03	0.57	75.1	30	2.24
570-106	385.73-385.93	20.1	5.67	22.6	2.17	131	17.1	47.7	22.8	<0.03	3.85	4.3	18.1	0.89
890-188	42.82-42.98	32.9	89.7	29.6	0.498	13.7	30.8	442	1.63	<0.03	0.56	32.3	14.5	2.37
890-188	93.10-93.39	44.2	27.2	12.2	5.56	43.8	50.0	471	12.1	<0.03	2.76	67	24.9	2.35

Borehole	Depth	B	K	Li	Mn	Sr	Cl	Br	Ca	Mg	Na	SO_4
	(m)	mg/kg	mg/kg	mg/kg	mg/kg	mg/kg	mg/kg	mg/kg	mg/kg	mg/kg	mg/kg	mg/kg
570-105	32.10-32.28	0.0555	66.2	0.111	1.99	0.0297	24.0	0.224	10.0	0.958	44.8	37.8
570-105	155.40-155.56	0.0569	31.9	0.0218	4.18	0.103	41.4	0.332	14.9	0.780	62.5	33.6
570-106	99.10-99.25	0.0250	19.3	0.000650	0.141	0.00425	9.46	0.0981	0.540	0.910	14.8	2.13
570-106	128.22-128.39	0.0360	71.4	0.0227	2.26	0.00626	14.6	0.157	0.420	0.480	42.9	13.6
570-106	179.63-179.87	0.0451	53.5	0.00371	3.84	0.0233	71.7	0.947	3.63	0.570	75.1	30.0
570-106	385.73-385.93	0.0201	5.67	0.0226	2.17	0.131	17.1	0.0477	22.8	3.850	4.28	18.1
890-188	42.82-42.98	0.0329	89.7	0.0296	0.498	0.0137	30.8	0.442	1.63	0.560	32.3	14.5
890-188	93.10-93.39	0.0442	27.2	0.0122	5.56	0.0438	50.0	0.471	12.1	2.76	67.1	24.9

Table 11. $\delta^{37}Cl$ for core leachates.

Borehole	Depth in borehole (m)	Description	$\delta^{37}Cl$ (±0.15‰)
550-112	6.66-6.95	Before major fault; sub-permafrost	+0.212
570-105	155.40-155.56	Muscovite granite; sub-permafrost	+0.242
570-106	179.63-179.82	Muscovite granite; sub-permafrost	+0.027
890-188	93.10-93.39	Muscovite granite; sub-permafrost	-0.071

2.6.2 Fluid inclusions and fracture minerals

Fluid inclusion analyses and isotope geothermometry will be used on the limited fracture infillings found in cores and rock fractures. A number of recent Finnish and Swedish studies are claiming to have found evidence of glacially formed and glacial age calcites; it is therefore important to examine these minerals at a site in permafrost.

Fracture mineralization is sparse at the Lupin site. To date, just over 20 calcite infillings have been recorded. Most appear to be magmatic and occur in sealed fracture zones. Core samples and grab samples from the mine walls at depths from 60 m to 1130 m have been collected. The limited amount of calcite available is divided for isotopic (^{13}C-^{18}O) and fluid inclusion analysis. Fifteen polished thin sections for fluid inclusion analyses have been prepared for calcites from the 170 m level to the 890 m level (Table 12), and are ready to be analyzed on the fluid inclusion stage. Concurrently, additional samples are being prepared.

Table 12. Samples prepared for calcite fluid inclusion analysis. The first term in the borehole code indicates the level in the mine and the second term is the number of the hole.

Borehole	Interval (m)
170-135	60.75
570-105	123.68-123.96
570-105	123.68-123.96
570-106	31.28-31.43
570-106	277.4-277.65
570-106	288.37-288.64
570-106	375.55-375.7
570-105	353.91-354.15
570-105	511.64-512.00
570-105	283.17-283.39
570-105	416.90-417.08
890-188	61.75-62.11
890-188	493.26-493.48

2.7 Freezing experiments

The purpose of these experiments was to advance the understanding of groundwater hydrogeochemistry and isotopic systematics in crystalline shield settings as influenced by sub-zero temperatures. The study approach involved a series of controlled laboratory freezing experiments with several shield groundwaters conducted in parallel with theoretical thermodynamic predictions for the same experimental design. Key objectives of the study were: i) to measure changes in elemental compositions and isotopic systematics related to the freezing of Canadian and Fennoscandian Shield groundwaters; ii) to assess the importance of geochemical and isotopic signatures resulting from 'freezing out' on the recognition and interpretation of paleofluids; and iii) to conduct a preliminary assessment of solute and mineralogic implications for flow system characterization and evolution of Shield groundwater composition.

2.7.1 Methodology

Two kinds of experimental approaches were applied. The column experiments were designed to achieve a slower rate of freezing than in the batch experiments. The elemental and isotopic compositions of the ice as a function of progressive freezing and of the final residual solution were determined. Detailed descriptions of the experimental procedures, sampling and analysis for both the batch and column experiments can be found in Zhang and Frape (2003).

The groundwaters used in the experiments of Zhang and Frape (2003) spanned the range of shield groundwater compositions that would be found down to repository depths. Using these shallow saline fluids, the type of residual concentrated freeze-out solution that would migrate in front of a downward propagating permafrost layer into the depth range of a typical repository can be observed. Groundwaters from present research sites including a Na-Cl-SO_4 groundwater from the URL in the Canadian Shield (Canada), a Na-Ca-Cl water from Hästholmen (Finland), a Na-SO_4-type water from Palmottu (Finland), and a Na-HCO_3-Cl water from Äspö (Sweden) were used in the batch experiments (Fig. 32). The results from the column freezing experiment using Na-SO_4-type groundwater from Palmottu reported by Zhang and Frape (2003) has been augmented with an additional experiment using a Ca-Cl brine from Sudbury. The results of both these column experiments are reported in the following sections.

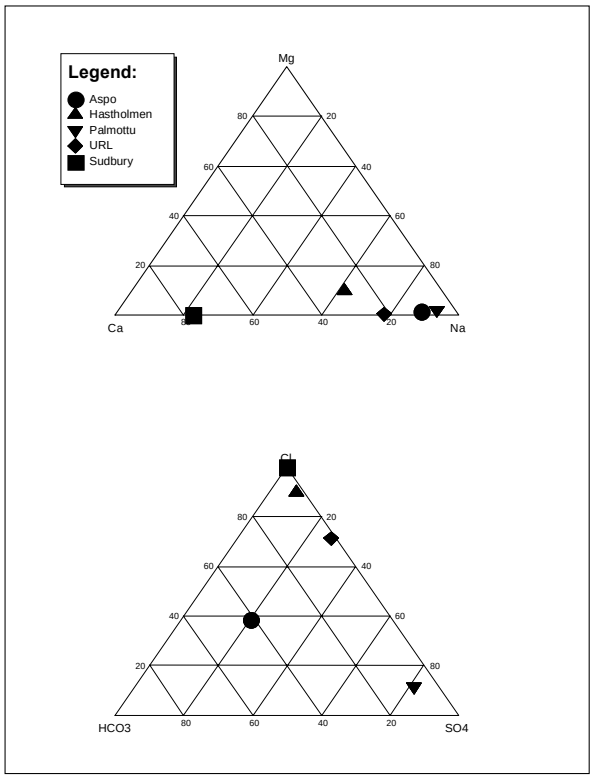

Figure 32. Trilinear diagrams showing the chemical compositions of groundwater samples used in this study.

2.7.2 Results and Discussion

In the column experiments, groundwater in a cylinder was frozen in stages by exposing small sections of the column to freezing conditions, while the remainder of the column was insulated. When the column was filled with ice, the residual solution was drained through an outlet at the bottom of the column. The ice was removed and cut into segments. The residual solution and the solutions from the melted ice segments were analyzed for their chemical and isotopic compositions (Zhang and Frape 2003).

Electrical conductivity measurements of the melted ice segments from both experiments are plotted in Figure 33; the residual solution from freezing of the dilute Sudbury groundwater is also plotted. Ice segment number 1 indicates earliest-formed ice (at the top of the column), while higher numbers indicate ice formed at later stages in lower portions of the column. A similar increase in the electrical conductivity of water from ice segments is seen with progressive freezing in both column experiments. Because conductivity is proportional to solution concentration, it is evident from these results that the ice formed during early stages of freezing contained smaller quantities of ions. During freezing, the residual solution becomes more concentrated due to salt rejection from the ice. Inclusions of this increasingly more concentrated residual solution as fluid trapped between or within ice crystals is the most likely source of the solutes measured in the ice during later stages of freezing.

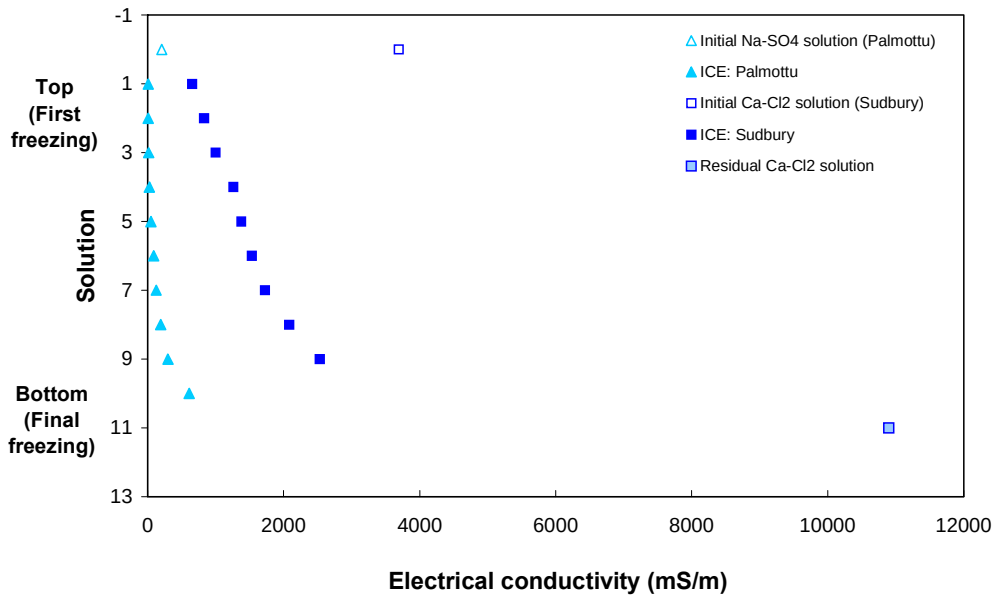

Figure 33. Electrical conductivity of water from ice segments and residual waters from the freezing experiments using groundwater from Palmottu, Finland and a diluted (1:10) Ca-Cl brine from Sudbury, Canada.

Changes in the major ion concentrations in the ice segments within the column with progressive freezing of the Palmottu and of the Sudbury groundwater (diluted by a factor of 10) are shown in Figure 34. With progressive freezing, the concentrations of all ions show a similar trend towards increasing concentrations, indicating that preferential incorporation of ions by the ice structure did not occur under these experimental conditions. This trend is approximately linear in the column experiment with Palmottu groundwater, which had lower initial ion concentrations than the Sudbury groundwater. Because the initial concentrations of ions in ice from the Sudbury groundwater were higher than in the Palmottu water, the increase in their concentrations with progressive freezing to the last ice segment (no. 9) is less pronounced.

In the freezing experiments with the Palmottu groundwater, the concentrations of major ions in the ice formed in the column experiment were more than one order of magnitude lower than measured for ice from the batch experiment during the early stages of freezing. At the slower freezing rate used in the column experiments, substitution for H+ and OH- in the crystal lattice of ice is likely the dominant mechanism for ion incorporation. Because the lower freezing rates used in the column experiments are closer to the rates expected under permafrost conditions, the solution concentrations measured better represent the type of solutions that would likely form during freezing due to permafrost.

The isotopic compositions of hydrogen, oxygen and chlorine measured in the ice segments and in the residual solutions from both column experiments are recorded in Table 13. It should be noted that in the second column experiment, the δ^2H and $\delta^{18}O$ values of the initial solution are those of diluted Sudbury groundwater (*i.e.* mixed signature of the Ca-Cl brine and doubly-deionized water). The original groundwater, or Sudbury S-138, has δ^2H and $\delta^{18}O$ signatures of -10.9 and –44 ‰, respectively (Fig. 35).

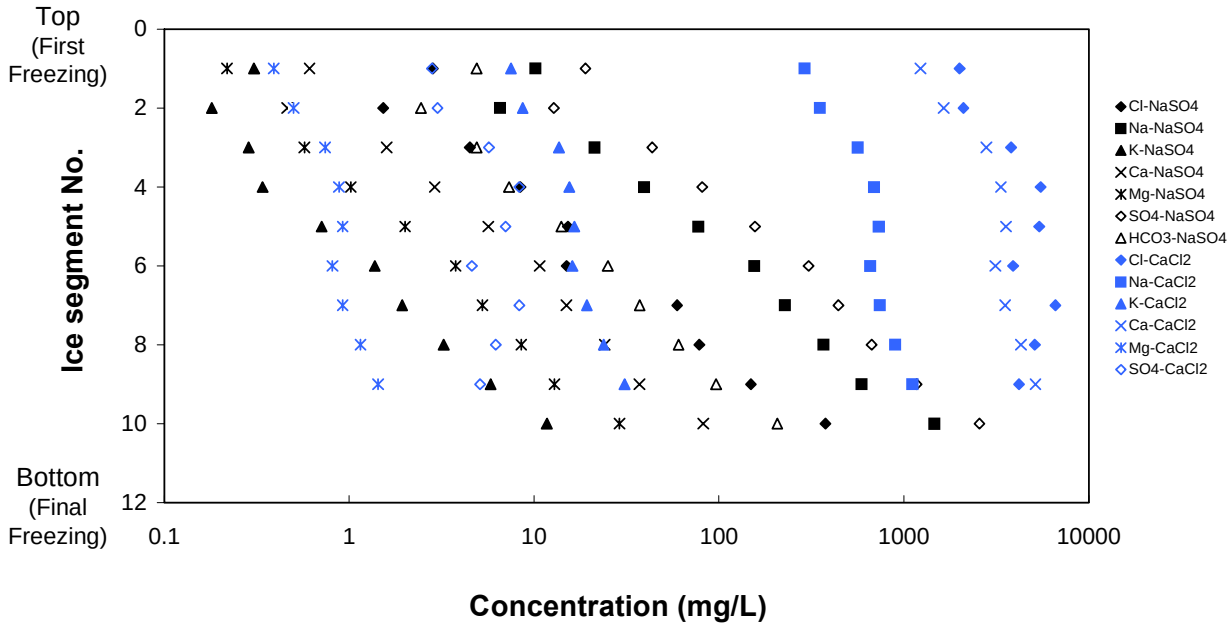

Figure 34. Concentration of major elements in the ice samples taken from column experiment with a groundwater from Palmottu, Finland ($Na\text{-}SO_4$) and a Ca-Cl groundwater from Sudbury, Canada.

Table 13. Hydrogen, oxygen and chlorine isotopic compositions measured in the column freezing experiment of the Palmottu groundwater, and in the diluted Ca-Cl type water from Sudbury (INS= Insufficient Cl^- for Analysis; N/A= not analysed).

Solution	Palmottu δ^2H (‰ VSMOW)	Palmottu $\delta^{18}O$ (‰ VSMOW)	Palmottu $\delta^{37}Cl$ (‰ SMOC)	Sudbury δ^2H (‰ VSMOW)	Sudbury $\delta^{18}O$ (‰ VSMOW)	Sudbury $\delta^{37}Cl$ (‰ SMOC)
Initial solution	-137.14	-18.65	0.87	-10.57	-74.93	-1.42
Ice segment 1	-124.45	-16.10	INS	-8.21	-60.73	-0.36
Ice segment 2	-126.05	-16.72	INS	-9.14	-63.85	-1.23
Ice segment 3	-129.80	-17.19	1.33	-9.50	-65.99	-1.33
Ice segment 4	-132.75	-17.63	1.30	-9.48	-67.60	-1.33
Ice segment 5	-136.95	-18.32	1.56	-9.68	-69.54	-1.34
Ice segment 6	-141.40	-19.00	1.41	-10.01	-69.81	-1.43
Ice segment 7	-144.35	-19.65	1.25	-10.02	-71.79	-1.34
Ice segment 8	-150.25	-20.40	1.10	-10.19	-72.70	-1.35
Ice segment 9	-154.75	-21.25	0.95	-10.87	-73.99	-1.34
Ice segment 10	-158.10	-21.69	0.72	N/A	N/A	N/A
Residual	-195.55	-26.45	0.83	-12.82	-97.27	-1.33

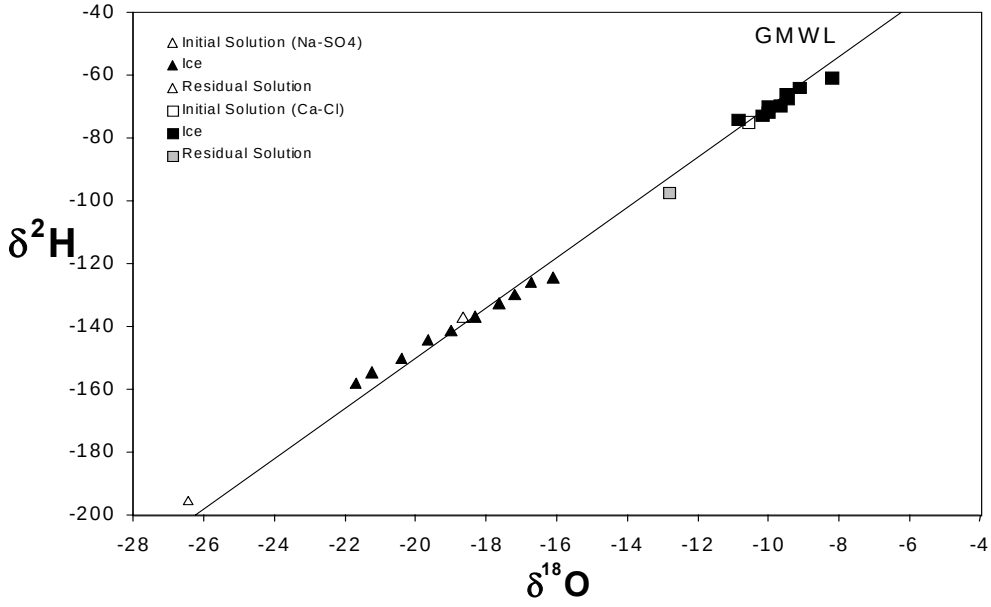

Figure 35. δ^2H vs. $\delta^{18}O$ for solutions from the column experiment with Palmottu ($Na\text{-}SO_4$) and Sudbury (Ca-Cl) groundwaters.

The enrichment in δ^2H and $\delta^{18}O$ measured in the ice from the column experiment with Palmottu groundwater is larger than that measured in the batch experiments (Fig. 35). Similar to the batch experiments, a linear relationship was observed between δ^2H and $\delta^{18}O$ for samples of ice and residual water taken from both column experiments. Favourable comparisons of the observed ^2H and ^{18}O isotopic fractionation in the experiment with Palmottu groundwater were found with those predicted using fractionation factors reported in the literature.

In the column experiment with the relatively dilute $Na\text{-}SO_4$ groundwater from Palmottu, the $\delta^{37}Cl$ signature for the first ice segment with measurable Cl^- (ice segment No. 3) is approximately +1.4 ‰ (Figure 36). This is enriched compared to the initial solution with a $\delta^{37}Cl$ of +0.87 ‰ by +0.53 ‰, and indicates that the heavier isotope (^{37}Cl) is preferentially incorporated into the ice. The Ca-Cl solution prepared by 1:10 dilution of a groundwater from Sudbury had an original Cl^- concentration of 16 000 mg/L, and a $\delta^{37}Cl$ signature of –1.4 ‰. The concentration of Cl^- in the first ice segment was 2000 mg/L, with a $\delta^{37}Cl$ signature of -0.4 ‰ (based on two replicate analyses). The enrichment in ^{37}Cl in ice is consistent with observations from the Palmottu column experiment, except that the observed shift in $\delta^{37}Cl$ is approximately double (+1.0 ‰). This is surprising, because based on the Palmottu column experiment no measurable chlorine isotopic fractionation would be expected when the Cl^- concentrations in the ice were greater than 100 mg/L. However, no fractionation is observed in the 2nd ice segment of the diluted Sudbury groundwater (Cl^- concentration of 2100 mg/L) or in the remaining ice segments; the $\delta^{37}Cl$ signatures of the ice segments are the same as the original solution, within analytical uncertainty. It is not known whether the chlorine isotopic fractionation observed in the 1st ice segment is real or an experimental artefact.

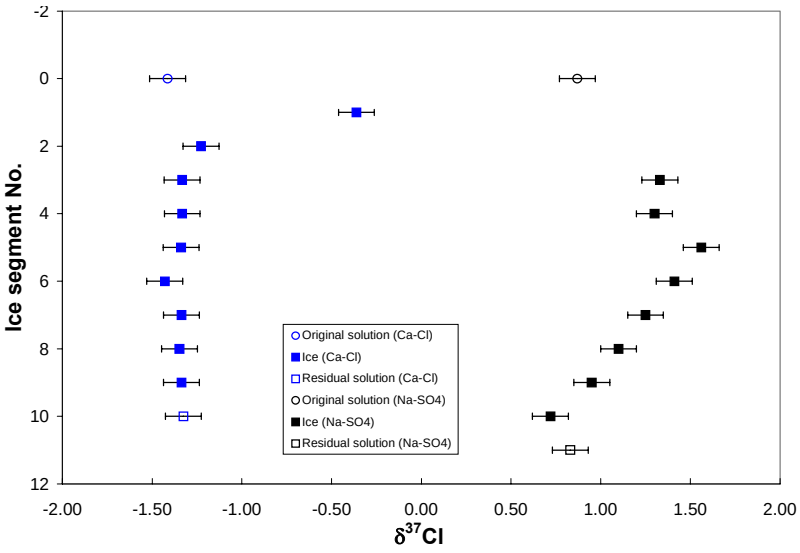

Figure 36. $\delta^{37}Cl$ signatures in ice segments during progressive freezing of the Palmottu (black) and diluted Sudbury (blue) groundwaters.

For the Palmottu groundwater, a gradual depletion in the chlorine isotopic composition was observed (Fig. 37A) from the early-formed ice to ice formed at the end of the experiment. A similar trend was seen in the hydrogen and oxygen isotopic compositions. As a result, a positive correlation between $\delta^{18}O$ and $\delta^{37}Cl$ was measured in the ice samples (Fig. 37B). However, the reasons for depletion in these isotopes are different. As more ice formed in the system, the residual solution became more depleted in both $\delta^{2}H$ and $\delta^{18}O$, which in turn resulted in a gradual decrease in the $\delta^{2}H$ and $\delta^{18}O$ values of the ice samples. In contrast, the chlorine isotopic composition remained unchanged in the solution with the freezing process, because the structurally-bound chloride only accounted for a very small percentage of the total amount of chloride in the solution. At the late freezing times, fluid inclusions became the major source of chloride in ice samples. As a result, the measured chlorine isotopic signatures mainly reflect those of the free chloride, *i.e.* the chlorine signature of the residual solution.

Compared to Canadian and Fennoscandian Shield groundwaters, the compositions of the experimental residual brine generally plot at higher sulphate concentration for a specific chloride concentration. In order to achieve the chemistry of typical concentrated brines found at shield sites, most of the sulphate must have been removed from the residual solutions. Two mechanisms for sulphate removal are (1) further concentration of the residual solution to precipitate SO_4 mineral phases such as mirabilite ($Na_2SO_4 \cdot 10H_2O$) and barite ($BaSO_4$) and/or (b) removal of sulphate by reduction to sulphide. Both processes could be invoked at typical shield sites under permafrost conditions. As for the conservative ions Br and Cl, the most concentrated residuals for all but the Palmottu waters are outside typical concentrated shield saline fluids and brines. In order to match typical shield fluids, the temperature of the very low volumes of residual fluid (< 2 % of original) would have to be decreased to below the eutectic point of hydrohalite (-21°C). This would allow precipitation of Cl phases and concentrate Br relative to Cl. The experimental data on $\delta^{2}H$ and $\delta^{18}O$, as well as many of the Shield groundwaters fall close to or on the GMWL.

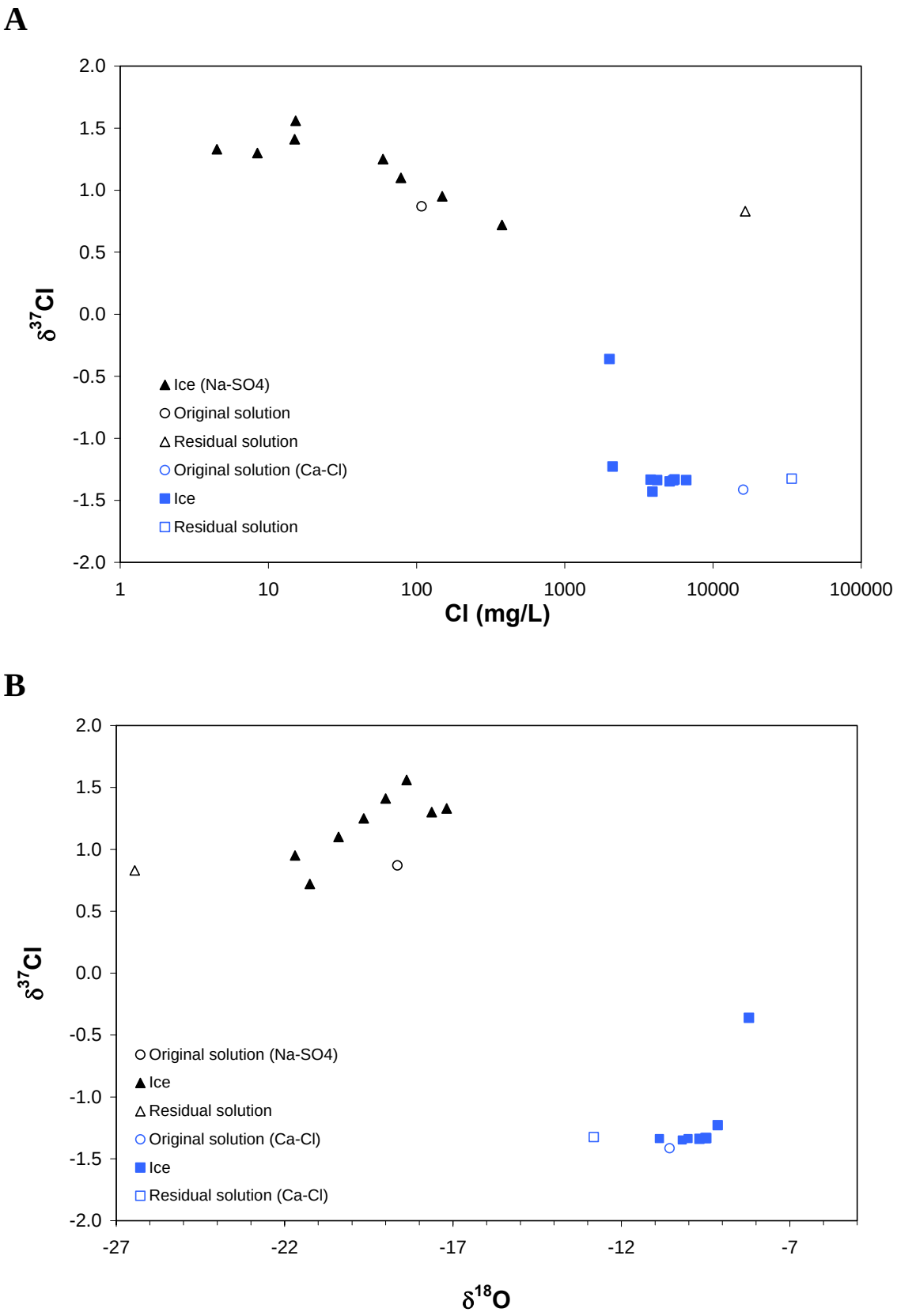

Figure 37. (A) Chlorine isotopic composition vs. Cl concentration; (B) Chlorine isotopic composition vs. oxygen isotopic composition. Data are from column experiments with Palmottu and diluted Sudbury groundwater.

3 Discussion of the results

3.1 Surface hydrology

The Lupin area is situated about 450 m above sea level (m.a.s.l) and has been dry land for a long time before the Quaternary. The landscape is relatively flat with a height variation in the range of 30 – 40 m. (Fig. 38). The highest locations (elevation over 479 m) are 3.5 – 5 kilometers to the NW, W or SW from the mine. The topography is characterised by low eskers and/or delta formations and flat boulder fields or outcrops (Ruskeeniemi *et al.* 2002). The mine is located on a hill, which is about 30 m above the lake surface.

The research area, like other permafrost areas, is characterised by a large number of smaller and larger lakes and ponds. They are located at variable topographic positions. Due to the impermeable frozen soil, water collects in any significant depression. Most of the lakes are shallow and are likely to freeze down to the bottom during winter. Generally, freezing begins in mid-September and all the lakes, including Lake Contwoyto, are frozen by mid-November. The ice starts to melt in early June and most of the lakes are open by late June. Some of the lakes/ponds are interconnected forming complex waterways, which collect the surface waters around the mine and discharge them to Lake Contwoyto. The lakes have three main water sources: 1) melt water in spring time, 2) precipitation and 3) melting ground ice/permafrost.

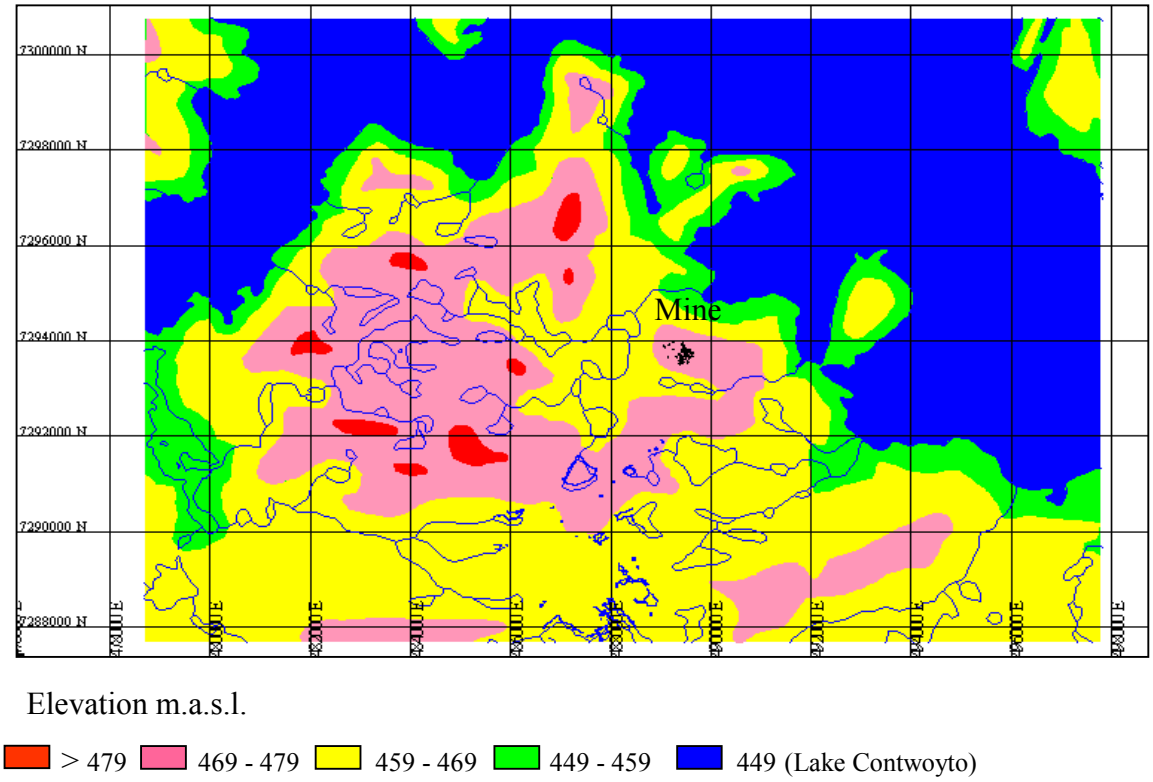

Figure 38. The regional topography and the main watercourses in the surroundings of Lupin. The area of the map is c. 19 km x 13 km (Ruskeeniemi *et al.* 2002).

The snow cover is rather thin and has a low water content due to the dry and cold climate. However, strong winds tend to build up thick snowdrifts in sheltered slopes where the melt water finds collects in local depressions. Only a small portion of the melt water percolates into the soil, because the ground is frozen and the active layer is very thin. Most of the annual rain falls in August – September, and the mean annual precipitation is 270 mm (see Ruskeeniemi *et al.* 2003). The moisture may originate either from the Atlantic or Pacific Oceans or from the Arctic Ocean in the north, which results in a considerable variation in the isotopic composition of the rainwater (IAEA/ISOHIS 2001). Melting ground ice provides an extensive and continuous water source during the warm summer months. The typical silt moraines in the area are saturated by a mixture of rainwater and water from melting ground ice prior to the freezing. The following summer this water is released by the advancing active layer, which may extend to depths of about two meters. Some of the observed springs are assumed to be dependent on this type of water source.

A fourth, still hypothetical water type could be water derived from discharging deep groundwaters. This situation might arise due to the presence of a talik structure related to a major fault.

3.2 Hydrogeological conditions

3.2.1 The unsaturated zone

Drilling from the mine at the 570-m level revealed the existence of an "unsaturated" or dewatered zone below the permafrost. Pressure monitoring at deeper saturated levels 890 m and 1130 m indicated that the highest water table is approximately at a depth of 620 m below surface (Fig. 28, borehole 1130-192). Consequently, there seems to be about 100 m of unsaturated zone below the permafrost. At least some of the pressure-monitored boreholes may be short-circuited via fracture zones, giving lower head values. However, water table logging at borehole 570-106 gives consistent head values with pressure data from the 1130-192 and 890-188 boreholes.

The question still remaining is whether the dry zone is a natural phenomenon related to the growth of the permafrost or if it is a local draining effect due to the mine. Based on the flow measurements carried out in a number of boreholes (see Ruskeeniemi *et al.* 2002) the groundwater inflow into the mine is roughly estimated to be about 20 000 m^3/y. The most productive boreholes were drilled during the period between 1992 and 1993. It is evident that even with these relatively low out-flow rates a depression in the groundwater table could be generated in the vicinity of the mine. However, there are indications, which suggest that the dry zone might be of natural origin:

- The longest pressure-monitored boreholes and the newly drilled research boreholes at 570-m level reach almost 600 meters away from the mine. They are drilled perpendicular to the schistosity and the interpreted main fracture directions. The intact sections between them are considered to prevent hydraulic connections with the mine. Thus, the measured pressures represent a large bedrock block, where the effect of the mine is assumed to be limited.

- The geophysical SAMPO soundings carried out in the area between the mine and Lake Contwoyto provided consistent information on a deep conductive

layer. This layer was interpreted to represent the upper surface of a saline groundwater. The survey could not be extended near the mine proper, because of man-made constructions. It turned out, however, that the western end of the west-east trending survey line 1 (see Fig. 2) almost overlaps the most critical boreholes used in head monitoring.

The original reasoning for conducting the SAMPO soundings was to detect a saline out-freezing front, if present, at the base of the permafrost, which occurs at a depth of 540 m in the mine. However, in most of the profiles the subhorizontal conductor was observed somewhat deeper than expected. As a rule, the SAMPO-results are in good agreement with the head-monitoring data (Fig. 39). Therefore, the upper surface of the interpreted conductor at around 650 m does not necessarily represent the depth of the permafrost, but probably indicates the groundwater table. From a methodological point of view, the resistivity contrast between unsaturated and saturated rock is clear enough to be observed by SAMPO soundings. In this case, the salinity in the saturated zone is not an issue, but the presence or absence of water is critical. The discrepancy between the geophysically interpreted depth of conductive layer and the water table close to the mine can be explained by the disturbance of the mine construction, or possibly by the extensive use of salts in the mine (the increase in the conductivity of the bedrock block causes a bias in the model calculations).

The SAMPO method has been successfully used in Finland to map deep groundwaters in four of Posiva's candidate sites for a radioactive waste repository (Paananen *et al.* 1991, Paananen *et al.* 1994a,b, Jokinen *et al.* 1995, Heikkinen *et al* 1992, 1996). The method was also successfully applied in determining the depth of saline water bodies below the Antarctic ice sheet (Ruotoistenmäki and Lehtimäki 1997, 1999). Clear indications of saline or brackish waters were obtained from the surveys, showing good agreement with the hydrogeochemical data. In Olkiluoto, the interpreted depth of saline water usually varied between 100 and 500 metres with typical water resistivities of 0.4 – 2 ohmm, corresponding TDS values between 3.2 and 16 g/L. These values are very comparable with the TDS values observed at Lupin, thus demonstrating the applicability and the resolution of the sounding method in comparable bedrock conditions.

Another important issue raised by the results of the SAMPO soundings was that the weak conductor observed in schist is consistently absent in granodiorite. Two separate sounding lines crossing the contact between the schists and the granodiorite were measured. In both cases the weak conductor dissappeared as soon as the contact was crossed (Paananen and Ruskeeniemi 2003). At the same time the bedrock resistivity increased from 10000 ohm to 30000 ohm and remained constant thereafter. All the apparent resistivity versus depth curves calculated for the numerous sounding points within the granodiorite show only homogenous highly resistive rock down to 1000 m, which was the limit for the applied configuration.

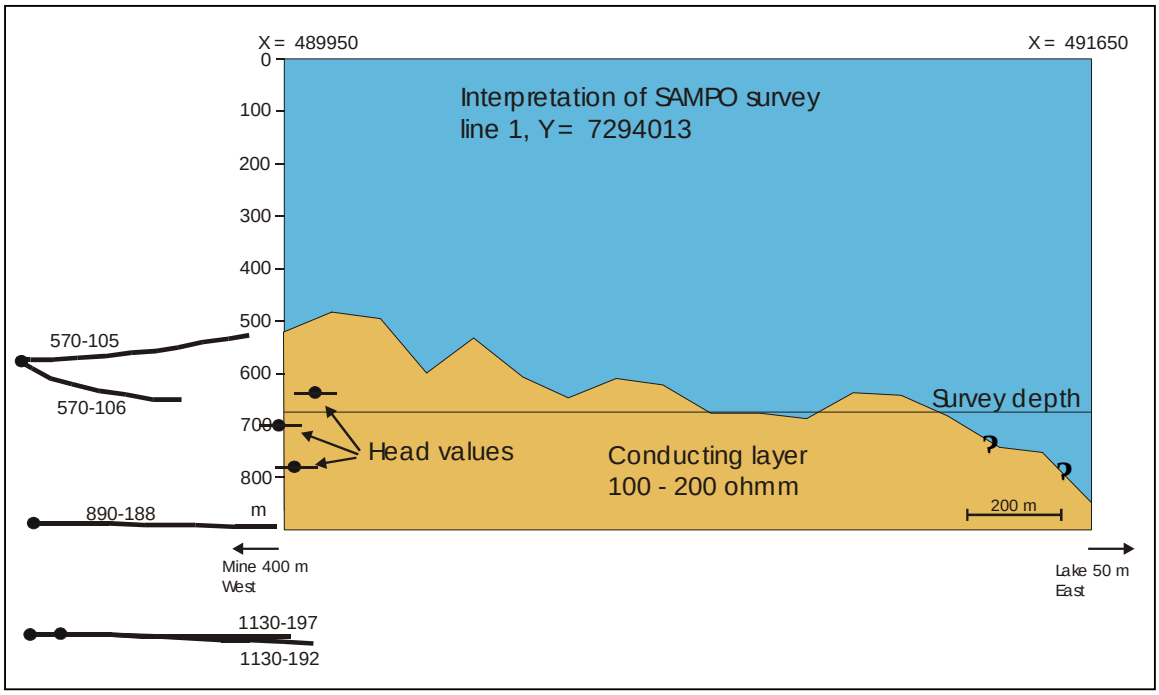

Figure 39. A collage of SAMPO survey line 1, E-W trending vertical section (see Fig. 2). Five boreholes and three head values from boreholes 890-188, 1130-192 and 1130-197 are also shown.

The southern test line close to the tailing ponds was trending across a shallow hill, where the plutonic rock is exposed. The granodiorite outcrops are sparsely fractured and because the rock type is not orientated the discontinuities parallel to the foliation are also missing. Vertical fracturing exists and there are some terraces, which probably indicate subhorizontal fractures, but their spacing is generally several metres or more. The lack of frost heaving, so typical for the schist outcrops, further underlines the intact nature of the granodiorite. It is suggested that the absence of the electromagnetic anomaly is due to the low porosity and consequently, the low water content in this type of rock.

In principal, the permafrost will extend deeper in formations where only small amounts of water have to be frozen to ice (*i.e.* the porosity is low). Although the permafrost is probably deeper in this type of rock than elsewhere at Lupin, it is not likely that it would extend to 800–1000 m, which was the depth limit of the Sampo survey. It is more plausible, that the low porosity and weakly connected migration routes have prevented the increase of salinity postulated to be due to out-freezing and/or the amount of the weakly saline matrix water is simply too low to generate a contrast strong enough to be observed at great depths.

3.2.2 Flow routes and the hydraulic properties of the bedrock

The hydraulic properties of the bedrock are very important when considering the possible hydrogeochemical affects of the propagating permafrost. To be effective the chemical and isotopic fractionation possibly related to the freeze-out process needs a continuous supply of water, as well as routes for the residual freeze-out fluid to escape.

On a broader scale, the groundwater flow conditions below permafrost linked with the overall long-term hydrogeochemical stability are strongly connected to the permeability of the bedrock. Consequently, considerable effort has been made to increase the understanding of the location and nature of the hydraulic zones within reach of the mine. Geophysical methods, down-hole video surveys and hydraulic testing have been applied to aid the interpretation.

In low-porosity crystalline rock, water is mainly found and focussed in zones of broken rock, *i.e.* water-bearing structures. An interconnected network of fractures rather than pervasive planar fault-type structures are responsible for the hydraulic conductivity within the first 350 m of bedrock east from the mine. However, frequently, but not always, the open fracturing is clearly related to healed fractured rock, where tight or sealed fractures are abundant. During drilling, many of these discontinuities tend to open resulting in high fracture frequencies in drill core samples. Thus, the core log alone is not necessarily a sufficient indication of potential hydraulic zones. However, the indirect geophysical methods benefit from the increased fracturing and can be applied to locate potential hydraulic zones. Indeed, some indications of such N-S trending, faulted zones were observed in the seismic survey (Ruskeeniemi *et al.* 2002).

Certain features seem to be typical for the open fracturing at Lupin. Both vertical and subhorizontal sets are present. Fracturing parallel to schistosity seems to be predominant in the former type, but the observation may be biased by the fact that most of the observations were from boreholes drilled across the schistosity. There are some fractures, which have apertures 1 – 2 mm or even larger, but a large majority have apertures well below 1 mm and sometimes only point-like channels are observed. Only rarely do these fractures appear in swarms. Usually, there are tens of meters or sometimes even a hundred meters of intact rock before the next open fracture is observed. Frequently, the open fracturing is related to fine-grained, relatively homogenous cordierite bearing phyllite or greywacke. Usually it is not possible to see any evidence of water flow from a single fracture, but gas bursts into the water-filled hole are easier to observe. Although the gas flow towards low-pressured holes cannot be used as an absolute indication of water flow, it is probably the case. Only a few fractures produce gas and most of them are at the lower end of the holes (Figs. 25 – 26). Gas production is typically related to single, minor fractures or shattered rock containing randomly oriented cracks. The gas emanation can be taken as evidence of a network with roots extensive enough to collect and conduct dissolved gas from a wider area. Clearly the aperture of the fracture and its length do not necessarily correlate. A clear example of this would appear to be the significantly wide fault 1.5 to 2.0 m in borehole 550-112 and the appearance of this fault with a width of only 10 to 30 cm at a distance of 50 m away on the ramp.

The hydraulic field is heterogeneous and nearby research holes give different pressure values, which may indicate that they are either not interconnected or are only poorly connected. Especially poor hydraulic connections along the strike of the schistosity have been observed around borehole 192 at 1130 m level, which has the highest head. No response was observed in the surrounding holes during a test where each hole was opened in turn. Although short-term, these tests would have revealed any direct connections since the holes are relatively close to each other. The calculated transmissivities based on the recovery of the hydraulic pressures range in the order of

10^{-7} m^2/s. The first estimate for the transmissivity of the intersected hydraulic zones in borehole 570-106 at the base of the permafrost is $8 \cdot 10^{-6}$ m^2/s.

On the other hand, the video survey showed that a lack of open fracturing is not the reason for the poor transmission or absence of pressure signals. Rather it is the degree of weak to absent connectivity. There are a number of open fractures, some of which give gas, along the length of the hole. Also the borehole 1130-192 has been flowing continuously for about ten years. The measured outflow under open-hole situation was 6.4 L/min in 2002 (Ruskeeniemi *et al.* 2002). The four-fold salinity (30 g/L) compared to the other holes is further evidence for discrete flow networks within the studied volume of rock.

Obviously, vertical connections dominate over the horizontal directions. The complex isoclinal folding and the juxtaposition of lithologies with contrasting rock mechanical properties may result in tube-like, steeply-dipping hydraulic structures, for example at the crest of a fold structure. The lithological units are steeply dipping (80–85°) towards NE. This geometry may explain the observed strong hydraulic and hydrogeochemical compartmentalisation.

Beyond 350 m distance there is a possibility for the existence of a more profound structure, which was referred to as V1 in Ruskeeniemi *et al.* 2002. In two long boreholes, 890-188 and 1130-192, the video survey terminated at a fragmented zone through which strong gas and water flow has been observed. Borehole 1130-197 is also long enough (570 m) to hit the same zone, but the video survey extends only to 423 m due to technical problems.

The existence of the structure could not be verified by the drilling at the 570 m level. However, the existence of other structures could be deduced from various observations. The main zones of bedrock-weakness were observed at borehole lengths:

- Z1: 180 m/borehole 570-105 – 200 m/borehole 570-106
- Z2 ; At both sides of an amphibolite sequence at 240 m and 270 m in borehole 570-105, 270 m and at 300 m in borehole 570-106

Broken drill core was observed in these sections, but the video survey confirmed that breaking of the core took place mainly during drilling. The rock in these zones contain numerous, randomly oriented healed minor fractures and shear seams. Nevertheless, some open fractures were observed (Fig. 24).

Hydraulic conductivity of those zones became evident through different observations:

- First a natural increase in salinity of returning drilling water was associated with Z1 in drill hole 570-105 (Fig. 10). Although weak, an indication of hole-to-hole interaction due to pressure response was also associated with Z1 (Fig. 13).
- The other zone Z2 was clearly manifested in hole-to-hole head monitoring (Fig. 13). A relatively clear increase in flushing-water consumption was also associated with the zone (Fig. 9).

The water table observed in borehole 570-106 may also be controlled by zones Z1 or Z2. A hydraulic "falling-head" test carried out in borehole 570-106 indicated a relatively high transmissivity associated with either of the zones or both together (section 2.2.6). At present, it is not known if these zones have lateral and/or vertical extensions.

The inflow to the borehole 570-105 observed at early stage may have been related to the drainage of these zones. Soon after the drilling was completed and the packers were installed, some water was collected from the section 160 – 515 m. The rate of inflow then decreased distinctly.

3.3 Hydrogeochemistry

Currently the Lupin dataset includes analyses of 80 rain, snow, ice, surface water and groundwater samples. They have all been analysed for major and minor elements including REEs. Representative samples from the upper levels and practically all the deep groundwater samples have been analysed for tritium and stable isotopes. Several of the boreholes have been sampled at different times to monitor possible changes in composition over time. A set of samples has been selected for detailed geochemical characterisation including ^{14}C and ^{37}Cl dating.

In addition, an extensive gas-sampling programme has been conducted in the boreholes at the 890 and 1130 m levels. A database containing information on the amount, the composition and the isotopic characteristics of the gas phase is being compiled at the University of Waterloo.

Figure 40 presents a trilinear diagram of the chemical composition of snow, rain, surface water and groundwater samples from Lupin. The groundwaters plot into three distinct fields based on their Br/Cl-ratio (Fig. 41). The variable, but high Na/Ca permafrost waters form a uniform group with a low Br/Cl ratio, while the deep groundwaters plot at the high-end of the diagram. The waters just below the permafrost have variable Na/Ca ratios and intermediate Br/Cl ratios. The surface waters are very dilute with Br/Cl ratios on the order of tens to hundreds, and would plot to the far right in the diagram. This is a common observation for shallow groundwaters and surface water that the authors have collected in Shield environments worldwide. The high Br/Cl ratios in recent, atmospherically derived samples are believed to be the result of anthropogenic loading of Br from the burning of coal and oil.

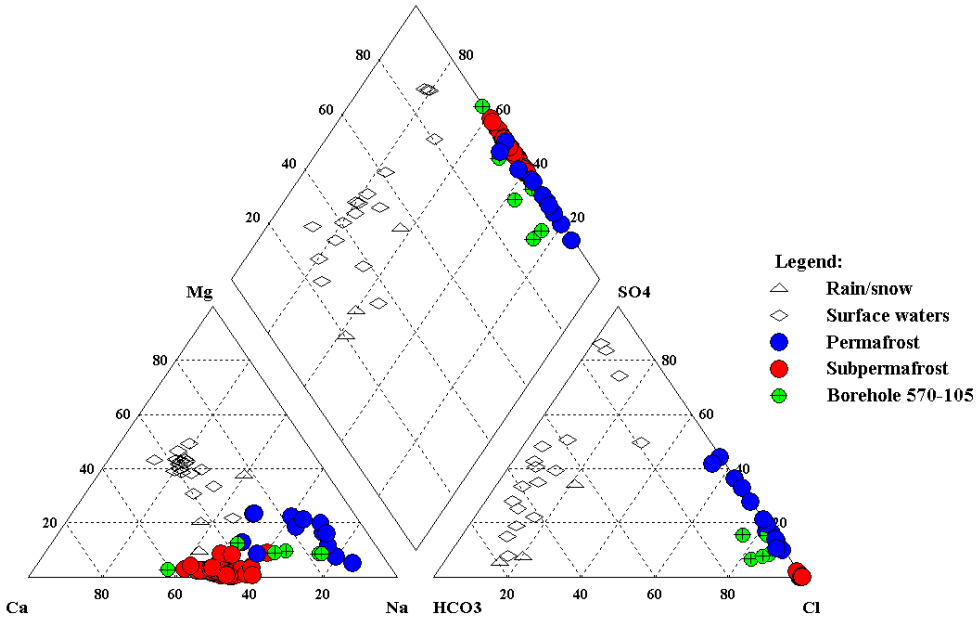

Figure 40. Trilinear diagram of the chemical composition of the hydrogeochemical samples from Lupin.

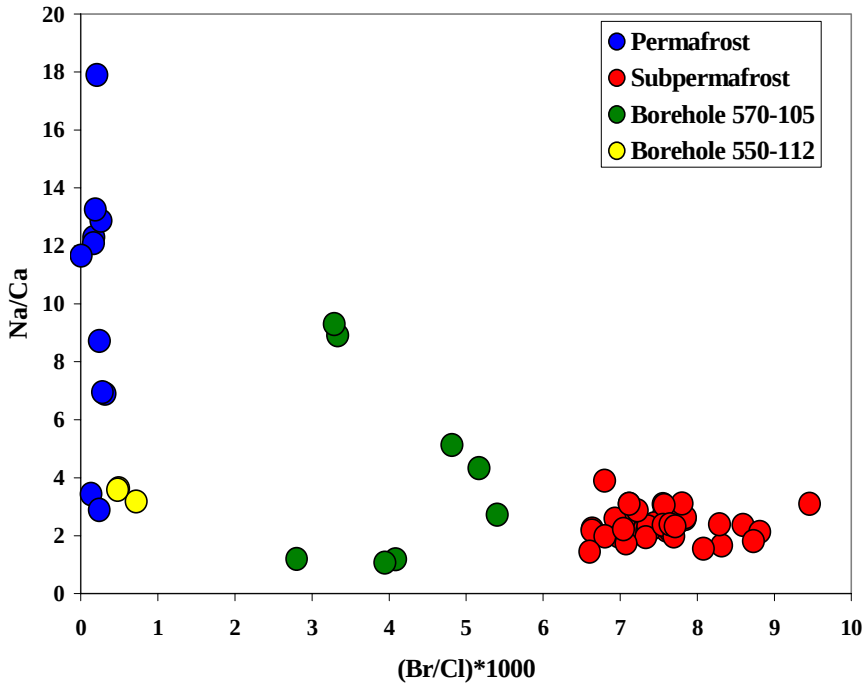

Figure 41. Variation of Na/Ca ratio versus (Br/Cl)*1000 in the Lupin water samples. Three distinct groups can be observed: waters in permafrost (blue), deep groundwaters (red) and those intermediate near the base of the permafrost (yellow). The base of the permafrost is at 540 m depth.

Figure 42 presents the stable isotope plot for the various Lupin waters. In general, the water samples, including the lake water, plot in a line below the global meteoric water line (GMWL). The snow and rain sample plot exactly on the line. The permafrost waters have a lighter isotopic composition than the lake water used for the mining activities, but they are heavier than the deep groundwaters. This relationship suggests that a formation water component is mixing with the man-made brine, while it migrates downwards. The fact that the stable isotopes of ^{2}H and ^{18}O can distinguish that a more dilute matrix or host fluid is present in the permafrost zone is significant to further studies that will help define the composition of the permafrost and subpermafrost fluids.

A permafrost water from 430 m level and a subpermafrost sample from borehole 1130-181 (sampling in February 2002) show anomalous isotopic compositions. The two other analyses from borehole 181 are consistent with the rest of the deep groundwater data from Lupin. Currently there is no explanation for these deviating numbers.

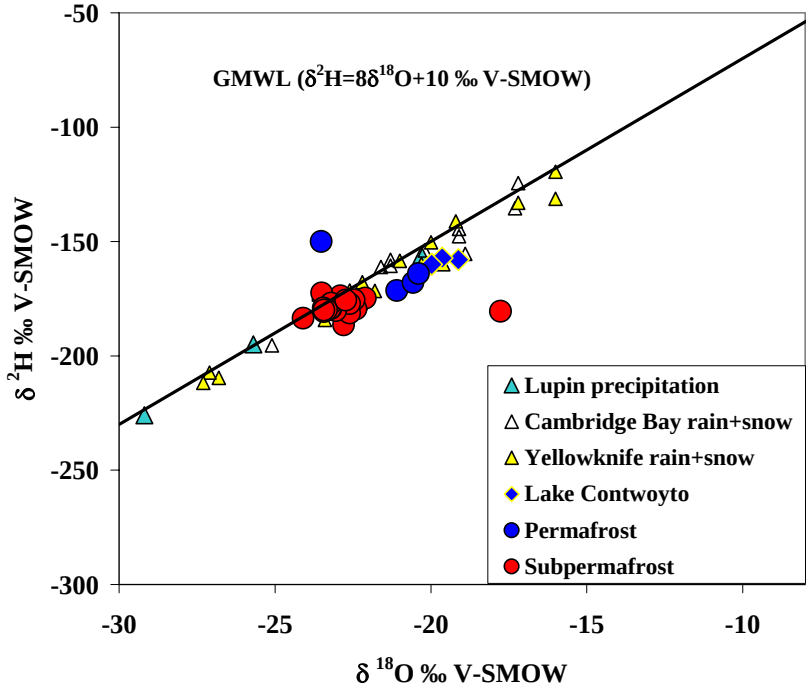

Figure 42. Stable isotope plot ($\delta^{2}H$ and $\delta^{18}O$) for the Lupin mine water samples compared to the Global Meteoric Water Line ($\delta^{2}H=8\delta^{18}O+10$; Craig 1961). Cambridge Bay and Yellowknife data are from the ISOHIS Database of IAEA (2001).

3.3.1 Groundwater in permafrost

All together 10 water samples were collected during Phase I above the 540-m level, which is placed as the lower limit of the permafrost in the vicinity of the mine. All waters have been sampled from dripping, more fractured parts of the rock exposed to the underground workings. The waters are typically sodium dominant Na-Cl or Na-Cl-SO4 type. In three samples Ca or Mg are also major components in addition to Na. The content of total dissolved solid (TDS) varies between 7.3 and 39.5 g/L and tends to

show a decreasing trend with depth. The most saline, naturally occurring waters are of the Na-Cl type (Ruskeeniemi *et al.* 2002).

There is a large variation in the measured pH. Most measurements show values between 6.8 and 7.5 (measured in the laboratory). Two exceptionally low values, pH 3.2 at 310 m and pH 3.3 at 390 m, were recorded. These low pH values in a mine environment are typically related to the oxidation of sulphides and hydrolysis of ferric iron. Highly variable SO_4 is observed. SO_4 increases with depth to 5000mg/L at 390 m after which concentrations decline to 1439 mg/L at 530m.

The NO_3 concentrations in the Lupin permafrost waters are exceptionally high. They range from 423 to 2630 mg/L. The highest values are from the 250-m level. The concentrations drop rapidly at the 330 m level, and at deeper levels within the mine, a concentration well below 1000 mg/L is reached. An explosive containing ammonium nitrate is commonly used at the mine and is the most likely source for the elevated NO_3 concentrations. The lower nitrate levels in the deeper groundwaters versus the shallower permafrost waters are due in part to the position of the structures being sampled. In the upper parts of the mine, most boreholes and seepage surfaces intersect a common fault/joint structure (named the ramp fault). A large spill of salt water (NaCl) entered this structure and flushed large amounts of nitrate in the process. Because the drilling waters were derived from Lake Contwoyto, they contained considerable tritium. The contaminated solution is assumed to be slowly moving downward within the upper part of the mine. This contaminated fluid provides an excellent tracer, but complicates acquiring representative permafrost fluids. The deeper groundwaters are primarily derived from fracture zones far from the mine environment (thus little opportunity -for NO_3 contamination), and well below the salt and tritium-contaminated solution. A reconnaissance survey of the nitrogen (^{15}N) and sulphur (^{34}S) isotopes in contaminated and uncontaminated groundwaters is on-going, and may add additional insight into the sources of these compounds and migration rates of the suspected contaminants within the permafrost zone of the mine.

The tritium values vary between 12.2 and 17.3 TU indicating the mixing of recent meteoric waters. It is reasonable to conclude that any tritium present at depth is the result of water pumped down for the mining activity (drilling, washing etc.) The 17.3 TU value from the 250-m level is higher than that presently observed from Lake Contwoyto (15.8 TU), which is the source of all process water used in the mine. (Ruskeeniemi *et al.* 2002).

As discussed in Ruskeeniemi *et al.* 2002, these and many other features denote contamination of permafrost waters due to the Na-Cl dosed-waters used in excavation and drilling through the permafrost. Many of the geochemical trends at Lupin, such as increased salinity and sulphate concentrations, are proposed to be derived from contamination but could theoretically have a component induced by freezing processes as well. The eutectic freezing temperatures for $Na_2SO_4 \cdot 10H_2O$ precipitation (-3.5 to -8.2 °C) and $MgSO_4 \cdot 6H_2O$ are within the range of temperatures recorded in the permafrost zone (-1.5 to -7.5 °C). However, the lack of representative uncontaminated borehole water, or any water from other structures than the ramp fault, from the upper levels to date has prevented the establishment of the “baseline” hydrochemical situation in the permafrost.

3.3.2 Groundwaters at the base of permafrost

As presented in Sections 2.2.5 and 2.3.3 the knowledge of the prevailing waters at the base of the permafrost is based on samples collected during and after the drilling of the boreholes at 570 m (Table 3) and at 550 m levels. It is encouraging to notice that the chemistry of borehole waters at the 570 m level seem to cluster well with the deep groundwaters rather than with the contaminated permafrost waters (see Fig. 11).

The bedrock immediately below the permafrost is practically dry based on the observations from the 570-level boreholes (see Section 2.3.2). However, borehole 570-105 seems to still produce small amounts of water half a year after the drilling. The borehole has been sampled several times and both open-hole samples and samples from packered sections are available. The first 160 m, *i.e.* the section nearest to the mine is cleaning up much quicker than the rest of the hole. The uranine levels show that the amount of flushing water is lowest within the first 45 m (see Table 3). Because the uranine is also very low in the latest open-hole sample (Lu/GTK/62) it is obvious that the water introduced into the borehole from bedrock section close to the mine is increasingly characterising the outflow from the borehole. This was confirmed by the sampling carried out in May/June 2003. A packer was installed at 120 m of borehole length, which showed that the water is coming in explicitly from the section 0–120 m (sample Lu/GTK/79).

The chemistry of the waters from the sections 0–45 m and 0–120 m, hereafter referred as proximal samples (in relation to the proximity to the mine), differs from the samples collected deeper in the borehole hereafter referred to as distal. As discussed above the latest open-hole sample Lu/GTK/62 is suggested to belong to the former group, and the chemical characteristics give support to this classification. Thus, two types of water are encountered at the base of the permafrost.

The proximal samples show the highest Cl concentrations (Fig. 43). The TDS in these waters is about 4 g/L, while the other borehole samples range from 0.8 g/L to 1.5 g/L. Also the water is of Ca-Na-Cl-SO_4 type, whereas the distal ones are Na-Cl waters. The deep groundwaters at Lupin are of Na-Ca-Cl or less commonly of Ca-Na-Cl type.

High NO_3 and SO_4 together with tritium values around 10 TU are generally considered to indicate contamination at Lupin. This kind of water was collected from a dripping fault exposed close to the drilling station (NO_3: 901 mg/L and SO_4: 3070 mg/L). In the proximal samples the NO_3 is << 20 mg/L, but SO_4 (640 – 800 mg/L) is clearly elevated compared to the deep groundwaters in general and also compared to the distal samples from this borehole (80 mg/L). The low tritium values in the samples indicate that recent meteoric waters (drilling water) are not mixed with the borehole waters. Currently, it is not possible to say whether the high SO_4 is related to the oxidation of exposed sulphides in the borehole or if it is of some other natural origin.

Compared to the flushing water, the tritium levels are about 2 units lower in the first open-hole samples from October-November 2002 (13 and 13.7 TU vs. 15.8 TU), which suggests the mixing of low-tritium formation water. This is in agreement with the uranine data. Most of the return waters collected during drilling point to similar compositions. More recent samplings show a clear cleaning trend for the borehole waters, both tritium and uranine have decreased to low values (1,5 TU and 3 µg/L in May 2003).

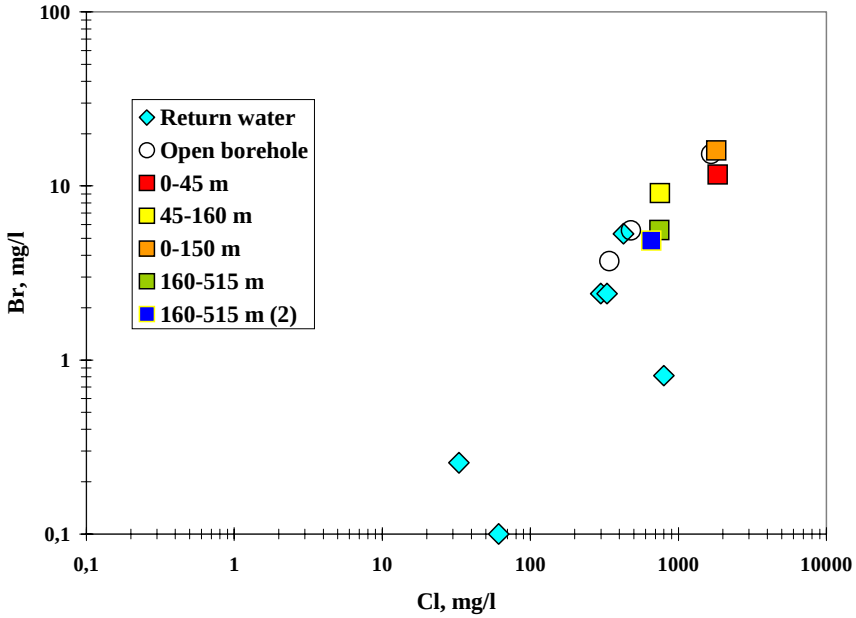

Figure 43. Br/Cl ratio in samples collected from borehole 570-105. The chemistry is corrected based on the uranine concentrations.

The water samples from the short borehole 550-112 seem to be more contaminated. Both the NO_3 and the SO_4 concentrations are very high, at the same level as in the fault in the ramp and so are the tritium levels (around 10 TU). The Br/Cl ratios also indicate similarity with the ramp waters (see Fig. 11). Sealing out the fault with a packer might provide an opportunity to collect more representative samples.

If the two samples, Lu/GTK/51 and Lu/GTK/52, collected behind the 160-m packer in borehole 570-105 and containing 30–40% formation water are considered representative, the following features characterize the waters at the base of the permafrost, far away from the mine:

- the waters are relatively dilute, TDS around 1,5 g/L
- the water is of Na-Cl type
- NO_3 concentrations are lower than 7 mg/L and SO_4 are around 80g/L
- pH measured in field is pH 6.25
- $\delta^{18}O$ and $\delta^{2}H$ are in the range of the deep groundwaters

The available data does not provide any evidence of highly saline waters below the permafrost. However, there is not yet enough information to unequivocally rule out the hypothesis of the presence of a saline freeze-out front. There is information only from one borehole and it is still an open question whether the samples represent melting permafrost or the fluids in the bedrock.

Zang and Frape (2003) conducted a series of laboratory experiments, in which the effects of the freezing-out process were studied using a number of groundwater samples from Canada and Fennoscandia (see section 2.7). Among other things, they concluded that it is very difficult to envision a situation where any significant amount of concentrated saline fluid could be generated in crystalline bedrock by this mechanism.

The amount of water in fractured crystalline rock is limited and the bedrock temperatures necessary to support the successive freezing corresponding to increasing salinity levels is unrealistically low. This result seems to be in agreement with the observations of the groundwater chemistry from Lupin.

Detailed geochemical and isotope research is on-going. A comparison of the water chemistry with the crush and leach data, which provide information on the matrix fluids, may help to evaluate the origin of the water collected from the base of the permafrost, and the evolution of these groundwaters. The core samples for the crush and leach experiments have been collected from boreholes at 570 and 890 m levels.

3.3.3 Deep groundwaters

Continued research with the deep groundwaters confirmed many features already recognised during Phase I. Sealing and re-establishing the environmental pressure in the holes turned out to have only a limited affect on the water chemistry. The only observed trend was that the salinities in some boreholes decreased after sealing.

The TDS in the deep groundwaters range from 2.2 to 36.3 g/L. Rather low salinities, TDS< 5 g/L are typical for levels 890 m and 1105 m. The TDS at 890 m level (TDS 2.7 – 3.6 g/L) is only slightly higher than observed at 570 m level. It is interesting that both the most dilute (2.2 g/L) and the most saline (36.3 g/L) waters are recorded from the 1130 m level. The most dilute waters are leaking from a bolthole and from a 40-m long uphanded borehole, and dripping from the ceiling at the end of the new exploration drift indicating that the source of water is somewhere above, but not very far from the drift. The flow rate and the chemistry of the outflow from the bolthole have remained constant at least three months, the period it has been monitored. Obviously, the dilute water body is not draining very quickly. The waters from the subhorizontal boreholes close to the bolthole are distinctly more saline, the TDS ranging from 6 up to 16 g/L. The most saline water at Lupin is coming from borehole 1130-192, which also has the highest hydraulic head observed. All the nearby boreholes have 2-4 fold lower salinities.

The deep groundwaters have rather consistent chemistries despite large differences in TDS (Fig. 44). The waters are of Na-Ca-Cl type, with the exception of Ca dominant waters which occur in two boreholes (201 and 219) at level 1130 m. Two previously Ca dominant holes became Na dominant after they were pressurised by sealing with packers. The good correlation between the trace elements and TDS also suggests that the waters may have a common origin (Fig. 45). The linear relationship suggests dilution as a result of mixing between highly saline water, and fresh, tritium-free water at depth.

Redox potential data from sealed boreholes (Table 4) indicates that Eh-values are generally slightly below zero. There were some indications of still decreasing trends, but the available time series indicate that the final values are not lower than about -50 – 0 mV. Dissolved oxygen concentrations were beyond the lower detection limit and are recorded at 0.0 mg/L in all cases. The measured pH range is from 8.2 to pH 8.6 under packed-off conditions. Compared to the long-term measurements done at Palmottu (Cera *et al.* 2002), the values fit very well with an iron-dominated redox system. As often observed in groundwater studies, iron concentrations in Lupin groundwaters are

very close to or below the detection limit for iron. The low concentration is possibly a major reason for the prolonged measurement times. Contrary to the deep groundwater redox data from Palmottu, sulfide-dominated Eh-values were not observed in Lupin waters. Due to the deep mine conditions, it was not possible to perform accurate sulfide analyses. However, the distinct smell of sulfide would have been detected, if the waters had contained it.

The tritium content in most of the waters, including the most dilute ones, is <0.8 TU. In some samples the tritium content is slightly above 1 TU, but this is probably related to the air contamination during sampling. So far, there are no indications that recent meteoric waters have infiltrated down to these depths. Also the lack of dissolved oxygen and the redox values (–10 – +24 mV in Eh scale), are in agreement with this interpretation.

Samples have been collected for dating the deep waters and the dissolved gas phase (^{36}Cl and ^{14}C). However, the isotopic signatures indicate that the gas is primarily thermogenic and most likely originates at depth. Additional carbon isotope analyses (both ^{13}C and ^{14}C) on the dissolved inorganic carbon component show indications that much of the DIC may have resulted from degradation of the methane after initial thermogenic methane formation. The CO_2 produced for example, by acetate fermentation, can be incorporated into the dissolved carbon pool. Three boreholes 890-188, 1130-181 and 1130-192 gave ^{14}C (pmc) values of 8.72, 2.78 and 16.2 respectively. However, the ^{13}C values were -8 ‰, -15 ‰ and +2 ‰ respectively. The enriched value for the 192 borehole (one of the most concentrated saline fluid), coupled to the holes higher than normal HCO_3 concentration, may indicate bacterial reduction/oxidation of methane. As well, very recent ^{13}C results on methane gas shows small (2‰) but consistent isotopic shifts in the gas signature of several boreholes. Further work will be concentrated on determining if the methane to DIC link is real, if it is a modern present day borehole bacterial situation or a palaeophenomenon.

Stable chlorine isotope results indicate that although permafrost samples are similar to either the salt used by the mine to mix brine, or to fluids with the rock matrix at Lupin, deeper samples are lighter than the brine-mix salt (Fig. 46). $\delta^{37}Cl$ signatures for the rock matrix from the preliminary crush and leach experiments are presented in section 2.6.1. Analyses of water samples from depths directly below the permafrost are on-going.

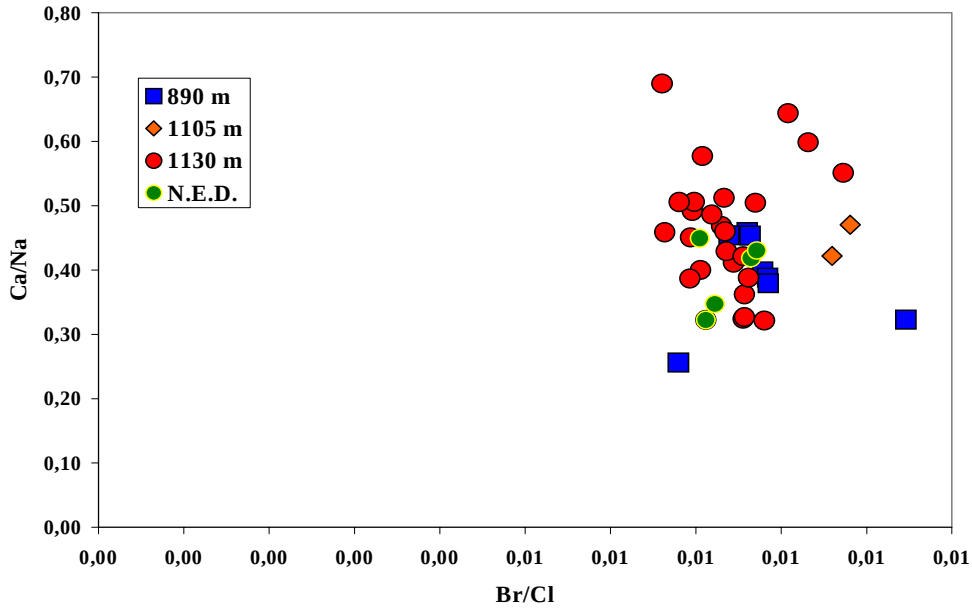

Figure 44. The deep groundwaters form a consistent group in the Ca/Na vs. Br/Cl diagram despite of the wide range in salinity. N.E.D. denotes New Exploration Drift at 1130 m level.

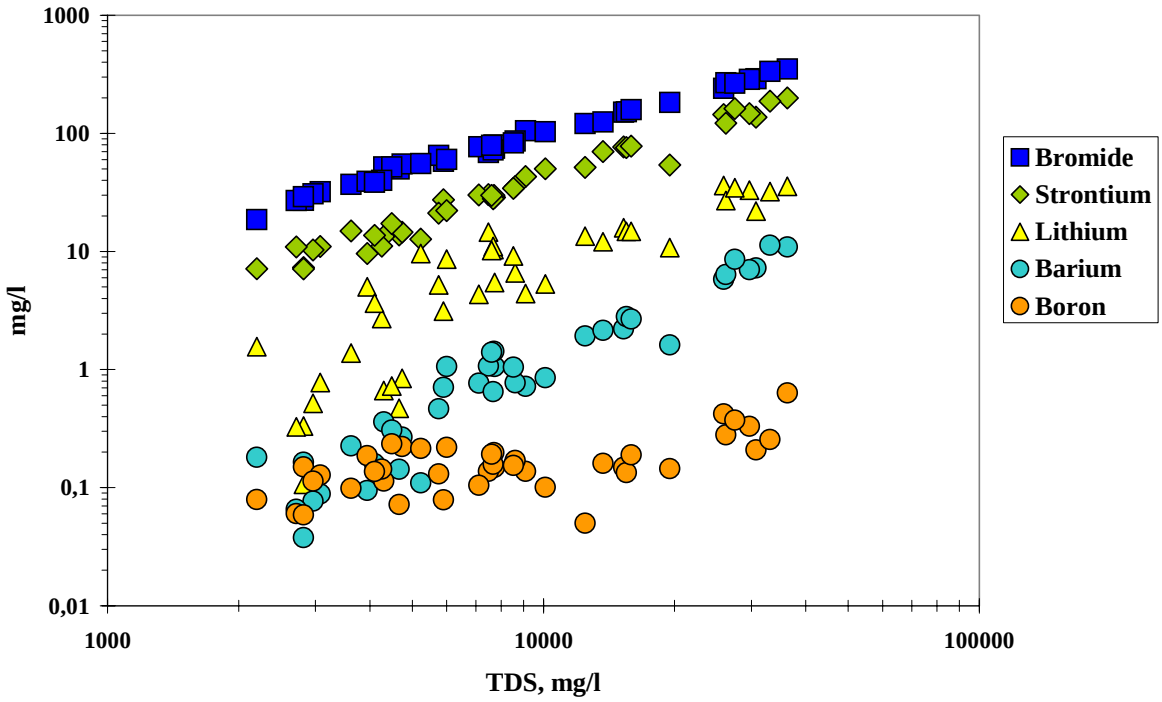

Figure 45. Trace elements and TDS have an excellent correlation in the deep groundwaters.

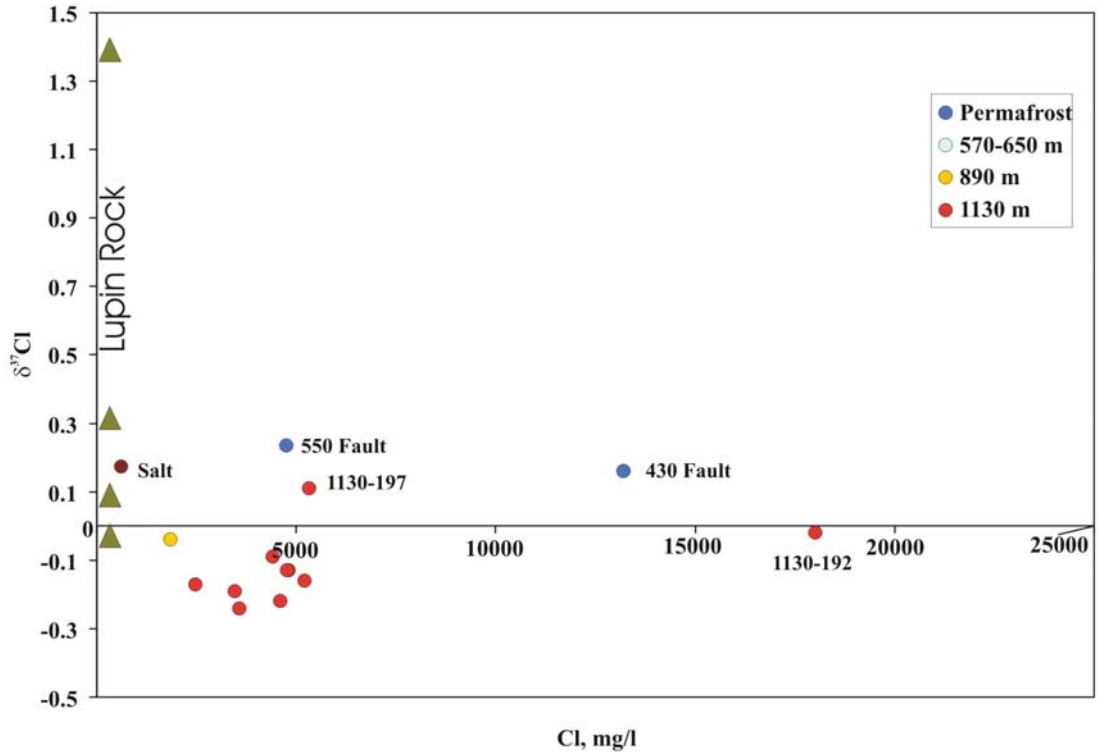

Figure 46. Stable chlorine isotopic signatures of groundwaters as a function of their Cl- concentrations. Note that the salt is scaled to fit the diagram. The Cl concentration is 607 000 mg/L.

4 Conceptualisation of the groundwater conditions at Lupin

4.1 Late Quaternary glaciations in Canada

The glacial history during the late Quaternary in Canada is similar to NW Europe. The Sangamon interglacial (Eemian in Europe) was succeeded by a marked cooling of the climate and the Wisconsin glacial stage (Weichselian in Europe) began about 116 000 years ago. There was considerable fluctuation in climate during this stage and consequently, there is considerable disagreement over the events of the ice advance and retreat in the early and middle Wisconsin (Trenhaile 1998, p. 142 onwards). Data for the middle Wisconsin (65 000 – 35 000 years ago) suggest that the climate was sometimes cooler and at other times similar to the present climate. In general, a trend of progressively cooling climate from 64 000 to 28 000 years ago has been observed in many areas. The late Wisconsin glacial stage is generally considered to extend between 35 000 and 10 000 years BP. During this period the Laurentide ice sheet covered an area of 16 000 000 km^2 in North America (Flint 1971). The ice sheet was comprised of several centres of ice accumulation (Dyke and Prest 1987). The Keewatin dome between Hudson Bay and Great Slave Lake was of major importance for the Lupin area (cf. Fig. 47). It is suggested that many areas of the Laurentide ice sheet developed upon pre-existing permafrost that had been produced during the Middle Wisconsin non-glacial interval (Fischer *et al.* 1985). Energy Balance Models indicate that in large areas, including Lupin and its surroundings, the ice sheet was cold-based during the last glacial maximum at 21 000 years BP, but during most of the late Wisconsin stage the ice-sheet was warm-based (*e.g.*, Peltier 2002). The maximum thickness of the Laurentide ice sheet over Hudson Bay has been assumed to reach 3,5 km or slightly more (Peltier 1998), or even exceed 4 km (Hughes *et al.* 1981). It is assumed that the crustal depression below the major domes may have exceeded 1 km. The retreat of the Laurentide ice sheet began slowly about 14 000 years ago and the last remnants in north eastern Canada disappeared 6000 – 7000 years ago (Dyke and Prest 1987). During the retreat, major confined ice lakes were formed along the ice margin.

A general warm period followed the disappearance of glacial ice with temperatures peaking during the middle Holocene between 6000 and 9000 years ago (Smith *et al*. 2001). Macrofossil analysis and radiocarbon dating of peat cores have been used to reconstruct the permafrost distribution in western Canada 6000 years ago. The results of this analysis suggest that mean annual temperatures were about 5°C warmer than present, and that the southern limit of permafrost was 300 to 500 km northward of its current position. Much of the present discontinuous permafrost zone may have been free of permafrost. Where permafrost did exist during this time, active layer thickness was probably greater than at present. Cooler conditions followed the Mid-Holocene warm period and permafrost once again became more extensive. Permafrost was probably established in northwestern Alberta by 3700 years ago and the climate at this time probably resembled the present climate regime. In the Mackenzie Delta region, permafrost growth and Pingo development occurred in response to the deterioration in climate that began about 5000 years BP.

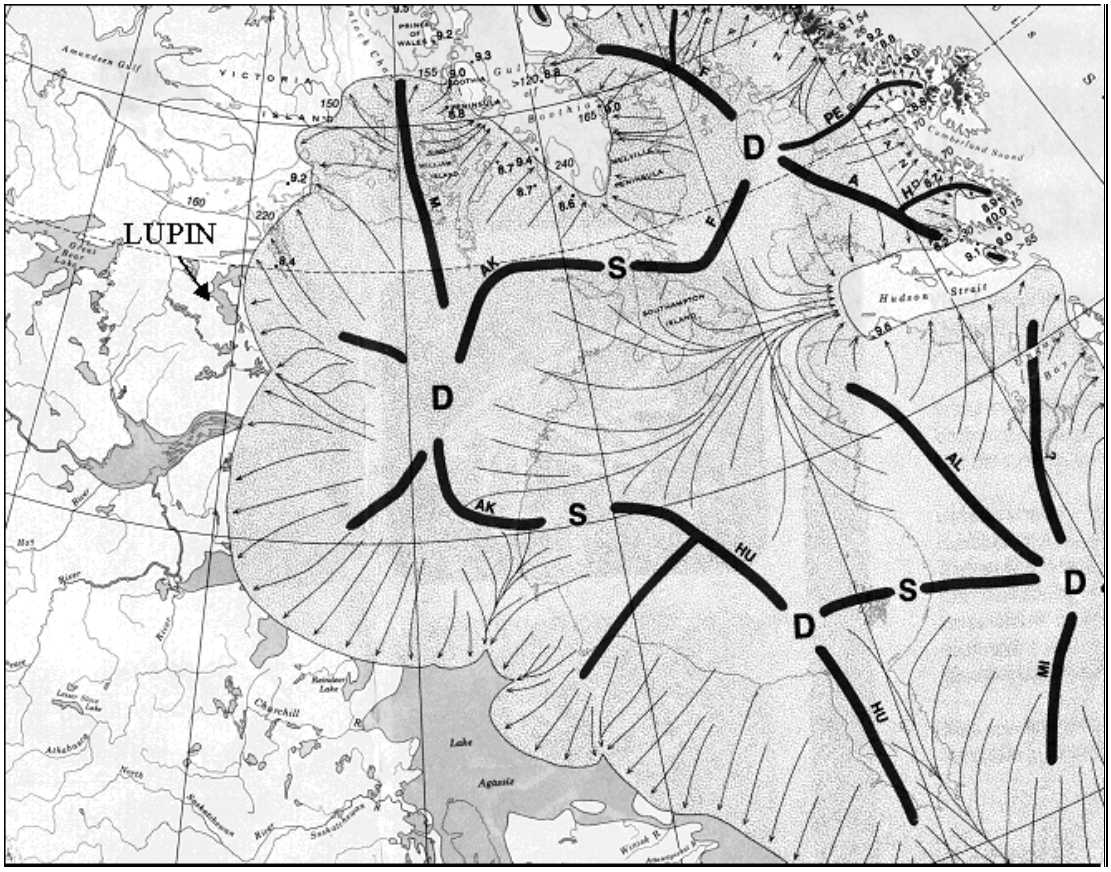

Figure 47. Reconstruction of the Laurentide ice sheet at 8500 BP. The westernmost dome is the Keewatin Dome. The retreat of the ice began around 14 000 years ago. An ice lake occupied the Lake Contwoyto basin until about 9000 years BP (Dyke and Prest 1987). D= dome, S= saddle and the curved, thick lines indicate the locations of ice divides.

4.2 Permafrost at Lupin

Lupin is located in the high north. It is likely that the area became glaciated soon after the cooling of climate during the Quaternary. However, it is possible that the area was not glaciated between 67 000 and 28 000 BP as Gascoyne *et al.* (1980) suggest. If this was the case, then the climate would have been favourable for the growth of deep permafrost, especially during the latter part of the period. Consequently, it is possible that Late-Wisconsin ice sheet developed on deep permafrost (Fischer *et al.* 1985). According to reconstructions of the Laurentide ice sheet presented in Dawson (1992), the Lupin area was continuously covered by ice from 28 000 BP to 9000 BP. It is likely that most, if not all, of the permafrost disintegrated during this long period due to geothermal heating. The strong ice-born striations observed in the outcrops demonstrate that at some point, the glacier did transform to warm-based, permitting basal ice flow.

When the ice gradually retreated from the area, huge amounts of meltwater streamed from the glacier forming eskers and outwash deltas typically found on the landscape. Large ice lakes formed along the ice margin. One of those was in the basin of present Lake Contwoyto (Fig. 47). It covered a wide area until the Burnside River broke open and let the waters to the Arctic sea at about 9000 years BP (Dyke and Prest 1987). It is

noteworthy that the bedrock below the lake basin was continuously isolated from cold air either by ice or a huge water body for tens of thousands of years. This implies that any possible relict permafrost had plenty of time to disintegrate below the lake and, on the other hand, the growth of permafrost was prevented during the early Holocene. It is plausible that Lake Contwoyto, or any other larger lake in the area, has a talik below extending through the permafrost.

Permafrost began to develop as land areas became exposed. Although the mean annual air temperature during early Holocene was several degrees higher than presently observed, the climate at high latitudes was still cold and the mean annual air temperature was well below zero. However, the present depth of permafrost was reached only during the last 5000 years, when the temperature gradually dropped to the present annual average of -12ºC. It is assumed that at high latitudes the present-day permafrost is in equilibrium with the current climate and has reached its maximum depth (*e.g.* C. Burn 2003 pers.com).

The freezing of ground is a physical process, which implies heat transfer that will move the system towards an energy balance consistent with the air temperature and geothermal heat flow. Numerous parameters, such as vegetation, thickness of snow cover, porosity and heat conductivity of the main rock types are involved. The rock parameters are particularly significant at Lupin, where research indicates a strong hydraulic anisotropy suggesting higher hydraulic conductivity of subvertical structures. The higher porosity and water content of these structures would retard the advance of freezing. Additionally, it can be argued that the topographic relief at surface is reflected to the base of the permafrost. In relation to the sea level, the base of the permafrost would be located higher in elevated areas than in lowland areas. The electromagnetic SAMPO soundings gave indications that the base of the permafrost (or the groundwater table) is highest close to the mine and is deeper in the vicinity of the lake (Paananen and Ruskeeniemi 2003). The mine is located about 50 m higher than the areas close to the lake.

The temperature measurements conducted in the mine in 1989 indicate that permafrost persisted down to the 540 m level where 0°C was recorded. The lowest value was recorded at 87 m depth (–6.8°C) and at 170 m depth (–5.8°C). In 2000 a thermistor installed in an exploration drift at 490-m level showed a constant value of 0.66º C for a prolonged monitoring period, confirming that the previous depth estimate for the permafrost was correct (Ruskeeniemi *et al.* 2002). The suggested depth fluctuation at the base of permafrost combined with crustal uplift might have some interesting implications with respect to gas accumulation and may in part explain the development of the observed dry zone below the permafrost.

4.2.1 Surface hydrology

The research area, like other permafrost areas, is characterised by a large number of smaller and larger lakes and ponds. Due to the impermeable frozen soil, water collects in any significant depression, forming small ponds or lakes. Some of the lakes/ponds are interconnected forming complex waterways, which collect the surface waters around the mine and discharge them to Lake Contwoyto. The lakes have three main water sources: 1) melt water in spring time, 2) precipitation and 3) melting ground ice/permafrost. The major load is probably released from the snow in late May. At this time the ground is

still frozen to the top and all melt water is sustained at surface. The annual precipitation is low, 270 mm on average, with roughly 2/3 of the total precipitation obtained as rain during the warm summer months.

The active layer (unfrozen soil) begins to form around late May/early June, when the sun starts to warm the ground and after most of the snow has melted. The layer is discontinuous at first, and will be found on exposed slopes facing south. The thickness of the active layer depends on the soil type, but probably varies between 0.5 m and 1.5 m. This layer is saturated with water due to the melting of ground ice formed during the previous freezing season. This implies that the soil cover is not able to retain significant amounts of water (precipitation, melt water), and the extra water is directed towards watercourses as run-off. The constant winds may increase the evaporation and drain the topsoils, but it is difficult to estimate the net effect of this process. The possible exceptions for the above are the eskers, which are highly porous compared to the fine-grained soil types. They are not able to readily retain water or ice in the pores, thereby providing routes for recharging waters down to the underlying frozen bedrock.

4.2.2 Hydrogeological conditions

Three "external" factors have significantly affected the development of the hydrogeochemical and hydrogeological system at Lupin: frozen ground, rebounding bedrock and hypothesized unfrozen talik structures through the permafrost. The first two mentioned are regional processes, while a talik may be considered either as a local or regional feature, depending on the dimensions of the structure and its impact. These features involve different mechanisms and they affect different parts of the hydrogeological system. It is fairly easy to identify some of the major impacts for each of these, but the integrated effect of these simultaneous processes is much more difficult to understand.

Freezing of water in the fractures and voids of the bedrock tends to seal the hydraulic conduits and prevents flow. However, due to an uneven distribution of dissolved solids during freezing, the grain boundaries or voids in ice or in rock matrix may remain liquid allowing diffusive-type migration. The sealing effect of the thick permafrost is well demonstrated in the mine's water budget, which shows that the annual mine discharge is very low, although it includes the water deliberately brought into the mine. There is some moisture right below the base of the permafrost due to the melting of the permafrost by the warm air flowing up, but deeper down the mine is dry. Moreover, borehole observations at the base of permafrost and hydraulic head measurements deeper in the mine reveal the existence of an unsaturated zone below the permafrost. The thickness of this zone is probably about 100 m. Whether this zone is a natural feature or due to mine drainage is still somewhat controversial, although the geophysical soundings suggest that the depression of the groundwater table extends far outside the mine. Regardless of the origin of the zone, it is clear evidence of limited recharge, as well as of limited lateral flow.

Isostatic adjustment of the underlying bedrock begins during the melting and retreat of the ice sheet. The uplift of the lithosphere plate is related to the slow mass flow in the asthenosphere. It is suggested that about 30 % of the uplift takes place during the initial thinning of the ice sheet and 50 % shortly after the retreat of the ice sheet. The remainder is residual uplift, which is an ongoing process (Andrews 1970), and may be

considerable. In southern Hudson Bay the rate of uplift is assumed to be up to 15 mm/year, with 120 – 160 m of uplift still expected (Dawson 1992). At Lupin the rate may be slightly more than 5 mm/year (Peltier 1996). On a regional scale, the uplift affects the hydraulic gradient, which in time changes the routes of water pathways, both subsurface and surface water courses. In the context of permafrost, the residual uplift is significant, because it is contemporaneous with the aggregation of permafrost. The rate of the uplift probably exceeded the rate of growth of permafrost, which may have some significance as well.

Based on the discussion above several questions remain unanswered. It is generally suggested that the glacial rebound predominantly affects and is eventually balanced by the movement on previously existing fault zones (Vuorela and Kuivamäki 1997; Kuivamäki *et al*. 1998). Is the concept different in rigid frozen bedrock? Additionally, does the uplift of the impermeable permafrost layer induce a kind of pumping effect, which could promote either flow downwards along taliks or upward flow of deep groundwaters? The role of taliks is discussed in later sections.

Hydraulic connections in the bedrock.

The characteristic features of the bedrock at Lupin are the frequent alternation of schistose lithologies with contrasting rock-mechanical properties, intensive folding and abundant, but tight fracturing. The contact of a plutonic massive is located about one kilometre west of the mine. A number of NE-SW trending major lineaments cut the geological units in the vicinity of the mine. Roughly N-S trending diabase dykes are evidence of the ancient tensional faulting in the area.

Although Quaternary deposits partly obscure the structures near the mine, the investigated bedrock area seems to represent a relatively intact block bordered by regional lineaments. The major structural features in the bedrock are related to ancient folding, which took place in at least two phases. On a broad scale, the lithologies showed predominantly plastic behaviour during these events. However, depending on the mineralogical composition and textures of the individual units, an intra-layer fracturing with variable intensity was generated. Sliding along the bedding planes and along contacts between different rock layers was also common. The high-temperature and/or high-pressure nature of most of the fracturing is evidenced by the alteration of the rock surfaces. Polished chloritic and/or graphitic surfaces with frequent re-mobilised sulfide veining or coating are typical mineralogical features. The folding of the rock units also generated a more pervasive texture parallel to the axial plane, schistosity due to the preferred orientation of certain mineral phases, and ruptures, especially in the crest areas of the folds. In the latter case, the fractures may extend across rock units.

Numerous, generally narrow faults (10 – 100 cm) cross-cut the lithologies at the mine-scale, but only rarely is related water flow observed. The distribution of open fracturing in boreholes is irregular as evidenced by video logging. The hydraulic conductivity is typically supported by few isolated fractures. Steeply dipping fracture sets parallel to the schistosity are dominant and subhorizontal, roughly westwards or eastwards dipping fractures are common as well. The apertures are generally around 1 mm or below, although a few larger ones have been observed. Abundant gas flow is observed in some fractures and, as a rule, the gas phase is present in all water producing boreholes.

There is little direct or indirect evidence of the lateral hydraulic connections in the area. Distinctly different salinities, a lack of hydraulic response in cross hole tests and different yields of groundwater between nearby boreholes at the same level point to strong compartmentalisation. Video surveys in a large number of boreholes confirmed that a lack of open fractures is not the reason for the limited interaction. It is more plausible that the fractures are short and poorly interconnected laterally. On the other hand, the continuous and abundant out-flow from year to year from a number of these holes indicates the existence of an extensive water reserve. At the moment, the most reasonable explanation is that the hydraulic conductivity is strongly anisotropic in nature, and is controlled by subvertical rock units parallel to the fold axis. The first hydraulic tests indicate that the transmissivities in these hydraulic zones would be in the range of 10^{-6} to 10^{-7} m^2/s.

The hydraulic situation is demonstrated schematically in Figure 48. Although open fractures exist, they are mainly short and poorly connected. In some mechanically more brittle rock types, fractures are more common and, correspondingly, there may be almost intact rock layers in between. In any case, even closely located boreholes may intersect different rock units with contrasting hydrogeochemical and hydraulic characteristics.´

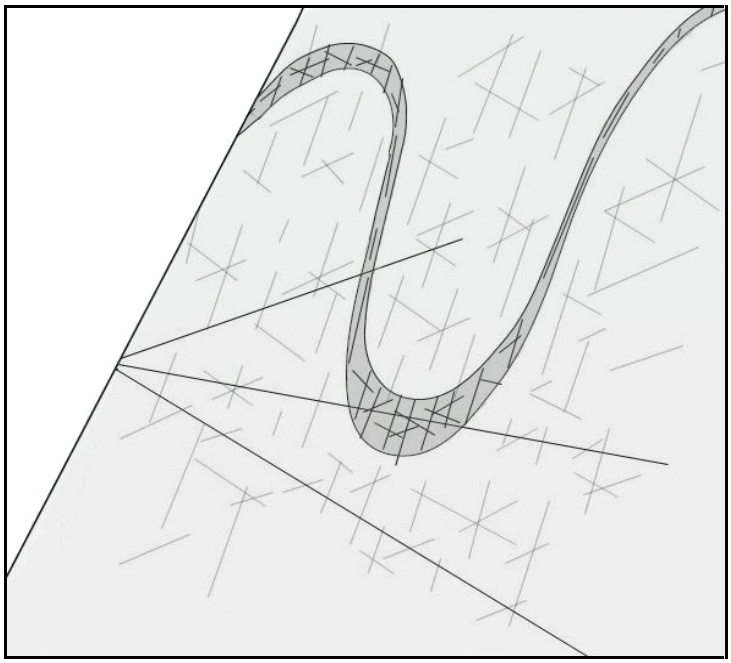

Figure 48. A schematic presentation of the different hydrogeological situations encountered in closely located boreholes when drilling a geologically complex system. The folded layer was more susceptible for fracturing during deformation, and forms a more hydraulically active zone, with major connections in directions perpendicular to the plane.

Fracture infillings.

The low porosity of the rocks and the impression of tightness of the fracture network are supported by the observations of fracture infillings. Often the actual infilling minerals are completely absent, but where present, the coatings are very thin and the mineralogical variation is limited. This is partly due to the rock types, which are relatively resistant to weathering and hydrothermal alteration (small portion of feldspars etc.), but mainly can be attributed to the restricted flow routes. It remains to be seen if fluid inclusion research on fracture calcites will provide indications of fluids of different age and composition, but based on the fracture logging, the situation looks monotonous. This is somewhat surprising, since the nearby plutonic massives and the cross-cutting diabase and granitic dykes provide evidence of younger events which suggests subsequent fluid movements.

Taliks and their impact on hydrogeological conditions.

In the Lupin area all shallow lakes will freeze down to the bottom during winter. The bottoms of larger lakes deeper than 2 – 3 m will remain unfrozen all year. These lakes have the potential to support a closed talik, which means a localized area of unfrozen ground completely enclosed by permafrost in all directions. These would not penetrate the deep permafrost at Lupin. Still larger lakes, more than 100 m in diameter may potentially have a significant influence on the local and regional hydrogeology, because they are likely to conceal taliks extending through the deep permafrost.

A simple rule for the formation of a talik was presented by Mackay (1992) and Burn (2002). If the water depth below the ice is greater than 2/3 of the maximum ice thickness, the temperature at the bottom remains above zero all year and there should be no permafrost beneath. Either its formation has been prevented or it has degraded due to the geothermal heat flow. Geothermal modelling and also field observations suggest that the interface between permafrost and talik is abrupt and vertical (Burn 2002; Delisle *et al*. 2003).

At Lupin the limiting water depth would be around 3 m. There are no bathymetric logs from the lakes, but it is assumed that some of the lakes in the area would fulfil this criteria. Most taliks of this type would be isolated “worm-holes”. However, some chains of lakes related to regional lineaments, may have partly interconnected unfrozen channels beneath. Such a major fault zone (the Norma fault) is located a few kilometres southeast of the mine. However, the most significant talik structure in the area would be related to the Lake Contwoyto. The lake is 1-3 km wide and more than 100 km long. Although there is no direct evidence on the existence of a talik, there is no reason to doubt its existence. Numerous geothermal model calculations reported in literature show that much smaller water bodies are sufficient for talik formation (*e.g.* Burn 2002; Delisle *et al*. 2003). Furthermore, the reconstructions of the retreat of the Laurentide ice sheet and the climate in the Holocene discussed in a previous section support the talik hypothesis.

Due to the lack of direct observations, the properties of a talik and its potential influences on the hydrogeological and hydrogeochemical conditions at Lupin are speculative. It is important to identify the kind of geological system in which the talik has formed. The formation of a talik is basically a physical heat transfer process, which

is actually more effective in an intact rock mass where less heat is required for the water/ice phase transformation. Thus, a talik may exist below a lake or other favourable location, but its impact on hydrogeological regime may be insignificant. This is probably the case with many taliks related to small lakes in the Lupin area. However, if a talik is related to a fault or other more permeable structure, the impact on hydrogeology is likely to be different.

The elongated and ragged shape of the Lake Contwoyto strongly suggests that the lake basin is formed on a large NNW-ESE trending fault valley, which is intersected by a number of northerly trending faults. This structural relationship suggests the basin may be highly fractured deep into the underlying bedrock. This does not necessarily imply that there are more open fractures and a higher hydraulic conductivity compared to the surrounding area. Ancient deformation events may have taken place under high temperatures and may have supported high fluxes of mineralised fluids. Thus, at depth, the healing due to recrystallisation and the precipitation of secondary minerals may result in a lowering of the permeabilities in fault zones compared to the surrounding bedrock. Nevertheless, close to the ground surface the fractured zones are more susceptible to superficial stresses (weathering, erosion), and to the wearing and crustal movements related to glacial cycles. The depth of the lake basin is not accurately known, although the deepest measured water depths are said to be around 30 m. It is evident that sedimentation (most recently the glaciogenic Quaternary sediments) has smoothed the relief considerably. The top-most lake sediments are composed of permeable sand and gravel layers, but deeper down silt and clay layers deposited from meltwaters during the ice lake stage may be of considerable thickness. These impermeable sediments together with the compressed basal moraines would tend to restrict the infiltration of the lake waters into the bedrock.

The closest distance between the mine and the assumed Lake Contwoyto talik is about 1300 m at surface, while at the 1130 m level the distance to the projected shoreline is only about 500 m (Fig. 49). From a hydrogeological point of view, the talik structures may provide a hydraulic connection between the surface and the deep groundwater system. Although they provide potential pathways for fluid transport, a driving force is also required to generate flow. The local flat topography would not provide a gradient which could force flow deeper than few tens of meters. A drawdown cone around the mine could cause suction towards it. However, it appears that the lateral hydraulic connections are relatively weak, at least towards the mine. None of the faults or fracture systems exposed to the mine drifts are known to leak water. Some were wet for a while, but drained shortly thereafter. The generously flowing exploration boreholes indicate that hydraulic zones exist in the vicinity of the mine. All these holes are drilled towards the lake. Currently, it is not known whether this water availability is linked to the assumed talik structure.

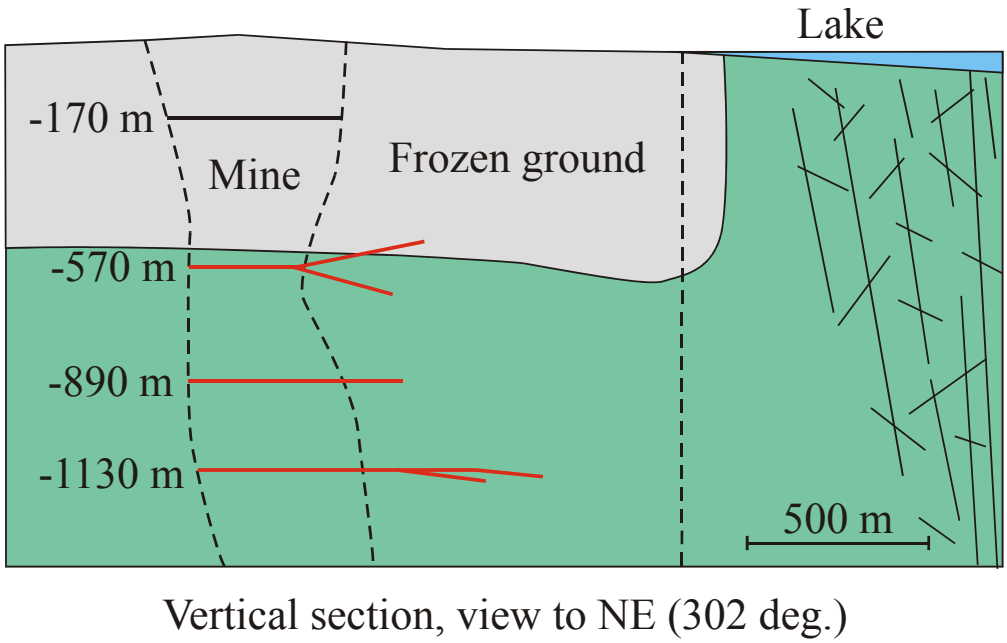

Figure 49. Cross-section showing the spatial relationship between the mine and the assumed talik below Lake Contwoyto (the mine workings are delineated down to about the 1400 m level). Additionally, the projections of the research boreholes at 570 m, 890 m and 1130 m extending closest to the talik are shown. The dashed vertical line indicates the approximate location of the shoreline.

4.2.3 Hydrogeochemistry

Despite considerable crustal depression and the rapid eustatic rise of the sea level during the melting of the ice sheet, marine waters did not invade the Lupin area. An ice-dammed lake occupied the basin of Lake Contwoyto and the valley of the Burnside River extending to the Arctic sea until about 9000 years BP (Dyke and Prest 1987). It is reasonable to assume that during and shortly after deglaciations the upper part of the bedrock was saturated with dilute and cold melt water. It is possible the high hydraulic pressures under most recent sub-glacial conditions forced the melt waters down to considerable depths along fracture zones, such as the one assumed to locate below Lake Contwoyto. Dilute water with high oxygen content and light oxygen isotope composition would be characteristic for the glacial melt waters (Ahonen and Vieno 1994). Older more saline waters would persist below the fresh groundwater layer.

The contribution to the salinity of residual fluids by the freezing of dilute, fresh waters is expected to be minor. The freeze-out process can effectively increase the salinity only when initially saline waters are involved. These types of water are generally found deeper in the bedrock, but the continuous advance of the freeze-out front is eventually prevented by increased groundwater salinity and increased temperature with depth. The small volume of available water and the lack of routes for the escaping residual fluids are most likely the limiting factors in crystalline rocks. Zhang and Frape (2003) came to the same conclusion based on the results of laboratory freezing experiments. Highly saline waters have not been observed directly below the permafrost at Lupin. The salinities at depths of 540 – 570 m are 2 – 3 g/L. Similar or slightly higher concentrations are observed throughout the 890 m level, where a number of boreholes

have been sampled. Interestingly, this water type is again encountered at 1130 m level in a newly excavated drift extending towards the Lake Contwoyto and pristine bedrock.

Strong hydrogeochemical compartmentalisation characterizes the deeper parts of the mine. At the 1130 m level, the salinities range from 2 g/L to 30 g/L which is approaching the salinity of seawater. Despite this variation in TDS, the groundwaters have consistent chemistry of Na-Ca-Cl type,with homogeneous isotope composition. The tritium content in most of the waters, including the most dilute ones, is less than 0.8 TU. This relationship suggests dilution as a result of mixing between highly saline water, and fresh, tritium-free water at depth. The fact that the salinities are not uniform may be attributed to the structural heterogeneity at the site as discussed above.

The measured pH range at 570 level is around pH 6, and at 890 m level and below, from 8.2 to pH 8.6. The sulphide bearing rocks have a distinct influence on groundwater pH values, if oxidizing waters are involved. This is observed in a fault exposed to the mine ramp, where man-made brine is slowly moving downwards. The measured pH values in this structure are generally below pH 6. Redox potential data from sealed boreholes at 890 and 1130 m levels indicate that Eh-values are slightly below zero (in Eh scale). These values fit very well with an iron-dominated redox system. As often observed in groundwater studies, iron concentrations in Lupin groundwaters are very close to or below the detection limit for iron. Sulfide-dominated Eh-values were not observed in Lupin waters. Dissolved oxygen concentrations were beyond the lower detection limit in all cases. To date, there is no indication that recent meteoric waters have infiltrated to these depths. Unfortunately, there are no flowing boreholes at higher levels, which would provide an opportunity to monitor the situation closer to the base of permafrost.

Gases found in the deep groundwater systems beneath the permafrost, are apparently thermogenic in origin. The site does have considerable metasedimentary rocks which were originally deep ocean sediments. The gas composition and age would therefore most likely be tied to the age of the metamorphic event (*i.e.* hundreds of millions to billions of years). In most cases, the gases, matrix fluids and many of the saline groundwaters have similar evolutionary histories.

5 Summary

The existence of structural heterogeneity at the Lupin site is evidenced by (i) salinity and gas differences in the 1130 m boreholes, which generally trend in the same direction through the same group of faults and geological units across the foliation. As an example, the proximity of highly saline zones on the 1130 level to a zone containing very fresh, non-tritiated water suggests variable, poorly connected structural pathways at the site; (ii) the heterogeneity of the hydraulic heads at the site; (iii) the apparent lack of hydraulic connection between boreholes during hydraulic testing; and (iv) the observed heterogeneity in gas flow from fractures versus fluid flow during down-hole video surveys.

One of the major implications of such a poorly connected system would be the limitation on recharge to depth or across the site. This is apparent from the large unsaturated zone (≈100 m thick) beneath the permafrost. The results from the electromagnetic soundings suggest that the groundwater table is consistently deeper than the assumed base of the permafrost for a distance of 2–3 kilometres away from the mine. In addition, the inflow of natural water into the mine is low, reflecting the low bulk permeability of the fractured rocks at this site (only 53, 000 m^3 of water were removed from the mine by pumping in 1999, including all water entering the mine via pipelines). Based on these two lines of evidence, it seems improbable that the observed unsaturated zone is the result of mine dewatering. However, regardless of the origin of the unsaturated zone (mine-induced drainage vs. permafrost limiting ingress), the area remains dry and is filling very slowly, as observed in borehole 570-106 after deeper boreholes were sealed. The possibility that crustal rebound is also affecting the unsaturated zone needs further investigation. In addition, the heterogeneity in salinity and the observed head measurements (with the possible exception of the non-tritiated fresh water sampled on the 1130 m level), would suggest that the connections to the assumed large talik structure connected to a major surface water body are poor.

Highly saline waters under high pressures have not been observed in or directly under the permafrost. The lack of such a large reservoir of high pressure, gas-rich saline fluid coupled with the structural heterogeneity discussed above constrains our conceptual model of the site. There are mine-induced contaminants moving slowly downwards in one large fault system. However, there appears to be a mixing or dilution of this saline, nitrate-rich contamination by a matrix fluid as seen in the results for a variety of stable isotopes (^2H, ^{18}O, ^{37}Cl) used to fingerprint the water and solutes. In addition, anomalies in some parameters such as sulphate concentrations in fluids from the permafrost zone may prove to be precipitates from the freeze out process (*e.g.*, $Na_2SO_4 \cdot 10H_2O$; $MgSO_4 \cdot 6H_2O$). If this proves to be the case, then these very soluble precipitates have remained undisturbed (possibly in a stagnant fracture system) until the man-made brine was introduced into the fault zone. This would have major implications in terms of demonstrating lack of flow or active hydraulic systems during the natural evolution of the flow system.

Gases found in the deep groundwater systems below the permafrost are apparently thermogenic in origin. The site does have considerable metasedimentary rocks which were originally deep ocean sediments. The gas composition and age would therefore most likely be tied to the age of the metamorphic event (i.e. hundreds of millions to

billions of years). In most cases, the authors assume that by association, the gases, matrix fluids and much of the saline groundwaters have similar evolutionary histories.

The inorganic carbon component of the system is very small. Carbon isotopes suggest that the DIC/bicarbonate component is sourced from very minor amounts of old methane that was converted from carbon dioxide by bacteria at some time in the past. The extremely small amounts of DIC (5 to 15 mg/L) would suggest a very minor impact of bacterial action in the system. The age of this activity is indeterminate at this point in the investigation.

6 References

Ahonen, L. 2001. Permafrost: Occurrence and physicochemical processes. Posiva Report 2001-05, 42 p.

Ahonen, L. and Vieno, T. 1994. Effects of glacial meltwater on corrosion of copper canisters. Nuclear Waste Commission of Finnish power Companies, Report YJT-94-13, 20 p.

Andrews, J.T. 1970. A geomorphological study of post-glacial uplift with particular reference to Arctic Canada. Institute of British Geographers Special Publication No. 2, 156 p.

Berger, A., Loutre, M.F. and Tricot, C. 1993. Insolation and Earths orbital periods. Journal of Geophysical Research 98/10, 10341 – 10362.

Burn, C. R. 2002. Tundra lakes and permafrost, Richards Island, western Arctic coast, Canada. Can. J. Earth Sci. 39 (8), 1281 – 1298.

Burn, C.R. 2003. Personal communication. Carleton University, Canada.

Cera, E., Ahonen, L., Rollin, C., Bruno, J., Kaija, J. and Blomqvist, R. 2002. Redox processes at the Palmottu uranium deposit. In: Maravic, H. von & Alexander, W. R. (eds.) Eighth EC Natural Analogue Working Group Meeting : proceedings of an international workshop held in Strasbourg, France from 23 to 25 March 1999. Luxembourg: Office for Official Publications of the European Communities, 183 – 200.

Cooper, H.H., Jr, and Jacob, E.C. 1946. A generalized graphical method for evaluation formation constants and summarizing well-field history. Transactions, American Geophysical Union, 27: 526 – 534.

Craig 1961. Isotopic variation in meteoric waters. Science 133, 1702 – 1703.

Dawson, A.G. 1992. Ice Age Earth: Late Quaternary Geology and Climate. Routledge, London and New York, 293 p.

Delisle, G., Caspers, G. and Freund, H. 2003. Permafrost in north-central Europe during the Weichselian: how deep?. – Proc. of 8th International Conference on Permafrost, Zurich, 187 – 191.

Dyke, A.S. and Prest, V.K. 1987. Late Wisconsian and Holocene history of the Laurentide ice sheet. Geographie Physique et Quaternaire 41, 237 – 263.

Fetter, C. W. 2001. Applied Hydrogeology (4th ed.) Prentice Hall, Upper Saddle River, NJ, 2001.

Fischer, D.A, Reeh, N. and Langley, K. 1985. Objective reconstruction of the Late Wisconsian Laurentide ice sheet and the significance of deformable beds. Geographie Physique et Quaternaire 39, 229 – 238.

Flint, R.F. 1971. Glacial and Quaternary Geology. New York, John Wiley.

Gascoyne, M., Schwarcz, H.P. and Ford, D.C. 1980. A palaeotemperature record for the Mid-Wisconsin in Vancouver Island. Nature 285, 474 – 476.

Heikkinen, E., Paananen, M., Kurimo, M., Öhberg, A., Ahokas, H., Okko, O., Front, K., Hassinen, P., Pitkänen, P., Cosma, C., Heikkinen, P., Honkanen, S. and Korhonen, R. 1992. Geophysical investigations in the Olkiluoto area, Finland. Summary report. Nuclear Waste Commission of Finnish power Companies, Report YJT-92-34.

Heikkinen, E., Saksa, P., Ruotsalainen, P., Ahokas, H., Nummela, J. and Paananen, M. 1996. Groundwater salinity model based on deep electromagnetic soundings. Oral presentation, SAGEEP-96, Keystone,Colorado, USA.

Horne, R.N. 1995. Modern Well Test Analysis: a computer aided approach. Petroway, Inc., Palo-Alto, CA.

Hughes, T.J., Denton, G.H., Andersen, B.G., Schilling, D.H., Fastook, J.L. and Lingle, C.S. 1981. The Last Great Ice Sheets: a global view. *In* The Last Great Ice Sheets (eds. G.H. Denton and T.J. Hughes). John Wiley & sons, 275 – 318.

IAEA, 2001. Global Network of Isotopes in Precipitation (GNIP) and Isotope Hydrology Information System (ISOHIS). http://isohis.iaea.org.

Jokinen, J., Paananen, M., Oksama, M. and Soininen, H. 1995. Interpretation of supplementary electromagnetic soundings at Olkiluoto study site, Eurajoki, southeastern Finland. TVO/Site Investigations, Work report PATU-95-21.

Kruseman, G.P. and de Ridder, N.A. 1994. Analysis and Evaluation of Pumping Test Data, 2nd edition. ILRI publication 47, Wageningen, The Netherlands.

Kuivamäki, A., Vuorela, P. and Paananen, M. 1998. Indications of postglacial and recent bedrock movements in Finland and Russian Karelia. Geological Survey of Finland. Nuclear Waste Disposal Research. Report YST-99, 92 p. + 1 app.

Long, A., Eastoe, C.J., Kaufmann, R.S., Martin, J.G., Wirt, L., and Finley, J.B. 1993. High precision measurement of chlorine stable isotope ratios. Geochim. Cosmochim. Acta 57, 2907-2912.

Mackay, J. R. 1992. Lake stability in an ice-rich permafrost environment: examples from the western Arctic coast. *In* Aquatic ecosystems in semi-arid regions: implications for resource management (eds. R.D. Robarts and M.L. Bothwell). National Hydrology Research Institute, Environment Canada, Saskatoon. Symposium Series 7, 1 – 26.

Paananen, M., Jokinen, J., Oksama, M. and Soininen, H. 1994a. Interpretation of electromagnetic soundings at Romuvaara study site, Kuhmo, eastern Finland. TVO/Site Investigations, Work Report PATU-94-45.

Paananen, M., Jokinen, J., Oksama, M. and Soininen, H. 1994b. Interpretation of electromagnetic soundings at Kivetty study site, Äänekoski, central Finland. TVO/Site Investigations, Work Report PATU-94-50.

Paananen, M., Lehtimäki, J., Kurimo, M., Jokinen, T. and Soininen, H. 1991. Interpretation of electromagnetic and electric soundings at Olkiluoto study site, Eurajoki, southwestern Finland. TVO/Site Investigations, Work Report 91-28 (In Finnish with an English abstract).

Paananen, M. and Ruskeeniemi, T. 2003. Permafrost at Lupin: interpretation of SAMPO electromagnetic soundings at Lupin. Geological Survey of Finland, Report YST-117. 22 p. + 4 app.

Peltier, R.W. 1996. Global sea level rise and glacial isostatic adjustment: an analysis of data from the east coast of North America. Geophysical Research Letters 23, 717 – 720.

Peltier, R.W. 1998. Implicit ice in the global theory of glacial isostatic adjustment. Geophys. Res. Lett. 25, 3957 – 3960.

Peltier, R.W. 2002. A design basis glacier scenario. Ontario Power Generation, Nuclear Waste Management Division. Report 06819-REP-01200-10069-R00, 63 p.

Ruotoistenmäki, T. and Lehtimäki, J. 1997. Estimation of permafrost thickness using ground geophysical measurements and its usage for defining vertical temperature variations in continental ice and underlying bedrock. In: King-Clayton, L. ... [*et al.*] (eds.) Glaciation and hydrogeology : workshop on the impact of climate change & glaciations on rock stresses, groundwater flow and hydrochemistry - past, present and future, 17 – 19 April 1996, Stockholm, Sweden : workshop proceedings. SKI Report 97:13, A64.

Ruotoistenmäki, T. and Lehtimäki, J. 1999. Analysis of flow parameters of continental ice and permafrost geometry in underlying bedrock using geodetic and

geophysical ground measurements on glaciated terrain in Queen Maud Land, Antarctica. In: Skinner, D. N. B. (ed.) 8th International Symposium on Antarctic Earth Sciences, 5 – 9 July 1999, Wellington, New Zealand : programme & abstracts. Wellington: Royal Society of New Zealand, 273.

Ruskeeniemi, T., Paananen, M., Ahonen, L., Kaija, J., Kuivamäki, A., Frape, S., Moren, L. and Degnan P. 2002. Permafrost at Lupin: Report of Phase 1. Geological Survey of Finland, Report YST-112. 59 p. + 3 app.

Sherwood Lollar, B., Frape, S. K., Fritz, P., Macko, S. A., Welhan, J. A. and Blomqvist, R. 1989. Gas geochemistry and its relationship to brines of the Canadian and Fennoscandian Shield. In: Geological Society of America 1989 Annual Meeting, St. Louis, Missouri, November 6 – 9, 1989. Geological Society of America. Abstracts with Programs 21 (6), A316.

Sherwood Lollar, B. Weise S. M., Frape S. K. and Barker J. F. 1994. Isotopic constraints on the migration of hydrocarbon and helium gases of southwestern Ontario. Bull. Can. Petrol. Geol., 42, 283 – 295.

Sherwood Lollar, B., Westgate, T. B., Ward, J. A., Slater G. F. And Lacrampe-Couloume G. L. 2002. Abiogenic formation of alkanes in the Earth's crust as a minor source for global hydrocarbon reserviors. Nature, 416, 522 – 524.

Smith, S.L., Burgess, M.M. and Heginbottom, J.A. 2001. Permafrost in Canada, a challenge to northern development. In Synthesis of Geological Hazards in Canada (ed. G.R. Brooks). Geological Survey of Canada, Bulletin 548, 241 – 264.

Soininen, H. and Jokinen, T. 1991. SAMPO, a new wide-band electromagnetic system. In: European Association of Exploration Geophysicists 53rd meeting and technical exhibition, Florence, Italy, 26 – 30 May 1991: technical programme and abstracts of papers (oral and poster presentations). Zeist: European Association of Exploration Geophysicists, 366 – 367.

Trenhaile, A.S. 1998. Geomorphology: A Canadian perspective. Oxford University Press, Toronto, 340 p.

Vuorela, P. and Kuivamäki, A. 1997. Problem of postglacial reactivation in the eastern part of the Fennoscandian Shield (Russian Karelia). In: King-Clayton, L. [*et al*.] (eds.) Glaciation and hydrogeology: workshop on the impact of climate change & glaciations on rock stresses, groundwater flow and hydrochemistry – past, present and future, 17 – 19 April 1996, Stockholm, Sweden : workshop proceedings. SKI Report 97:13, A82 – A83.

Zhang, M. and Frape, S.K. 2003. Evolution of shield brine groundwater composition during freezing. Ontario power Generation, Report No: 06819-REP-01200-10089-R00, 49 p.